Identification and Manipulation of Molecules Regulating Axonal Outgrowth and Synapse Formation during Post-Injury Axonal Remodeling

Dissertation

der Fakultät für Biologie

der Ludwig-Maximilians-Universität München

Angefertigt am Institut für klinische Neuroimmunologie, LMU München

Eingereicht von

Anne Jacobi

München, 2014

ERKLÄRUNG

Hiermit versichere ich ehrenwörtlich, dass meine Dissertation selbständig und ohne unerlaubte Hilfsmittel angefertigt worden ist. Die vorliegende Dissertation wurde weder ganz, noch teilweise bei einer anderen Prüfungskommission vorgelegt. Ich habe noch zu keinem früheren Zeitpunkt versucht, eine Dissertation einzureichen oder an einer Doktorprüfung teilzunehmen.

München, den 02.07.2014

Dissertation eingereicht am: 02.07.2014

1. Gutachter: Prof. Dr. Hans Straka

2. Gutachter: Prof. Dr. Anja Horn – Bochtler

Tag der mündlichen Prüfung: 12.11.2014

Evolution of a PhD (Winner of the public award of the Graduate Center Photocompetition 2011)

Table of Contents

Table of Contents

List of Abbreviations

Akt	Protein Kinase B (PKB), serine-threonine proteine kinase
AAV	Adeno-associated virus
ASIA	American Spinal Injury Association (Impairment Scale)
C1 (…)	cervical region 1 (…) of the spinal cord
cAMP	cyclic adenosine monophosphate
CA3	hippocampal Cornu Ammonis 3
ChABC	Chondrotinase ABC
CSPGs	Chondroitin sulfate proteoglycans
CNS	central nervous system
Cre	recombinase to cut out floxed genes
(h)CST	(hindlimb) corticospinal tract
DRG	dorsal root ganglion
E	embryonic day
EAE	experimental autoimmune encephalomyelitis
FGF	fibroblast growth factor
FGFR	fibroblast growth factor receptor
GFP	Green Fluorescent protein
GlyT2	Glycine Transporter 2
ICCP	International Campaign for Cures of spinal cord injury Paralysis
Jak	Janus kinase (JAK, or "Just another kinase")
KO	Knock Out
L1 (…)	lumbar region 1(…) of the spinal cord
LPSN	long propriospinal neurons
MAGs	Myelin associated glycoproteins
mTOR	mammalian target of rapamycin

List of Abbreviations

NCS1	Neuronal calcium sensor1
NL1 (4)	Neuroligin 1 (4)
NT3	Neurotrophin 3
OMgp	Olidgodendrocyte myeline glycoprotein
P4	postnatal day 4
PNS	peripheral nervous system
PTEN	Phosphatase and tensin homolog
RGCs	retinal ganglion cells
SCI	spinal cord injury
SPSN	short propriospinal neurons
SOCS3	Suppressor of cytokine signaling 3
STAT3	signal transducer and activator of transcription 3
SynCAM	synaptic cell adhesion molecule
T (…)	thoracic region of the cord (eg. T8= thoracic cord level 8)
TF	Transcription factor

Abstract

Spinal Cord Injury (SCI) is a devastating disease which leads to long lasting neurological deficits including sensory and motor-dysfunction below the site of injury. The persistence of these deficits is due to the low capacity of the adult central nervous system (CNS) to regenerate after injury. However, over the last decade it has been shown, that axonal tracts in the spinal cord can in principle remodel after injury. The corticospinal tract (CST), an important descending motor tract that is involved in the fine movement and coordination of the fore- and hindlimbs, serves as a good model to study this remodeling. A key aspect of CST remodeling after injury is the formation of intraspinal detour circuits that contribute to functional recovery. Which molecules regulate the formation of these new detour circuits is so far unknown. In my thesis, I aimed to identify these regulatory molecules and to understand their contribution to the establishment of detour circuits after injury.

First, I investigated, whether activating the intrinsic growth program can induce *de novo* sprouting of CST collaterals and thereby improve functional recovery. To do so, I induced sustained expression of STAT3, a growth-promoting transcription factor, via viral gene transfer in cortical projection neurons. This allowed me to show that enhanced activation of the intrinsic growth program was sufficient to increase sprouting of CST collaterals after injury.

Second, I performed *in situ* hybridizations for guidance and synaptogenic molecules to screen for candidates that could influence targeting of CST collaterals following spinal cord injury. I can show that all the molecules studied are also expressed in the adult CNS and that several cues among them, Semaphorin 7a, SynCAM4, Slits and Neuroligin 1, are differentially expressed in subsets of spinal interneurons suggesting that they could be involved in target finding during detour circuit formation.

Finally, I focused our attention on the establishment of new synapses during post-injury detour circuit formation. Recently, the family of fibroblast growth factors (FGF's) has been shown to be important during presynaptic differentiation in the development of the cerebellum and CA3 pyramidal neurons in the hippocampus. FGF22 in particular can promote the establishment of excitatory synapses and therefore is an interesting candidate that could regulate the formation of CST synapses during post-injury remodeling. To test this, I deleted the FGF22 ligand (using FGF22KO mice) or specifically ablated its main receptors, FGFR1 and FGFR2, in the hindlimb CST. Deleting FGF22 or both receptors impaired bouton formation and maturation of the newly formed CST collaterals and as a result limited the formation of detour circuits following spinal cord injury. This leads to a profound delay of functional recovery in mutant mice after spinal cord injury. These results identify FGF22 signaling as a first regulator of synapse formation during axon remodeling in the injured adult central nervous system.

In summary, the results presented in my thesis provide new insights into the molecular regulation of detour circuit formation and identify promising therapeutic targets (such as STAT3 and FGF22) that can foster axonal remodeling after spinal cord injury.

Zusammenfassung

Eine Rückenmarksverletzung hat für die betroffenen Patienten verheerende Folgen und führt häufig zu dauerhaften sensorischen und motorischen Funktionsausfällen unterhalb der Verletzungsstelle. Diese Funktionsausfälle sind häufig dauerhaft, da Nervenzellverbindungen im zentralen Nervensystem des Erwachsenen nicht mehr regenerieren können. In den letzten Jahren konnte jedoch gezeigt werden, dass Nervenzellverbindungen im Rückenmark nach einer Verletzung dazu fähig sind sich zu reorganisieren. Der kortikospinale Trakt (CST), ein wichtiger herabsteigender Fasertrakt, der die Ausführung der Feinmotorik und die Abstimmung der Extremitäten koordiniert, ist dabei ein besonders gutes Model zur Untersuchung dieser neuronalen Umstrukturierung. So konnte gezeigt werden, dass der CST nach einer Durchtrennung einen intraspinalen „Umgehungskreislauf“ bildet und damit schließlich zur funktionellen Erholung beiträgt. Welche Moleküle die Bildung dieses Umschaltkreislaufes regulieren, ist soweit nicht bekannt. In meiner Doktorarbeit habe ich entsprechend versucht erste Signalwege zu identifizieren, welche bei der Umstrukturierung nach einer Rückenmarksläsion eine Rolle spielen.

Im ersten Teil meiner Arbeit, untersuchte ich, ob die Aktivierung des intrinsischen neuronalen Wachstumsprogramms die Ausbildung neuer CST Kollateralen veranlassen kann. Dazu induzierten wir eine andauernde Expression von STAT3, einen wachstumssteigernden Transkriptionsfaktor, in kortikalen Projektionsneuronen mittels viralen Gentransfer und konnten zeigen, dass dies zu einer vermehrten Aussprossung neuer CST Kollaterale nach einer Läsion führt.

Zusammenfassung

Im zweiten Teil meiner Arbeit führte ich einen *in situ* Hybridisierungs-Screen durch, um potentielle Kandidaten, welche das gerichtete Wachstum von Axonen und die Herstellung von synaptischen Verbindungen nach einer Rückenmarksverletzung fördern könnten, zu identifizieren. Ich konnte zeigen, dass alle untersuchten Moleküle, die während der Entwicklung des ZNS das gerichtete Wachstum von neuronalen Verbindungen steuern, auch im adulten ZNS exprimiert werden. Einige dieser Moleküle, unter anderem Semaphorin 7a, SynCAM4, Mitglieder der Slit Familie und Neuroligin1, zeigen ein interessantes Expressionsmuster, welches auf deren mögliches Mitwirken bei der Entstehung intraspinaler Umgehungskreisläufe hindeuten kann.

Im letzten Abschnitt meiner Arbeit, untersuchte ich, welche Moleküle die Ausbildung neuer Synapsen nach einer Läsion steuern. Vor kurzem wurde entdeckt, dass die Familie der Fibroblasten Wachstumsfaktoren (FGFs) eine wichtige Rolle während der präsynaptischen Differenzierung im Kleinhirn und Hippocampus spielen. Insbesondere für FGF22 konnte gezeigt werden, dass es die Ausbildung von exzitatorischen Synapsen induzieren kann und somit möglicherweise auch die Bildung neuer Synapsen des CSTs beeinflussen könnte. Um dies zu untersuchen, habe ich Mäuse verwendet, die entweder FGF22 defizient waren (FGF22 KO Mäuse) oder in denen die beiden FGF22 Rezeptoren, FGFR1 und FGFR2, in den Neuronen des Hinterbein-CST genetisch entfernt wurden. Unsere Ergebnisse zeigen, dass das Fehlen von FGF22 oder seiner Rezeptoren nach einer Läsion bei den neu auswachsenden CST Kollateralen zu einer deutlichen Reduktion der Synapsenbildung und – Reifung führt. Dies behindert entsprechend die Ausbildung der intraspinalen Umgehungskreisläufe und verzögert die funktionelle Erholung nach einer Rückenmarksverletzung. Unsere Ergebnisse identifizieren den FGF22-FGFR Signalweg als einen wichtigen Regulator der Neubildung von Synapsen im geschädigten zentralen Nervensystem des Erwachsenen.

Zusammenfassung

In der Gesamtschau geben die Ergebnisse meiner Arbeit neue Einblicke in die molekulare Regulation der Ausbildung von Umgehungskreisläufe und neue Hinweise auf vielversprechende therapeutische Ansätze (mit STAT3 oder FGF22), die die Umstrukturierung von Nervenzellverbindungen nach einem Rückenmarkstrauma verbessern könnten.

1. Introduction

1.1 Epidemiology of Spinal Cord Injury (SCI)

With an occurrence of 18.5 people/million (source: The International Campaign for Cures of spinal cord injury Paralysis, ICCP), spinal cord injury impacts about 3000 new cases in Germany every year (Köning and Frowein, 1989). Surviving a traumatic injury of the spinal cord is most often followed by a "new" life in a wheelchair and the person usually depends on other people's help for the rest of her / his life. Most of the patients are young males (70%) with an average age between 16 and 30 years (Hulsebosch et al., 2002; Sadowsky et al., 2002). Most of the traumatic injuries occur due to accidents (2/3 of all cases), i.e. sports, traffic or work (Figure 1). In addition to striking life changing circumstances for the patient, the economic impact, in terms of long term cost of care and cost of social welfare support, reaches a high level every year (Westgren and Levi, 1998). For example, the costs for the United States alone reach up to 7.7 billion dollars annually (National Spinal Cord Injury Statistical Center, University of Alabama at Birmingham).

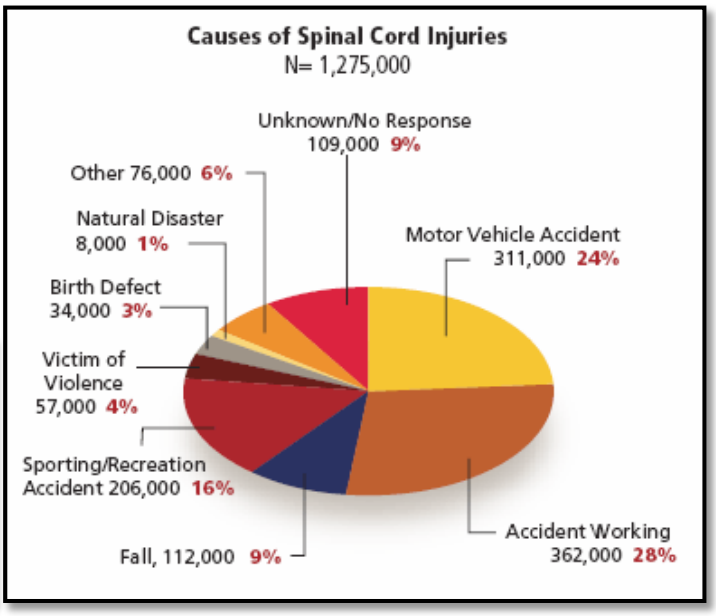

Figure 1: Causes of Spinal Cord Injuries; Over 50% of SCI are caused by accidents, one half by vehicle (i.e. motorbike) or during work (reprint permission from Christopher Reeve Foundation).

An insult to the spinal cord results in a change of the normal motor, sensory or autonomic function. This can be temporary or permanent as well as either complete or incomplete (Classification in the ASIA impairment scale, Figure 2). A complete injury leads to a total and irreversible loss of voluntary movement and sensation below the segment of injury. After an incomplete injury however, some function below the segment of injury remains (Raineteau and Schwab, 2001; Fawcett et al., 2007). Thereby in incomplete injuries some degree of spontaneous functional recovery in patients might be observed (Wernig and Müller, 1992; Dietz et al., 1998). These injuries are of course more amenable to therapies than complete injuries. The level where the injury occurs is also crucial, as this can either lead to paraplegia or quadriplegia (Figure 2). An injury at the level of the cervical spinal cord (between C1 and C7) causes quadriplegia, which happens in 52% of all cases and is classified by a loss of use of all four limbs and torso. A lower level of injury (between T1 and L5) instead leads to paraplegia, which happens in 47% of all cases and causes impairment in motor and sensory function of the lower extremities.

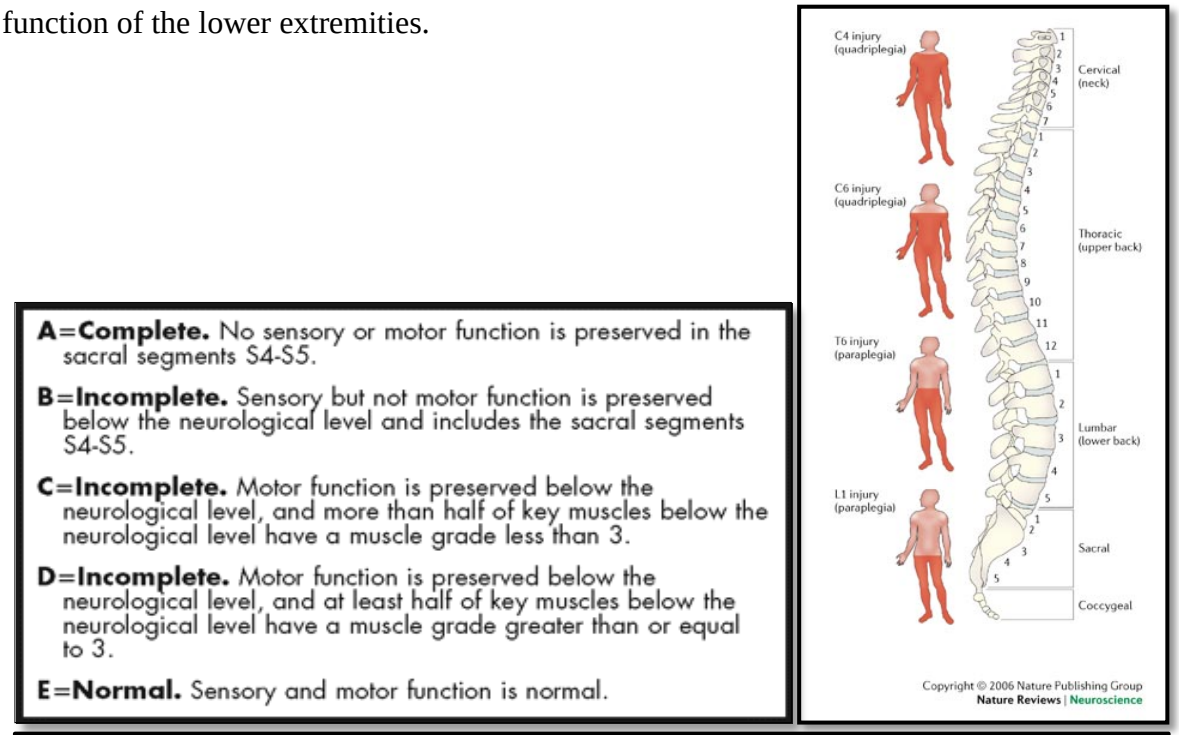

Figure 2: Spinal cord injury classification according to the American Spinal Injury Association (ASIA) Impairment Scale (Modified from Thuret et al., 2006; reprint permission from Nature Publishing Group)

1.2 Clinical Treatments to Date

Clinical treatments and strategies which are currently available do not lead to full recovery of sensory and motor function after spinal cord injury. However, they are designed to prevent secondary damage, help recovery as much as possible and usually are targeting different pathophysiological phases following the injury.

1.2.1 Pathophysiology of SCI

A spinal trauma leads to spinal vertebrate luxation or the break of spinal bones and thereby to a local injury of the spinal cord with a disruption of spinal nerve tracts (primary damage). This phase, directly after the insult, is called acute phase or spinal shock and includes the momentary complete loss of all reflexes, a reduced blood flow and a change of the whole biochemical environment (Ditunno et al., 2004; Martirosyan et al., 2011). The acute phase is quickly followed by the sub-acute phase which is featured by the release of free radicals, an inflammatory response with the influx of macrophages and the development of a vasogenous as well as a cytotoxic edema (Dusart and Schwab, 1994; Bethea and Dietrich, 2002; Sharma and Olsson, 1990). In the ensuing late phase a scar is formed, which includes the appearance of reactive astrocytes, necrosis, apoptosis, Wallerian degeneration (Zhang et al., 1997), demyelination and expression of growth inhibitory factors like Nogo-A and OMg or MAGs in the vicinity of the scar that inhibit regeneration at the lesion site (secondary damage; Filbin, 2003; Pernet and Schwab, 2012) (Figure 3).

1.2.2 Clinical Intervention to SCI

Depending on the phase in which the patient is, there are different strategies which are applied to avoid the spread of nerve degeneration or to induce functional recovery as much as possible.

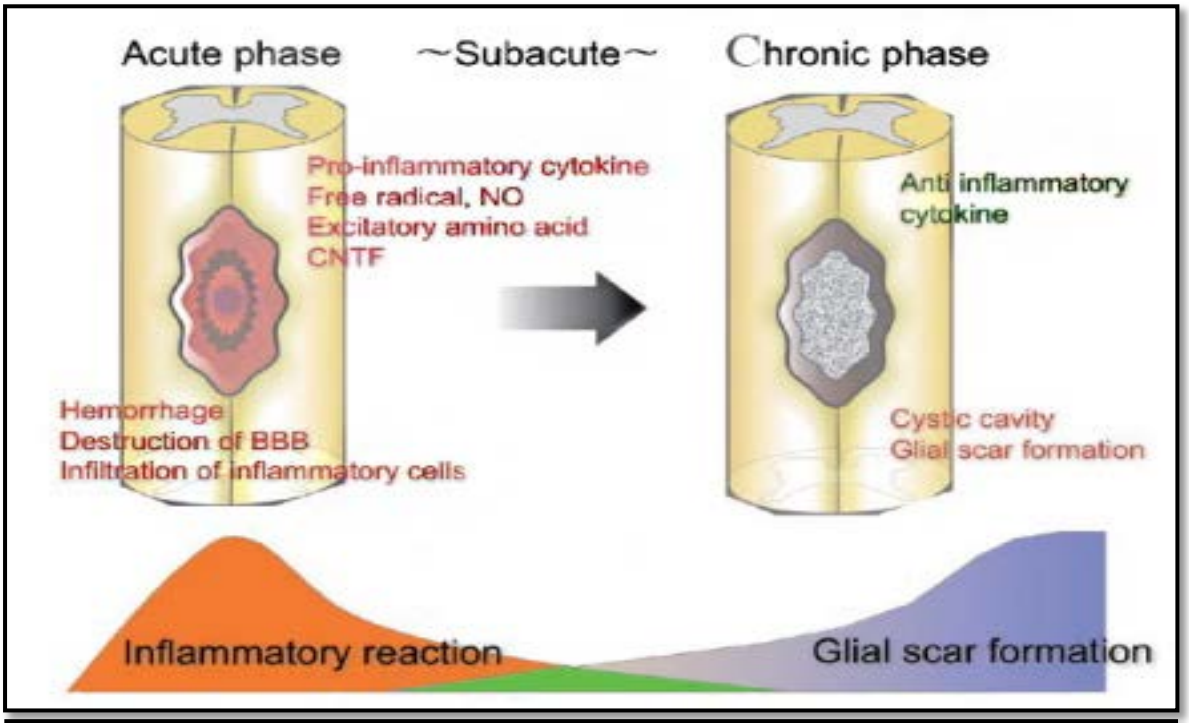

Figure 3: Phases of Spinal Cord Injury. The acute phase, with destruction of BBB and hemorrhage development. The sub-acute phase, with release of free radicals and NO plus inflammatory response. And finally the chronic phase, including glia scar formation. (Modified from Nakamura and Okano, 2013; Re-print permission from Nature Publishing Group)

In the acute and sub-acute phase, the first step is to remove mechanical causes, like broken bones during a reconstructive surgery. After that, most of the patients in many countries receive a cocktail of corticosteroids including methylprednisolone (MPS), which is designed to decrease inflammation and the release of free radicals. It is supposed to lead to fundamental increased functional recovery if applied within 8hrs after trauma (Bracken et al., 1984; Bracken et al., 1990; Bracken et al., 1997). Today this therapy is considered controversial and

often withdrawn as long term studies showed low efficiency, strong side effects (Hurlbert and Hamilton, 2008) such as diabetes mellitus, osteoporosis and psychosis and several follow up studies couldn't reproduce the beneficial long term effects which had been shown in the first studies of the NASCIS (National Acute Spinal Cord Injury Study I and II) (George et al., 1995; Gerhart et al., 1995; Nesathurai et al., 1998; Shepard et al., 1994; Hurlbert, 2008). Considering these insecurities and potential risks, a lot of effort is put into finding new therapeutic treatments. More recently an additional drug has been shown to be glia- and neuro-protective – Asialoerythropoetin (AsialoEPO). Here, the reduction of secondary damage, such as apoptosis, the inflammation processes and the ability to restore vascular integrity (for review see Matis and Birbilis, 2008; Mofidi et al., 2011) has been shown in experimental models for SCI and thereby showing exceptional preclinical characteristics and giving high promises into clinical human trials.

The chronic time after the acute phase is usually accompanied with trying to re-activate neural connections that have been destroyed due to the injury. Here, the only therapeutic intervention that is standard of care and internationally applied to maximize functional recovery in human SCI is rehabilitative training, such as weight-supported treadmill training (Edgerton et al, 2004; Dietz and Harkema, 2004; Dietz and Fouad, 2014). The treadmill training has shown some success in patients with functionally incomplete spinal cord injury (ASIA B-D) and therefore became routine in the rehabilitation centers. The body weight supporting harness and the movement of the legs via a robot or physiotherapist leads to a restoring of natural walking and a sensory feedback input (Maegele et al., 2002; Dietz et al., 2010). The improvements of locomotor capability depend on the location and on the size of the injury (Wernig et al., 1998); however they are maintained over a long period of time. Patients with

complete injury, unfortunately, haven't been able to maintain stepping movements after the training sessions were finished (Wirz et al., 2001).

1.3 Experimental Models to study Spinal Cord Injury

Trying to understand what happens within the injured human spinal tissue is studied in experimental models in order to discover different therapeutic treatments. Some studies focus on the prevention of toxicity, apoptosis or inflammation and hence are all driven by the aim to reduce cell death and scar formation (Kigerl et al., 2009; Liu et al., 1997; Nicholson et al., 2000; Fitch et al. 1999; Popovich et al., 1999). Others are trying to promote axonal growth and regeneration, and thereby restore function. For instance, attempts are carried out in which grafts that can bridge the lesion sites are applied directly after the injury and into the lesion area so that the injured fibers are able to regrow along those (Li et al., 1998; Bamber et al., 2001; Taylor et al., 2006).

Another strategy is to neutralize the growth inhibiting environment of the scar by applying IN-1 antigen, a blocker for the neurite growth inhibitor Nogo-A. In doing so, regeneration of sprouting fibers and their growth over longer distances is seen (Schnell and Schwab, 1990; Brösamle et al., 2000; Chen et al., 2000). In contrast to block inhibition, other studies apply growth promoting factors such as neurotrohpins (BNDF or NT3) (Jakeman et al., 1998; Jain et al., 2005; Sasaki et al., 2009; Houweling et al., 1998; Novikova et al., 2000) or gene transcription factors inducing axonal growth (Bareyre et al. 2011) after injury to promote induction of axonal growth. All these studies show promising potential to either be transferred into clinical studies at some point or at least to help us gain a greater insight into the pathophysiology of spinal cord injury.

The different attempts mentioned above are carried out in experimental animal models of SCI and are crucial to a better understanding of human injuries. Indeed experimental designs are trying to model the physical processes by which human SCI occurs and to replicate the variety of chronic pathologies that characterize its long term effects (Stokes and Jakeman, 2002; Filis and Schwab, 2012). The variations in biological processes between species contribute to difficulties in generalizing only one experimental model and its findings to the human condition. Therefore, depending on the question that is to be answered, different models are chosen. For example, is the primary focus of the experiment fiber regeneration and sprouting, or is the focus of the study on neuroprotective investigations?

1.3.1 Contusion Injury

The contusion injury is the most commonly used model to study SCI. Here, a determined weight is dropped onto the exposed spinal cord (New York University – Multicenter Animal Spinal Cord Injury Studies (NYU-MASCIS) impactor device). With different standardized weights one can mimic defined grades of spinal cord injury. The outcomes of this injury are very similar to human injuries, a necrotic center which is surrounded by histologically normal-appearing myelinated fibers and portions of gray matter (Figure 4a). The cell loss starts immediately after the initial impact and continues radially in all directions so that the lesion expands over time (several days to weeks). This expanded time frame of cell loss offers an opportunity for therapeutic intervention to rescue the neural cell populations (Hulsebosch 2002).

1.3.2 Dorsal Hemisection Injury

The second, most common, used model is the dorsal hemisection. It is a model to precisely and reproducibly study SCI. Here, the dorsal spinal cord is transected with a very fine pair of

scissors (iridectomy scissors). To induce paralysis of the hindlimbs in the mouse model, which represents humans paralysis the best and easiest, the hemisection is usually placed at a thoracal level of T8 – T9 (Figure 4b). This model induces a precise and local lesion with very defined histological consequences and spares parts of the cord. This sparing of parts of the spinal cord also represents a hallmark of most SCI in humans. Due to the mentioned advantages above, the dorsal hemisection is a very suitable model to study axonal regeneration at the lesion site as well as axon remodeling or reorganization (Bareyre et al., 2004).

1.3.3 Full Lesion Injury

A full or complete lesion injury is the term used to describe a complete transection of the spinal cord. Here the spinal cord is also transected with a fine pair of scissors, but no tissue is spared. Following the injury, the two stomps of the spinal cord retract leaving a “gap” between the two spinal extremities. It results in a complete and permanent loss of the ability to send sensory and motor impulses to the region below the lesion site and is also a very good model to study axonal regeneration at the lesion site. However it is noteworthy to say, that even in complete lesion models, some axons might be left intact in the ventral part of the spinal cord (You et al., 2003).

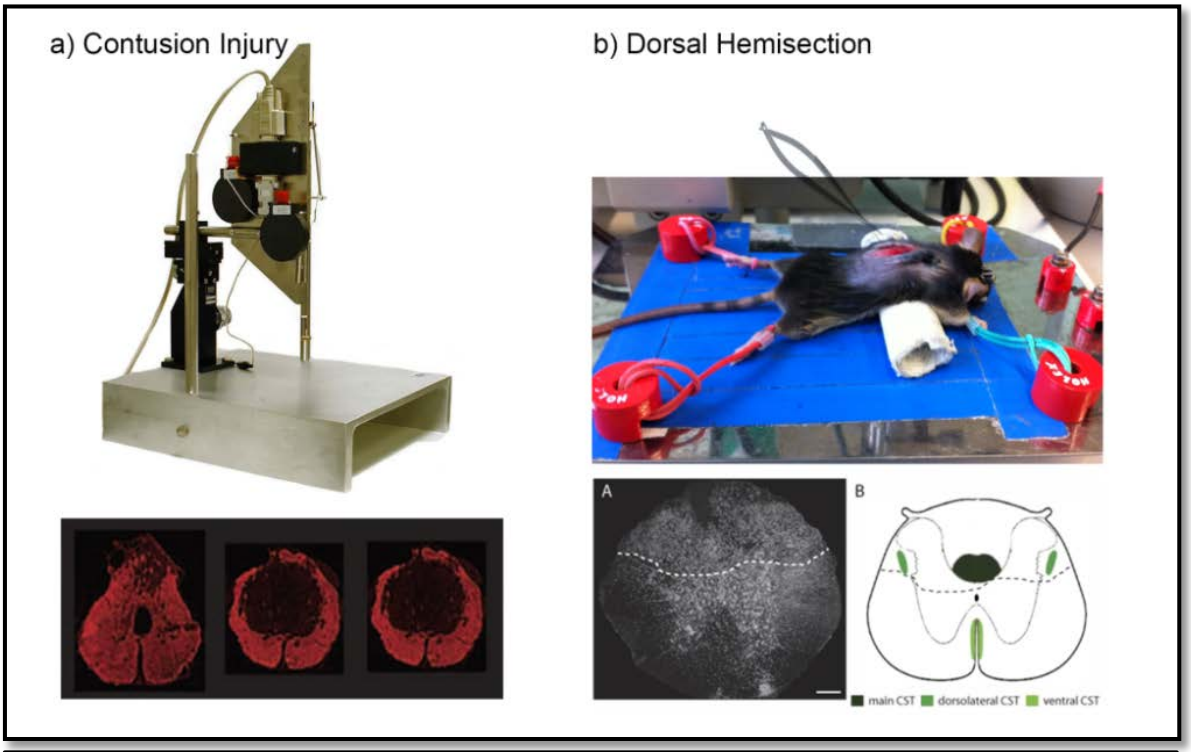

Figure 4: Models to study SCI. a) Contusion Injury; Mechanical device (MASCIS Impactor) and representative cross sections from the lesion center (GFAP staining) (adapted from Ishii et al., 2012). b) Dorsal Hemisection; Induction of a lesion with a pair of fine iridectomy scissors leads to transection of dorsal part of spinal cord, thereby leaving the ventral part intact (as indicated in bottom images from Lang et al., 2012).

1.4 Axonal Remodeling following SCI

For a long time it has been postulated that the adult CNS is not able to remodel or reorganize after a CNS injury, i.e. after traumatic brain injury or SCI. Over the last years this dogma has been proven wrong. First studies in mice could show some spontaneous recovery after injury which also to some extend happens in humans (Burns et al., 1997; Dietz et al., 1998; Dietz 2002; Curt et al., 2004; Fouad et al., 2001). Most of the studies, that show this potential of plasticity, have been investigating spinal cord lesions, in particular lesions of the corticospinal tract (CST) (Terashima et al., 1995; Weidner et al., 2001; Fouad et al., 2001; Bareyre et al., 2004; Courtine et al., 2008; Lang et al., 2012).

1.4.1 Anatomy of the Corticospinal Tract (CST)

The corticospinal tract (CST) is one of the major descending pathways from the motor cortex down to the spinal cord. The mammalian CST controls fine movements like grasping or stepping. It originates in the pyramidal cells of layer V of the motorcortex. About 95% of these cells send their axons down to the spinal cord via the brain stem and cross over to the contralateral side (pyramidal decussation) at the end of the medulla oblongata (spinomedullary junction in the mouse). In humans they cross at the level of the lateral funiculi and form the lateral corticospinal tract, whereas in the mouse they form the main CST (Terashima, 1995). The left over 5% of the axons do not cross contralaterally and thereby travel ipsilaterally in the white matter down to the spinal cord. Once the axons reached their target area in the spinal cord, they branch into the gray matter and connect (most of the time via interneurons) to the lower motor neurons in the ventral horn. Depending on their target area, the fibers are divided into the forelimb CST and hindlimb CST. The forelimb CST terminates in the cervical spinal cord (C3-C5 level), the hindlimb CST terminates in the lumbar spinal cord (L1-L5).

1.4.2 Detour Circuit Formation

The establishments of new circuits in the CNS to overcome or bypass a lesion, and thereby forming new circuits, have been shown in several publications over last decade. In 2001, Fouad et al. could show that after an incomplete thoracic hemisection, the CST is able to form new collaterals in the cervical region (C3-C5) (Fouad et al., 2001). That this sprouting is functionally meaningful was shown a couple of years later by Bareyre et al. in 2004. Here the authors demonstrated the establishment of a detour circuit which is formed by contacts of the newly born collaterals onto long propriospinal neurons (LPSN) which extend their axons from

C3-C5 in the ventral and lateral horn (Giovaneli Barilari and Kypers, 1969) down to the lumbarsacral enlargement (Alstermark et al., 1987; Dietz et al., 2002) (Figure 5). The LPSN are known to coordinate forelimb and hindlimb movements (Jankowska et al., 1974; Grillner et al., 1975). These interneurons are spared by an incomplete, dorsal hemisection and are able to transduce signals coming from the new CST collaterals onto the hindlimb motoneurons hence creating a new circuit (Bareyre et al., 2004) (Figure 5c+d). Electrophysiological experiments demonstrated that information coming from the cortex can be transmitted to the hindlimb motoneurons. Also the authors show in behavioral experiments that spontaneous functional recovery at least in parts is mediated by the detour circuit formation (Bareyre et al., 2004).

The importance of newly formed intraspinal circuits has been further strengthened by several publications investigating the spontaneous axonal plasticity of the corticospinal tract after injury (Weidner et al., 2001; Courtine et al., 2008). A recent publication from van den Brand et al., (2012) for instance shows that plasticity and recovery can take place also in cases of severe spinal cord injury. Here, after two lateral lesions in the thoracal spinal cord, they injected a chemical solution of monoamine agonists which triggers cell responses of spinal neurons and replaces the neurotransmitter cocktail which would come from the brainstem pathways in the healthy mouse. The cocktail is able to induce activation of lower spinal intercircuits and thereby of lower body movement. The authors then electrically stimulated the spinal cord with electrodes implanted in the spinal canal. This localized stimulation sends continuous electrical signals through nerve fibers to the chemically excited neurons. After a couple of weeks of training the rats not only voluntary initiated walking but also were able to climb obstacles and steps. They could show that this recovery is also due to a strong

remodeling process of supraspinal and intraspinal connections as well as cortical projections from the CST (van den Brand et al., 2012).

Intraspinal remodeling can not only be shown following traumatic lesions of the spinal cord but also following inflammatory lesions of the spinal cord. In an animal model of multiple sclerosis model (EAE), it has been shown that the CST can show sprouting ability above the inflammatory lesion. This leads to a detour circuit formation due to the increased contact formation onto spinal interneurons surrounding the lesion site and in the lumbar target area (Kerschensteiner et al., 2004). An additional paper supports this remodeling by showing the sprouting ability of the CST along blood vessels after EAE induction (Muramatsu et al., 2012).

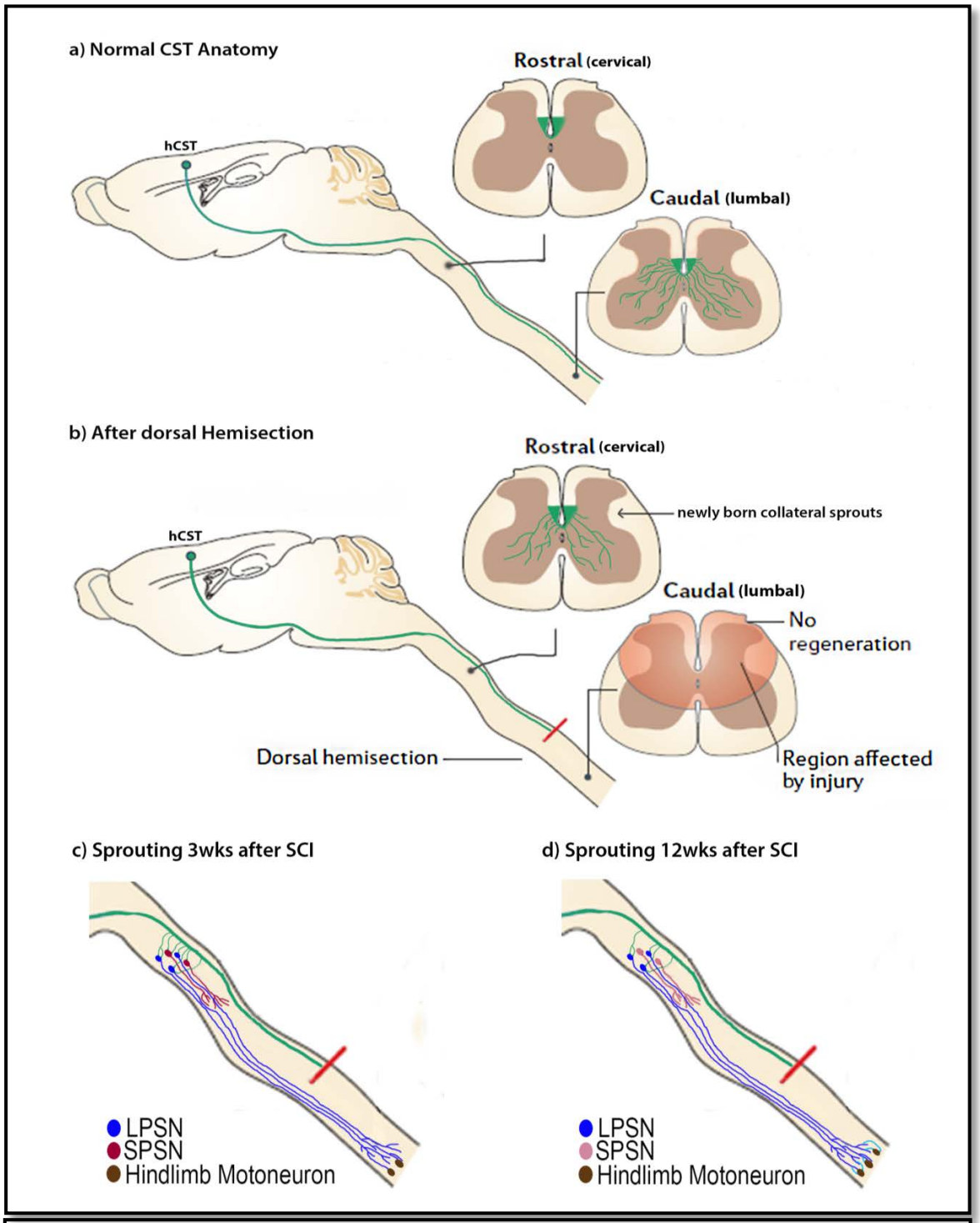

Figure 5. Model of Detour Circuit Formation. a) Unlesioned hindlimb CST (hCST) travels down the spinal cord and sends sprouts into the gray matter of the lumbar enlargement. b) After dorsal hemisection (T8) regeneration of collaterals from lesion site fails. Instead the lesion leads to spontaneous sprouting of the hCST in the cervical spinal cord (C3-C5). c) 3wks after lesion new collaterals form contacts onto excitatory spinal interneurons (SPSN and LPSN). d) 12wks after lesion only contacts onto LPSN remain, which run in the ventral horn and thereby are able to bridge the lesion site. Also the number of contacts onto the hindlimb motoneurons increases (Harel and Strittmater, 2006; Re-print permission from Nature Publishing Group).

The last decade of research has shown that the spinal cord after an injury has the capability to spontaneously form new intraspinal circuits (Fouad et al., 2002; Bareyre et al., 2004; Kerschensteiner et al., 2004; Courtine et al., 2008; van den Brand et al., 2012). Studying this process in further detail and thereby learning more about intrinsic factors, which might play a key role for the establishment of such circuits, will be important in coming one step closer to potential therapeutic treatments for human spinal cord injury.

For the successful formation of the detour circuit after a dorsal hemisection (Bareyre et al., 2004), several steps are required.

1.4.2.1 Directed Axonal Growth

In the first phase of the detour circuit formation, the newly born axon collaterals have to know where to grow to and thereby find their target area. In case of the detour circuit formation after a dorsal SCI, they have to grow into ventral-medial part of the cervical spinal cord, where the cell bodies of the LPSNs originate (Alstermark et al., 1987). First, the axons need to initiate growth which is possibly promoted via growth promoting molecules such as STAT3 or Semaphorin 7a. Second, once the axons have initiated growth, these need to be guided toward their appropriate target cells. Several molecules that induce axonal outgrowth and axon guidance have been shown to be important during neural development (for review Niclou et al., 2006; Guan and Rao, 2003), among others Netrins (Kennedy et al., 2006), Semaphorins (Behar et al., 1996), Slits (Lopez-Bendito et al., 2007) and Ephrins (Eberhart et al., 2000). Also, first studies now show their expression in the adult CNS, indicating a potential important role in injury induced spinal remodeling (Wehrle et al., 2005; Marillat et al., 2002; Mann et al., 2007; Bundesen et al., 2003).

1.4.2.2 Synapse Formation

Once the axon collaterals have reached their target cells, they have to contact those. This process is called synapse formation and requires a very defined course of events. To date it is not entirely clear which exact time course synapse formation follows, but studies conducted during CNS development agree that it can either be induced pre-synaptically or post-synaptically (Gerrow and El-Husseini, 2006).

Presynaptic-induced formation usually starts with the recruitment of presynaptic molecules upon initial contact (presynaptic differentiation) such as molecules for the assembly of the vesicle release machinery. This phase is followed by the creation of an active zone and the accumulation on the postsynaptic density (postsynaptic differentiation). The postsynaptic-induced synapse formation first recruits preformed postsynaptic scaffold proteins upon initial contact which then signals the presynaptic machinery to assemble. Either way, the recruitment of receptors to the postsynaptic side represents the last phase of the synapse formation. There are several molecules which are known to be important for the process of synapse formation during the development of the CNS, such as SynCams (Biederer et al., 2002), Neuroligins (Scheiffele et al., 2000) or FGF's (Umemori et al, 2004), which act as presynaptic organizers and EphrinBs (Henkemeyer et al., 2003) or Neurexins (Graf et al., 2004), which can act as postsynaptic organizers (Dalva et al, 2007; Shapiro et al., 2007; Tallafuss et al., 2010). Whether these are also important during contact formation after SCI, has been started to be investigated in the last couple of years (Thomas et al., 2008, Zelano et al., 2007, Budensen et al., 2003, Moreno-Flores et al., 1999).

1.4.3 Molecular Regulation of Detour Circuit Formation

1.4.3.1 STAT3 – a Gene Transcription Factor to Induce Axonal Growth

It is well known that the CNS is not capable of regenerating axons after injury. The peripheral nervous system (PNS) however has shown to be able to induce the regrowth of injured axons via the activation of an intrinsic growth program. The activation of transcription factors (TF's) such as c-Jun, CREB, SMAD, Atf-3 (Raiwich and Makwana, 2007; Zou et al., 2009; Seiiffers et al., 2007) and in particular the signal transducer and activator of transcription 3 (STAT3) (Qui et al., 2005; Aaronson et al., 2002), have been shown to take place after injury. STAT3 usually appears in the cytoplasm in an inactive state. Only the binding of cytokines like interleukin 6 (Il6, Zhong et al., 1994), ciliary neurotrophic factor (CNTF, Rajan et al., 1996) or leukemia inhibitory factor (LIF, Kunisada et al., 1996) to their receptors leads to phosphorylation of the Janus kinase (JAK) and in turn the phosphorylation of STAT3 and thus its homodimerization. This activated form now is transported to the nucleus where it binds to DNA-response elements which activate the transcription of specific genes (Zhong et al., 1994) (Figure 6). The sustained activation of STAT3 has been shown to be a key requirement for the timely induction of the intrinsic growth program in the dorsal root ganglion (DRG, Bareyre et al., 2011). Further studies implicated an important role of STAT3 during neuronal growth initiation. For instance the nuclear accumulation and phosphorylation of STAT3 is correlated to the regenerative responses of the neuron after injury (Bareyre et al., 2011). Also deletion or inhibition this TF impairs the initiation of PNS regeneration (Bareyre et a., 2011) or blocks the growth promoting effect after a lesion in the CNS (Qiu et al., 2005). Also, STAT3 overexpression as well as the blockage of its inhibitor SOCS3, can improve sprouting of the central DRG projections (Bareyre et al., 2011).

Finally, the co-deletion of SOC3 and PTEN enables robust and sustained axonal regeneration via concurrent activation of mTOR and STAT3 in the retinal ganglion cells (RGCs) after crush injury (Sun et al., 2011).

These key findings after injury and its previously described role during the neuronal development, i.e. axon pathfinding, neurite outgrowth and glial cell differentiation (Dziennis and Alkayed, 2008, Gautron et al., 2006), give rise to STAT3 being a very good candidate to initiate the intrinsic growth program after SCI and thereby induce growth of newly born CST collaterals.

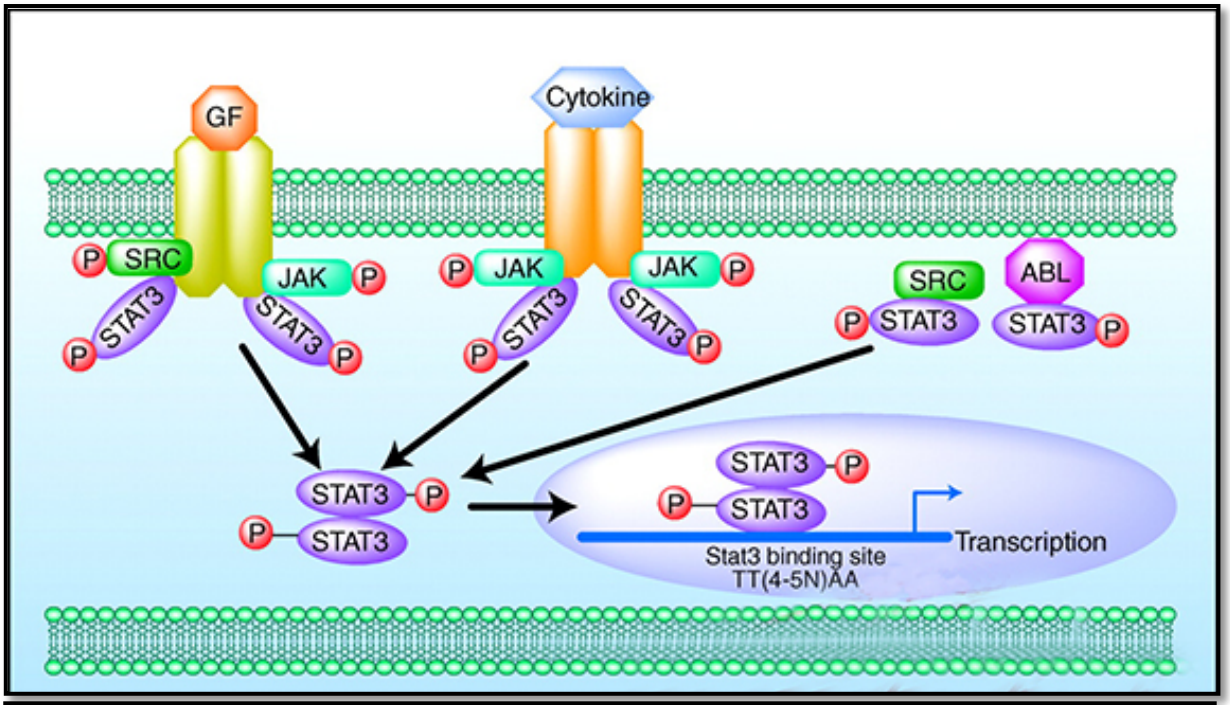

Figure 6: STAT3 Signaling Pathway. After binding of several cytokines (e.g., IL-6 receptor) to the JAK, Jak itself gets phosphorylated and thereby initiates the phosphorylation of STAT3. After STAT3 is phosphorylated on a tyrosine residue by activated tyrosine kinases in receptor complexes, it forms homodimers and heterodimers and translocates to the nucleus. In the nucleus, STAT3 dimers bind to specific promoter elements of target genes and regulate gene expression (Modified from Huang, 2007; Re-print permission from American Association for Cancer Research).

1.4.3.2 Fibroblast Growth Factors and their Receptors: Important Inducers for Presynaptic Differentiation

The family of fibroblast growth factors contains of 22 FGF's in human and mice and its four corresponding receptors (FGFR1 – FGFR4) (Figure 7a). The receptors are cell surface receptor tyrosine kinases (RTK's) with a transmembrane domain, an extracellular binding domain for the FGF's and an intracellular domain with its tyrosine kinase activity which interacts with intracellular signal transduction molecules (Böttcher and Niehrs, 2005). Binding of the FGF ligand to its receptors leads to dimerization of the receptor (Figure 7b) and downstream to the activation of the intracellular pathways such as the RAS/ MAPK pathway (Wang et al., 1996; Kouhara et al., 1997) or the PLCɣ/Ca^{2+} pathway (Hall et al., 1996; Doherty et al., 1996). Each receptor responds to only a certain subset of ligands (Zhang et al, 2006; Guillemot and Zimmer, 2011). The FGF10 family which also includes FGF7 and FGF22 binds specifically to FGF receptor 1 and 2 and has been shown to be involved in early synapse organization (Figure 7c, Fox et al., 2007). The importance of FGF22 for presynaptic differentiation during CNS development has also been shown by Umemori et al. in 2004. The authors purified putative target – derived presynaptic organizers from the developing mouse brain and identified FGF22 as the major active species. In additional experiments they could show that FGFR2bAP, a blocking protein which binds FGF22, inhibited presynaptic differentiation of mossy fibers in vitro and in vivo (Umemori et al., 2004). Also this paper points toward FGFR2b being the major receptor for FGF22 as experiments with the FGFR2c isoform do not show that effect on synapses. A couple of years later another publication could show even more precisely the involvement of the FGF10 family in presynaptic differentiation (Terauchi et al., 2010).

In this very nice study the authors show, that depending on which ligand binds to the receptor, either inhibitory (FGF7) or excitatory (FGF22) synapse formation in the CA3 region of the developing mouse hippocampus is induced (Figure 7d; Terauchi et al., 2010). To show this, they used Knock-out mice for either FGF7 or FGF22 and were able to demonstrate, that depending on which factor was missing, the inhibitory, GABAergic or excitatory, glutamatergic synapses showed deficits in clustering of synaptic vesicles (SV) in the pre-synapse and of VGAT or VGLUT1 labeling respectively. Also analyzing the excitatory or inhibitory postsynaptic currents in FGF22KO or FGF7KO showed decrease in frequency, indicating functional consequences of the change in the vesicle pools.

These three studies (Umemori et al, 2004; Fox et al., 2007; Terauchi et al., 2010) show the important role of the FGF10 family and their receptors in synaptogenesis during development thereby making them interesting candidates for studying their role in synapse formation during detour circuit formation after SCI.

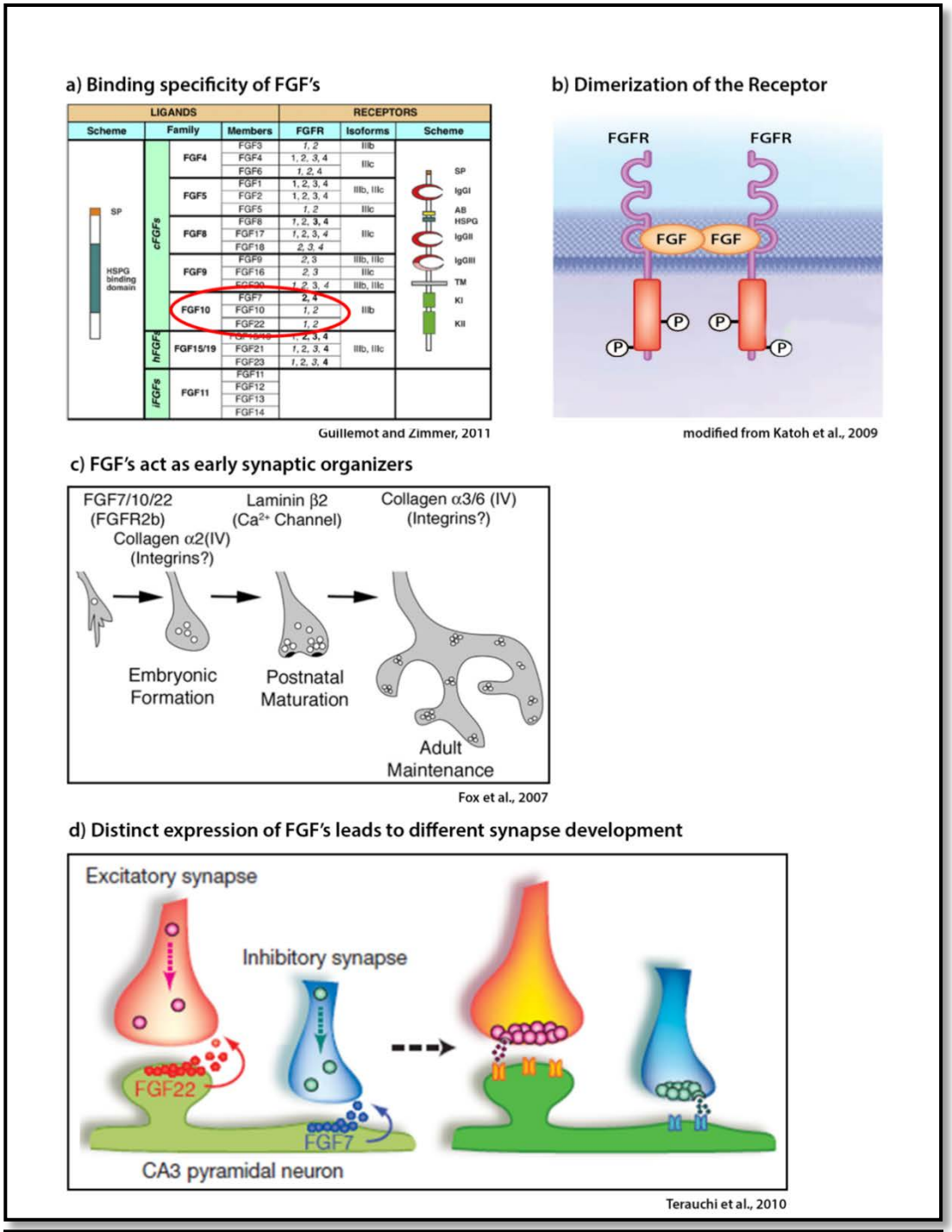

Figure 7. The FGF family involved in presynaptic differentiation. a) Structure and binding specificity of the different FGF's to the receptors. The FGF10 family (outlined in red) binds mainly to FGFR1 and 2. b) Binding of the ligand leads to dimerization and phosphorylation of the receptor and thereby to activation of the downstream pathways. c) Sequential expression of synaptic organizers. FGFs of the 7/10/22 subfamily act through FGFR2 to cluster synaptic vesicles in embryos. Additional molecules like Collagen a2, b2 laminins, Collagen a3 and a6 follow in the maturation process. d) Scheme of distinct synapse development. FGF22 induces excitatory, FGF7 inhibitory synapse development (Re-print permission from Elsevier for a and c; Re-print permission from Nature Publishing Group for b and d)

2. Aims of the Thesis

With the different studies of my thesis I am trying to gain more insight into the different aspects and phases of spinal cord injury induced detour circuit formation. In my thesis I will focus on the two phases of detour circuit formation and therefore asked the following questions:

1) Which factors are important inducers of axonal outgrowth during spinal remodeling?

In previous studies of our lab and in other studies it has been shown that STAT3 - a transcription factor which regulates the transcription of several growth promoting molecules (Zhong et al., 1994, Akira, 2000) – is important for initiation of peripheral nerves to regenerate (Bareyre et al., 2011) and for the initiation of axonal growth for regeneration in the CNS (Pernet et al., 2013). In the first aim of my thesis, I thought of investigating if STAT3 is also crucial for initiating the growth of the newly born CST collaterals during detour circuit formation. To test this, I specifically ablate STAT3 in the cells of layer V of the motorcortex (the origin of the fibers of the corticospinal tract in the spinal cord) and analyze if the deletion of STAT3 changes the pattern of axonal outgrowth of the collaterals after injury. In an additional set of experiments, I aim to overexpress STAT3 in CST fibers via gene therapy in the layer V neurons of the motorcortex. Deleting or overexpressing STAT3 in the CST allows us to specifically analyze the role of STAT3 in SCI induced axonal outgrowth.

2) Which axon guidance and synaptogenesis molecules could guide growing collaterals and induce synapse formation during detour circuit formation?

A lot of developmental studies have shown that for the precise growth and targeting onto specific neurons, certain axon guidance and synaptogenic molecules are needed (for review

see Kolodkin and Tessier-Lavigne, 2011 and Fox and Umemori, 2006). For instance, Netrins (Serafini et al., 1996), Slits (Lopez-Bendito et al., 2007) and Semaphorines (Behar et al., 1997) have been shown during development to guide axons to their target area and once the axon reached its target cell, synaptic molecules such as SynCAMs (Biederer et al., 2002), Neuroligins (Scheiffele et al., 2000) and molecules from the Ephrin family (for review see Klein, 2012) are important inducers for contact formation via pre- or postsynaptic differentiation during development. In the second aim of my thesis, I was investigating if some of these developmental cues are also expressed in the adult CNS and if so, whether they play an important role during spinal remodeling after SCI. To answer these questions I perform an *in situ* hybridization expression profile of the cues on different types of spinal interneurons such as excitatory short (SPSN) and long propriospinal neurons (LPSN) (retrogradely labeled) or inhibitory glycinergic interneurons (transgenetically labeled) in the cervical spinal cord of healthy and lesioned mice. The expression profile aims at helping to find interesting candidates for the establishment of the detour circuit formation.

3) Which role does the fibroblast growth factor 22 signaling play in the process of synapse formation during injury induced remodeling?

Developmental studies have shown that FGF22 and its receptors are important inducers of excitatory presynaptic differentiation, i.e. in the cerebellum (Umemori et al., 2004), in nerve terminals of motorneurons (Fox et al., 2007) or in the hippocampus (Terauchi et al., 2010). In the third aim of my thesis I was investigating if FGF22 and its receptors are important for synapse formation of the newly born CST collaterals onto the LPSN in the adult CNS after SCI. To test this, I specifically ablate FGFR1 and FGFR2 in the hindlimb CST (genetically or via gene therapy Figure 8a), or analyze the impact of the deletion of FGF22 (Figure 8b) on the detour circuit formation after injury.

These different approaches to suppress FGF22 signaling allow me to study its role specifically in synapse formation after injury induced remodeling.

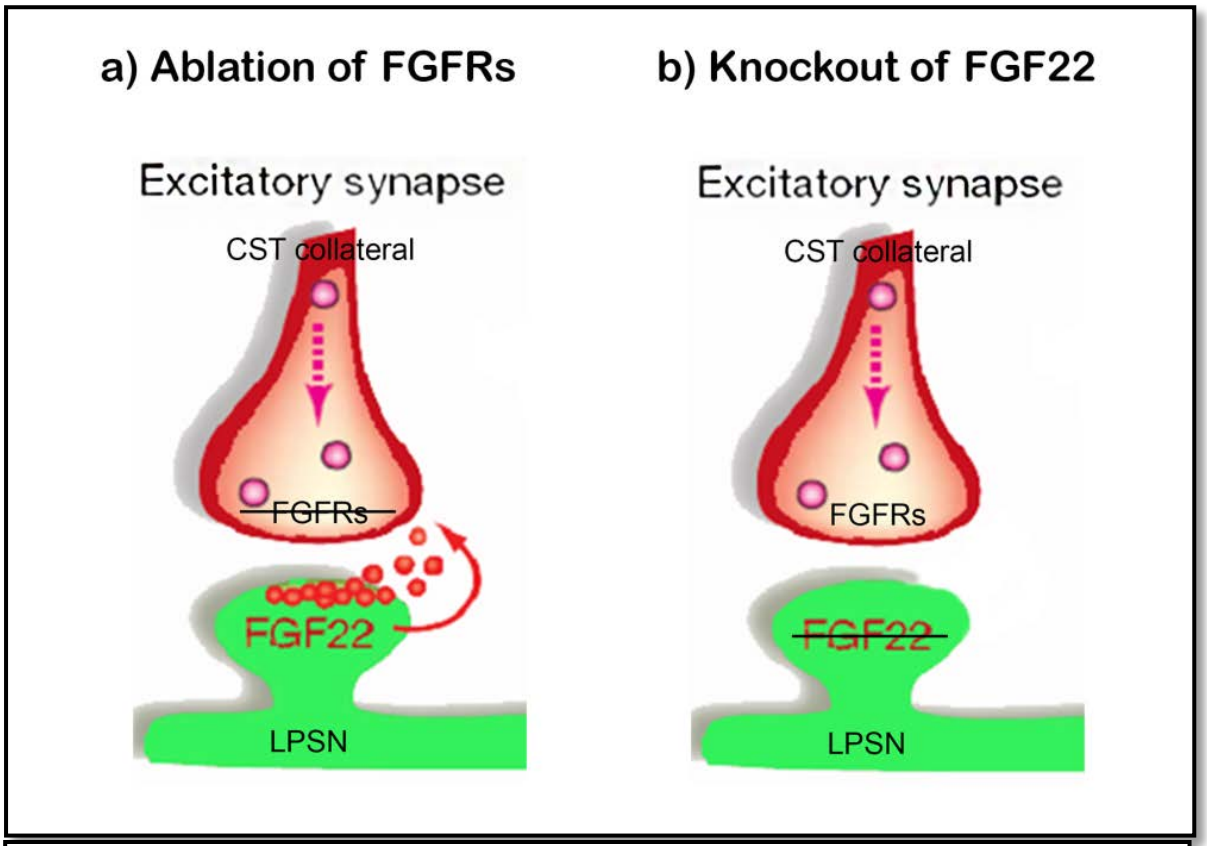

Figure 8: The different attempts of ablating FGF22 or its receptors in the adult spinal cord. a) Specific Knockout of FGFR1, FGFR2 or both at the same time in the axons of the hindlimb CST (red neuron). b) Full Knockout of FGF22 leads also to a loss of FGF22 in the LPSN (green neuron) of the cervical spinal cord. (Modified from Terauchi et al., 2010, Re-print permission from Nature Publishing Group)

3. Results

The work during this doctoral thesis has resulted in two peer-reviewed publications and one manuscript currently submitted to Nature Neuroscience for peer-review. They are included in this thesis and constitute Chapter III.

- Lang C, Bradley P, **Jacobi A**, Kerschensteiner M, Bareyre FM. (2013). STAT3 promotes corticospinal remodeling, regeneration and functional recovery after spinal cord injury. EMBO Rep 2013 Oct; 14(10):931-7.

- **Jacobi A**, Schmalz AM and Bareyre FM. (2014). Abundant Expression of Guidance and Synaptogenic Molecules in the Injured Spinal Cord. *PLoS One 2014 Feb 11;9(2):e88449*

- **Jacobi A**, Loy K, Schmalz AM, Hellsten M, Umemori H, Kerschensteiner M, Bareyre FM. (2014). FGF22 signaling regulates synapse formation during post injury remodeling of the spinal cord. *A manuscript to be submitted.*

LMU | KLINIKUM DER UNIVERSITÄT MÜNCHEN

INSTITUT FÜR KLINISCHE NEUROIMMUNOLOGIE
Hermann und Lilly Schilling Stiftung
in Assoziation mit der Neurologischen Klinik

Klinikum der Universität München · Institut für Klinische Neuroimmunologie
Marchioninistraße. 15 · 81377 München

To the

Dekanat der Fakultät für Biologie
Biozentrum
Großhaderner Str. 2

82152 Planegg-Martinsried

Prof. Dr. med. Martin Kerschensteiner

Telefon +49 (0)89 / 2180 – 78 282
Telefax +49 (0)89 / 2180 – 78 285
Martin.Kerschensteiner@med.uni-muenchen.de

http://www.klinikum.uni-muenchen.de/Institut-fuer-Klinische-Neuroimmunologie/de/index.html

Postanschrift:
Klinikum der Universität München
Forschungseinheit Therapieforschung
Marchioninistr. 17
D-81377 München

Ihr Zeichen	Unser Zeichen:	Munich 18.06.2014
xxxxxx	Ker:mso	

Re: Thesis of Anne Jacobi, author contributions

To whom it may concern,

The scientific work presented in the cumulative doctoral thesis entitled "**Identification and manipulation of molecules regulating of axonal outgrowth and synapse formation during post-injury axonal remodeling**" by **Anne Jacobi** has resulted in two peer-reviewed publications (1 first author and 1 co-author) and one manuscript which will be submitted in the close future (first author). All manuscripts are included in the thesis and constitute chapter 3. The contribution of Anne Jacobi - the author of the thesis - to each publication is listed as follows:

1) **STAT3 promotes corticospinal remodelling, regeneration and functional recovery after spinal cord injury**
   Lang C, Bradley P, **Jacobi A**, Kerschensteiner M, Bareyre FM
   An article published in EMBO Rep 2013 Oct; 14(10):931-7.

Anne Jacobi was responsible for several of the animal surgeries (specifically the spinal cord injuries, retrograde tracing of the CST) performed in this study. In addition, she was responsible for the tissue processing and evaluation for the analysis of the STAT3 expression in the cortex. This encompassed sacrificing the animals, dissecting and cutting the spinal tissue, performing the immunohistochemistry, (acquiring the images on a confocal microscope and image

processing – was performed by Claudia Lang) and performing data analysis. For this analysis Anne Jacobi dissected and processed the tissue (cutting and staining) and performed the confocal imaging of the experimental groups before and 3 weeks after lesion (the rest of the study was carried out by Claudia Lang). The other experiments and evaluations for this study have been carried out by Claudia Lang (as mentioned above) and Dr. Peter Bradley (who performed the electrophysiological recordings)

2) **Abundant Expression of Guidance and Synaptogenic Molecules in the Injured Spinal Cord**

Anne Jacobi, Anja Schmalz, Florence M Bareyre

An article published in PlosOne 9(2), e88449

For this study Anne Jacobi was responsible for all experimental procedures and data analysis. She performed all the surgeries (such as dorsal hemisection, anterograde and retrograde tracing of the CST and retrograde tracing of the propriospinal neurons), tissue processing, immunohistochemistry, and in situ hybridization and microscopy and evaluation for the experiments. Anja Schmalz helped performing in situ hybridizations and evaluations of the experiments.

3) **FGF22 signaling is necessary for correct post-injury spinal remodeling**

Jacobi A, Kristina Loy, Schmalz A, Umemori H, Kerschensteiner M, Bareyre FM.

A manuscript to be submitted to Nature Neuroscience in the next weeks (2014)

Anne Jacobi was responsible for the majority of all the experimental procedures and data analysis, such as all the surgeries (such as dorsal hemisection, anterograde and retrograde tracing of the CST and retrograde tracing of the propriospinal neurons), tissue processing, immunohistochemistry, in situ hybridizations, behavioural tests, microscopy and evaluations of the experiments. Exceptions are the CST maturation analysis (Suppl. Figure 3 and 4) that was performed by Anja Schmalz, and the behavioural tests and evaluations that Kristina Loy supported in performance and evaluation.

Anne Jacobi

Prof. Dr. Martin Kerschensteiner

3.1

STAT3 promotes corticospinal remodeling, regeneration and functional recovery after spinal cord injury

Lang C, Bradley P, **Jacobi A**, Kerschensteiner M, Bareyre FM

An article published in EMBO Reports (EMBO Rep 2013 Oct; 14(10):931-7)

EMBO reports

TRANSPARENT PROCESS

scientific report

STAT3 promotes corticospinal remodelling and functional recovery after spinal cord injury

Claudia Lang[1], *Peter M. Bradley*[1], *Anne Jacobi*[1], *Martin Kerschensteiner*[1,2+*] & *Florence M. Bareyre*[1,2++*]

[1]Institute of Clinical Neuroimmunology, Ludwig-Maximilians Universität, and [2]Munich Cluster for Systems Neurology (SyNergy), Munich, Germany

If and how neurons remodel their connections after CNS injury critically influences recovery of function. Here, we investigate the role of the growth-initiating transcription factor STAT3 during remodelling of the injured corticospinal tract (CST). Endogenous STAT3 expression in lesioned cortical projection neurons is transient but can be sustained by viral gene transfer. Sustained activation of STAT3 enhances remodelling of lesioned CST fibres and induces *de novo* formation of collaterals from unlesioned CST fibres. In a unilateral pyramidotomy paradigm, this recruitment of unlesioned fibres leads to the formation of midline crossing circuits that establish ipsilateral forelimb activation and functional recovery.

Keywords: axonal remodelling; corticospinal tract; neuronal plasticity; spinal cord injury; STAT3

EMBO *reports* (2013) **14**, 931–937. doi:10.1038/embor.2013.117

INTRODUCTION

Lesions to the spinal cord lead to the transection of axonal tract systems and are often followed by devastating motor and sensory deficits. If the lesion of the spinal cord is complete, severe deficits persist. If the lesion is however incomplete, some functional recovery can occur in rodents as well as humans [1–3]. Over the recent years, a number of studies have investigated the anatomical basis of this recovery process using the corticospinal tract (CST) as a model system [2,4,5]. The results show that while long-distance regeneration of transected CST fibres generally fails, lesioned CST connections spontaneously attempt to remodel after injury. We have previously identified intraspinal detour circuits that are formed by sprouting of CST collaterals in the cervical cord and the establishment of CST contacts onto long propriospinal neurons as key components of the endogenous remodelling process [2,6]. Despite the formation of these detour circuits, spontaneous functional recovery in most cases remains incomplete. To further improve functional recovery, we thus need to devise strategies that can extend endogenous remodelling.

How the induction of axonal remodelling is regulated and how it can best be therapeutically supported is so far incompletely understood. As axonal remodelling requires the reorganization of connections distant from the lesion site, strategies that affect the intrinsic growth capability of the entire neuron are conceptually most suited [7]. We have previously identified the sustained activation of the transcription factor STAT3 (signal transducer and activator of transcription 3) as a crucial requirement for the timely induction of the intrinsic growth programme in dorsal root ganglion neurons [8]. A key role for STAT3 during neuronal growth initiation is supported by the following findings: (i) The nuclear accumulation and phosphorylation of STAT3 correlate with the regenerative response of the neuron after injury [8,9]. (ii) Deletion of STAT3 impairs the timely initiation of PNS regeneration [8] and STAT3 inhibition blocks the growth-promoting effect of a conditioning lesion in the central nervous system [10]. (iii) STAT3 overexpression or the deletion of its inhibitor, SOCS3, can improve sprouting of central dorsal root ganglion projections [8] and promote optic nerve regeneration *in vivo* [11].

Here, we investigate whether and how growth initiation by STAT3 affects the remodelling of lesioned and unlesioned central nervous system axons and the resulting functional recovery after spinal cord injury.

RESULTS AND DISCUSSION

Endogenous STAT3 does not contribute to axonal remodelling

In the peripheral nervous system, the sustained expression and phosphorylation of STAT3 are crucial for the timely initiation of axonal outgrowth after lesion [8]. To examine whether STAT3 is also expressed and activated in lesioned cortical projection neurons, we investigated the expression of STAT3 and its activated phosphorylated form (p-STAT3) immunohistochemically in the hindlimb motor cortices of mice perfused at different timepoints from 6 h to 3 weeks following a dorsal mid thoracic hemisection. In unlesioned animals, only very few layer V pyramidal neurons in the motor cortex (that were identified on the basis of their typical morphology after NeuroTrace labelling) expressed either p-STAT3

[1]Institute of Clinical Neuroimmunology, Ludwig-Maximilians Universität, Marchioninistrasse 17, Munich 81377, Germany
[2]Munich Cluster for Systems Neurology (SyNergy), Munich, Germany
*These authors contributed equally to this work.
+Corresponding author. Tel: +49 89 2180 78282; Fax: +49 89 2180 78285; E-mail: martin.kerschensteiner@med.uni-muenchen.de
++Corresponding author. Tel: +49 89 2180 78279; Fax: +49 89 2180 78285; E-mail: florence.bareyre@med.uni-muenchen.de

Received 4 February 2013; revised 15 July 2013; accepted 16 July 2013; published online 9 August 2013

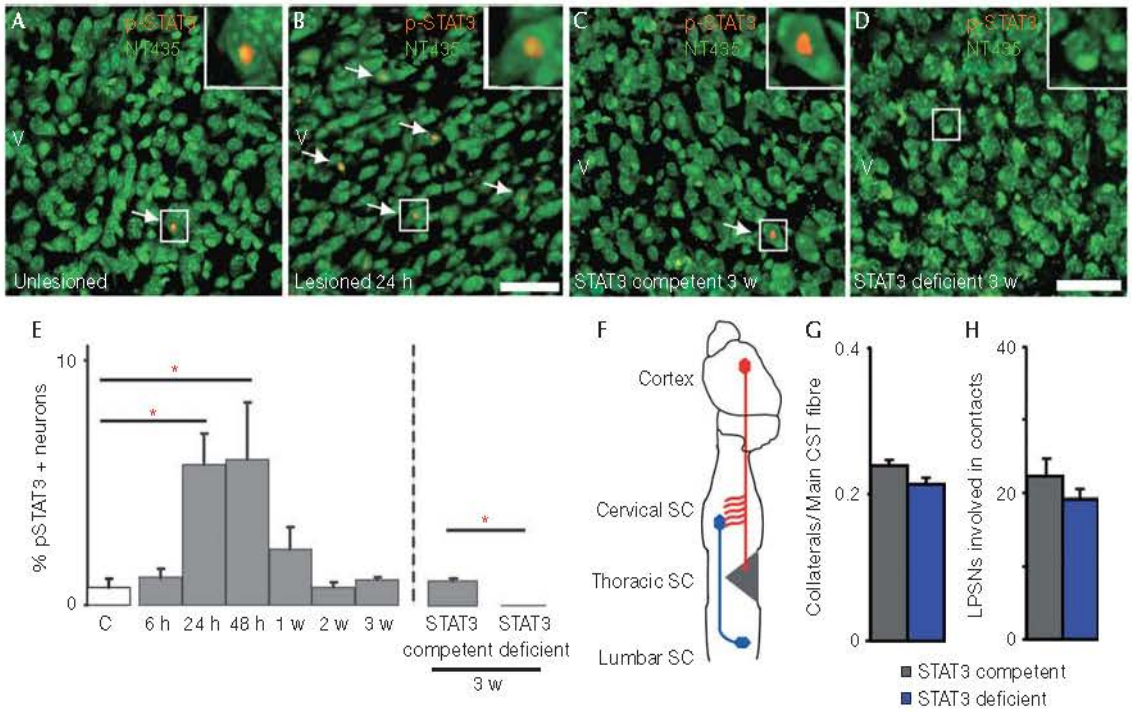

Fig 1 | Transient upregulation of p-STAT3 expression in cortical neurons does not contribute to endogenous CST remodelling after injury. (**A–D**) Confocal images of the expression of the activated form of STAT3, p-STAT3, in layer V cortical neurons (green, NeuroTrace 435; red, p-STAT3) of unlesioned (**A**), lesioned STAT3-competent (**B**, 24 h after lesion; **C**, 3 w after lesion) and STAT3-deficient mice (**D**). Arrows indicate p-STAT3-positive neurons (magnified in insets). (**E**) Quantification of p-STAT3 expression in layer V cortical neurons of unlesioned mice (white bar, $n = 5$) and mice perfused at different timepoints following thoracic hemisection (grey bars, STAT3-competent mice; blue bar, STAT3-deficient mice; $n = 5–6$ for each timepoint). (**F**) Schematic representation of the analysis of CST remodelling after a mid thoracic hemisection. (**G,H**) Quantification of axonal sprouting in the cervical spinal cord (**G**) and of the percentage of long propriospinal neurons contacted by CST fibres (**H**) in STAT3-competent (grey bars, $n = 9$) and STAT3-deficient (blue bars, $n = 12$) mice perfused 3 w following thoracic hemisection. All bars and error bars in this figure represent mean ± s.e.m. Statistical analysis was performed using a one-way ANOVA with Tukey test for E (left panel) and *t*-tests for E (right panel), G, H. $^*P < 0.05$. Scale bars equal 50 μm in B (also for A) and in D (also for C). ANOVA, analysis of variance; CST, corticospinal tract; SC, spinal cord; STAT3, signal transducer and activator of transcription 3.

(Fig 1A,E) or STAT3 (supplementary Fig S1 online). The number of p-STAT3-positive cortical projection neurons was then significantly increased at 24 h after lesion. However, even at this time, only a small subset of cortical projection neurons expressed STAT3 (supplementary Fig S1 online) or p-STAT3 (Fig 1B,E). Moreover, in these neurons, STAT3 expression and phosphorylation were only transiently induced and had returned to baseline levels at 1 week after injury (Fig 1E and supplementary Fig S1 online).

To assess whether those neurons that transiently expressed STAT3 are primarily responsible for endogenous attempts of axonal growth and remodelling, we selectively deleted STAT3 expression in cortical projection neurons. For this purpose, we crossed *Emx*-Cre mice, which express Cre recombinase in the forebrain [12], with $STAT3^{fl/fl}$ mice [13]. As expected, no STAT3 or p-STAT3 expressions are detected in cortical projection neurons of Cre-positive $STAT3^{fl/fl}$ mice (Fig 1C–E; supplementary Fig S1 online). Deletion of STAT3 did not appear to affect neuronal survival as similar densities of neurons were present in layer V of the motor cortex in Cre-positive and Cre-negative littermates (supplementary Fig S2 online). We then performed mid thoracic dorsal hemisections in STAT3-competent (Cre-negative) and conditional STAT3-deficient (Cre-positive) mice and examined the effects of STAT3 deletion on CST growth, remodelling and functional recovery. Our analysis revealed no differences between STAT3-competent and conditional STAT3-deficient mice in all parameters analysed (Fig 1F–H; supplementary Fig S3 online). In particular, we did not detect differences in the formation of intraspinal detour circuits as similar amounts of cervical collaterals formed at 1 week (supplementary Fig S3 online) and 3 weeks (Fig 1G) after injury, which did not differ in length, complexity and number of boutons (data not shown) and contacted similar proportions of long propriospinal neurons (Fig 1H). Consistent with these observations, no differences in the recovery of hindlimb locomotion were detected between STAT3-competent and conditional STAT3-deficient mice (supplementary Fig S4 online). These results show that the transient expression of STAT3 in cortical projection neurons is unlikely to contribute to the induction of the endogenous remodelling processes.

STAT3 enhances sprouting of lesioned CST fibres

As the transient induction of STAT3 expression in a subset of cortical neurons after central lesions is thus insufficient to induce a robust neuronal growth response, we next investigated whether the exogenous induction of sustained STAT3 expression would be sufficient to promote axonal growth. To induce sustained STAT3

expression in cortical neurons, we injected recombinant adeno-associated viruses (rAAV) expressing STAT3 into the hindlimb motor cortex. Immunohistochemical analysis of STAT3 expression and phosphorylation confirmed the efficiency of viral gene transfer to corticospinal projection neurons (Fig 2A–E). To assess the effect of sustained STAT3 expression on the response of lesioned CST fibres, we injected rAAV-STAT3 or Control rAAV into the hindlimb motor cortex and lesioned the main dorsal and the minor dorsolateral component of the CST by a mid thoracic dorsal hemisection. Our results show that while sustained STAT3 expression did not affect lesion volume ($0.307 \pm 0.02\,mm^3$ versus $0.316 \pm 0.03\,mm^3$ in mice injected with Control rAAV and rAAV-STAT3 respectively, $n=7$ mice per group) it significantly increased CST sprouting at the lesion site and moderately improved axonal growth beyond the lesion site (supplementary Fig S5 online). To assess to what extent sustained STAT3 expression can also support the remodelling of CST fibres distant from the lesion site, we quantified the formation of intraspinal detour circuits [2] after mid thoracic hemisections in mice injected with rAAV-STAT3 and Control rAAV. Indeed mice injected with rAAV-STAT3 showed an increased formation of cervical CST collaterals at 3 weeks after injury (Fig 2F–I). The intraspinal contact pattern of these collaterals, however, was not affected by this rather moderate increase in collateral number and a similar proportion of long propriospinal neurons were contacted in mice injected with rAAV-STAT3 and Control rAAV (Fig 2J). Taken together, this suggests that the endogenous growth response of lesioned CST projection neurons is sufficient to promote the formation of detour circuits at an 'optimal' rate that is not improved further by the presence of more CST collaterals. We noted, however, that unlesioned mice injected with rAAV-STAT3 showed a marked increase in the formation of cervical collaterals (Fig 2K–N) that resulted in a significantly higher number of contacts onto the long propriospinal neurons (Fig 2O). This indicated that sustained STAT3 expression might be able to also induce the remodelling of fibres that have not been primed to grow by their previous transection.

STAT3 recruits unlesioned CST connections

To further investigate the capability of STAT3 to recruit unlesioned fibres to the remodelling process, we induced a unilateral lesion of the left CST at the level of the medulla oblongata ('unilateral pyramidotomy,' Fig 3A). We then assessed whether and how unlesioned fibres from the contralateral, right forelimb portion of the CST remodel in response to the unilateral denervation. In animals injected with Control rAAV, no significant difference in the number of CST fibres that exited the right CST is detected at 1, 3 or 12 weeks after pyramidotomy (Fig 3B,E). Further, CST fibres that exit the CST rarely crossed the spinal midline (Fig 3B,F). In contrast, in animals injected with rAAV-STAT3, more CST collaterals exited the CST at 3 weeks after injury (Fig 3C,E). These newly formed collaterals extended towards the denervated side of the spinal cord resulting in a significant increase in the number of midline crossing fibres that was first detected at 3 weeks (Fig 3C,F) and persisted for at least 12 weeks after lesion (Fig 3D,F). We next examined the projection pattern of these newly formed midline crossing CST collaterals and found that in animals injected with rAAV-STAT3, CST collaterals extended significantly further into the denervated spinal cord and often projected to the intermediate and ventral laminae of the spinal cord (Fig 3G,H). As the cell bodies of short propriospinal neurons and spinal motoneurons that control forelimb movement are located in these laminae, we next labelled these cell populations using retrograde tracing and assessed whether they are targeted by midline crossing CST collaterals at 12 weeks after pyramidotomy. Our results show that the proportions of short propriospinal neurons and spinal motoneurons that are contacted by CST collaterals are increased more than 4- and 10-fold, respectively in animals injected with rAAV-STAT3 (Fig 3I–L). The finding that neuronal growth initiation by STAT3 is sufficient to induce the *de novo* formation of these midline crossing circuits indicates that the guidance signals that attract newly formed collaterals are endogenously present in the denervated spinal cord. It is interesting to note in this context that sustained STAT3 expression is not the only way to induce the remodelling of unlesioned CST fibres. Indeed previous studies have, for example, shown that the overexpression of the neuronal calcium sensor1 in projection neurons [14], or of neurotrophin 3 in the spinal target area [15] can induce sprouting and midline crossing of unlesioned CST fibres. Notably, a recent study further indicates that in primates, the CST can spontaneously extend midline crossing collaterals after spinal cord injury [16].

Midline crossing circuits improve functional recovery

To investigate whether the newly formed midline crossing CST circuits induced by sustained STAT3 expression can foster functional recovery, we performed the following analyses after unilateral pyramidotomy. First, we used the staircase test, which measures the capability of mice to remove sugar pellets placed on different stairs of a staircase, to evaluate skilled forelimb grasping as previously described [17]. While mice from both experimental groups showed similarly impaired forelimb grasping immediately after injury, mice injected with rAAV-STAT3 performed significantly better in the staircase reaching task compared with mice injected with Control rAAV from 5 weeks after pyramidotomy onwards (Fig 4A,B). To assess the contribution of midline crossing circuits to this recovery, we followed the recovery process for 10 weeks and then lesioned the contralateral CST on the level of the pyramids. This lesion removes all midline crossing CST connections and leads to a complete reversal of functional recovery (Fig 4B). To further confirm the contribution of midline crossing circuits to functional recovery, we recorded forelimb flexor electromyographs (EMGs) after intracortical stimulations (Fig 4C,D) [4]. In unlesioned animals, EMG responses could be elicited in 100% of the cases by stimulation of the contralateral forelimb motor cortex ($n=24$ stimulations, Fig 4E). In the days following pyramidotomy, this response was basically abolished (Fig 4E). However at 12 weeks following pyramidotomy, nearly all sites in the ipsilateral cortex of animals treated with rAAV-STAT3 elicited EMG responses (Fig 4E). This finding is consistent with the idea that newly formed midline crossing CST fibres mediate this recovery. To confirm the contribution of new CST connections below the level of the pyramids to the recovery, we performed an additional pyramidotomy of the intact side in rAAV-STAT3-treated mice that had previously recovered responsiveness to stimulation. In these mice, the second pyramidotomy completely abolishes the response to cortical stimulation (Fig 4E). Further analysis of the cortical stimulation parameters revealed lower stimulation thres-

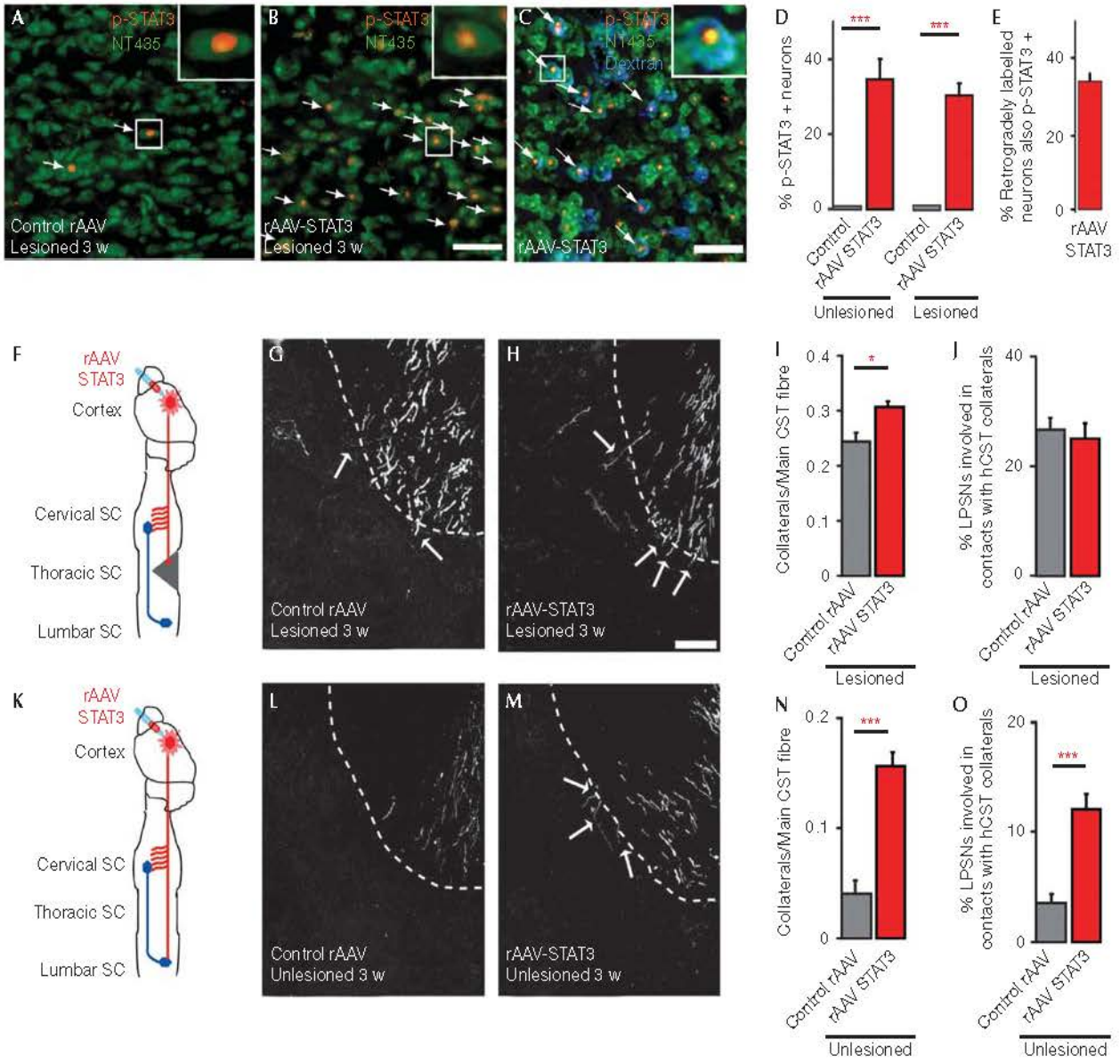

Fig 2 | Sustained STAT3 expression induces sprouting of lesioned and unlesioned fibres in the cervical spinal cord following injury. (A,B) Confocal images of p-STAT3 expression in layer V cortical neurons (green, NeuroTrace 435; red, p-STAT3) of mice injected with Control rAAV (A) or rAAV-STAT3 (B) and perfused 3 w following a mid thoracic hemisection. Arrows indicate p-STAT3-positive neurons (magnified in insets). (C) Confocal images of p-STAT3 expression in hindlimb CST projection neurons that were retrogradely labelled from the lesion site (blue, neurons retrogradely labelled with dextran tetramethylrhodamine; green, NeuroTrace 435; red, p-STAT3) in mice injected with rAAV-STAT3 and perfused 3 w following a mid thoracic hemisection. (D) Quantification of p-STAT3 expression in layer V neurons in the transduced area of the hindlimb motor cortex of unlesioned mice (left panel) either untreated (C same as in Fig 1E) or injected with rAAV-STAT3 (red bar) and lesioned mice (right panel, perfused 3 w after injury) injected with Control rAAV (grey bar) or rAAV-STAT3 (red bar, $n = 3$–5 mice per group). (E) Quantification of p-STAT3 expression in hindlimb CST projection neurons that were retrogradely labelled from the lesion site in mice injected with rAAV-STAT3 ($n = 4$). (F) Schematic representation of the analysis of cervical CST sprouting and remodelling following a mid thoracic spinal cord injury. (G,H) Confocal images of cervical hindlimb CST collaterals in lesioned mice injected with Control rAAV (G) or rAAV-STAT3 (H) and perfused 3 w following injury. Arrows indicate collaterals as they exit into the grey matter. (I,J) Quantification of the number of collaterals exiting the hindlimb CST in the cervical spinal cord (I) and of the percentage of long propriospinal neurons contacted by CST fibres (J) in mice injected with Control rAAV (grey bars, $n = 9$) or rAAV-STAT3 (red bars, $n = 9$) 3 w following spinal cord injury. (K) Schematic representation of the analysis of cervical CST sprouting and remodelling in unlesioned mice. (L,M) Confocal images of cervical hindlimb CST collaterals in unlesioned mice injected with Control rAAV (L) or rAAV-STAT3 (M). (N,O) Quantification of the number of collaterals exiting the hindlimb CST in the cervical spinal cord (N) and of the percentage of long propriospinal neurons contacted by CST fibres (O) in unlesioned mice injected with Control rAAV (grey bars, $n = 5$) or rAAV-STAT3 (red bars, $n = 8$). All bars and error bars in this figure represent mean ± s.e.m. Statistical analysis was performed using *t*-tests. $^*P < 0.05$; $^{***}P < 0.001$. Scale bar equals 50 μm in B (also for A), 25 μm in C and 50 μm in H (also for G,L,M). CST, corticospinal tract; rAAV, recombinant adeno-associated viruses; SC, spinal cord; STAT3, signal transducer and activator of transcription 3.

scientific report

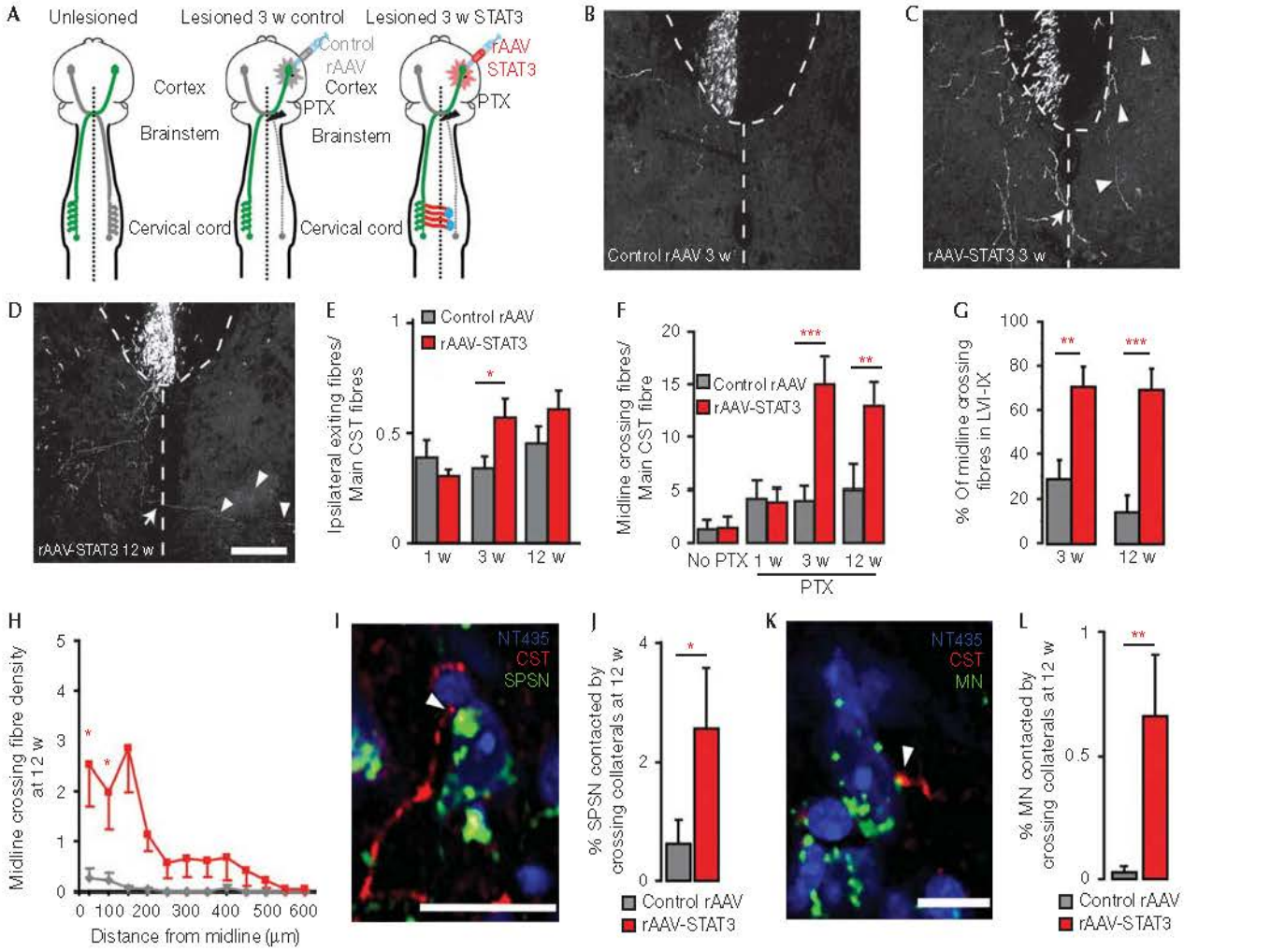

Fig 3 | Sustained STAT3 expression induces *de novo* formation of midline crossing circuits following pyramidotomy. (A) Schematic representation of the analysis of CST remodelling after unilateral pyramidotomy and injection of Control rAAV or rAAV-STAT3. (B–D) Confocal images of midline crossing fibres in mice injected with Control rAAV (B) or rAAV-STAT3 (C,D) and perfused 3 w (B,C) or 12 w (D) following pyramidotomy. Arrows indicate midline crossing fibres, arrowheads indicate examples of fibres that have already crossed the midline. (E,F) Quantification of the number of fibres exiting ipsilateral to the pyramidotomy from the main CST (E) and crossing the spinal midline (F) in mice injected with Control rAAV (grey bars) or rAAV-STAT3 (red bars) and perfused 1, 3 or 12 w ($n = 7$–10 mice per group) following pyramidotomy. (G) Quantification of the percentage of midline crossing fibres that project to the contralateral (denervated) laminae VI to IX in mice injected with Control rAAV (grey bars) or rAAV-STAT3 (red bars) and perfused 3 or 12 w following pyramidotomy ($n = 7$–10 mice per group). (H) Quantification of the density of midline crossing fibres in the contralateral (denervated) side of the spinal cord at different distances from the midline in mice injected with Control rAAV (grey line) or rAAV-STAT3 (red line) and perfused 12 w following pyramidotomy ($n = 7$–8 mice per group). (I,K) Confocal images (single planes) of contacts between midline crossing forelimb CST collaterals (red) and a short propriospinal neuron (I, green) or a motoneuron (K, green) in mice injected with rAAV-STAT3 and perfused 12 w following the pyramidotomy. (J,L) Quantification of the percentage of short propriospinal neurons (J) and motoneurons (L) contacted by midline crossing forelimb CST collaterals in mice injected with Control rAAV (grey bars) or rAAV-STAT3 (red bars) and perfused 12 w following injury ($n = 7$–8 mice per group). All bars and error bars in this figure represent mean ± s.e.m. Statistical analysis was performed using a two-way ANOVA followed by Bonferroni test for E–G, and a one-way repeated ANOVA followed by Tukey test in H and *t*-tests for J, L. $^{*}P < 0.05$; $^{**}P < 0.01$; $^{***}P < 0.001$. Scale bars equal 200 µm in D (also for B,C) and 25 µm in I and 10 µm in K. ANOVA, analysis of variance; CST, corticospinal tract; rAAV, recombinant adeno-associated viruses; SC, spinal cord; STAT3, signal transducer and activator of transcription 3.

holds and shorter latencies to an EMG response in mice 12 weeks after injection with rAAV-STAT3 compared with mice injected with Control rAAV (Fig 4F,G).

Taken together, our electrophysiological and behavioural analyses indicate that the midline crossing CST circuits induced by sustained expression of STAT3 are functional and contribute to improved recovery of forelimb function after injury. While the viral gene transfer strategy used in this study is not directly translatable to a clinical setting as treatment was initiated before injury, we believe that strategies that enhance endogenous remodelling processes have considerable therapeutic potential. This has been documented by a number of recent studies in rodents [18,19] as well as first reports in humans [20]. The recruitment of unlesioned fibres to the remodelling process, for

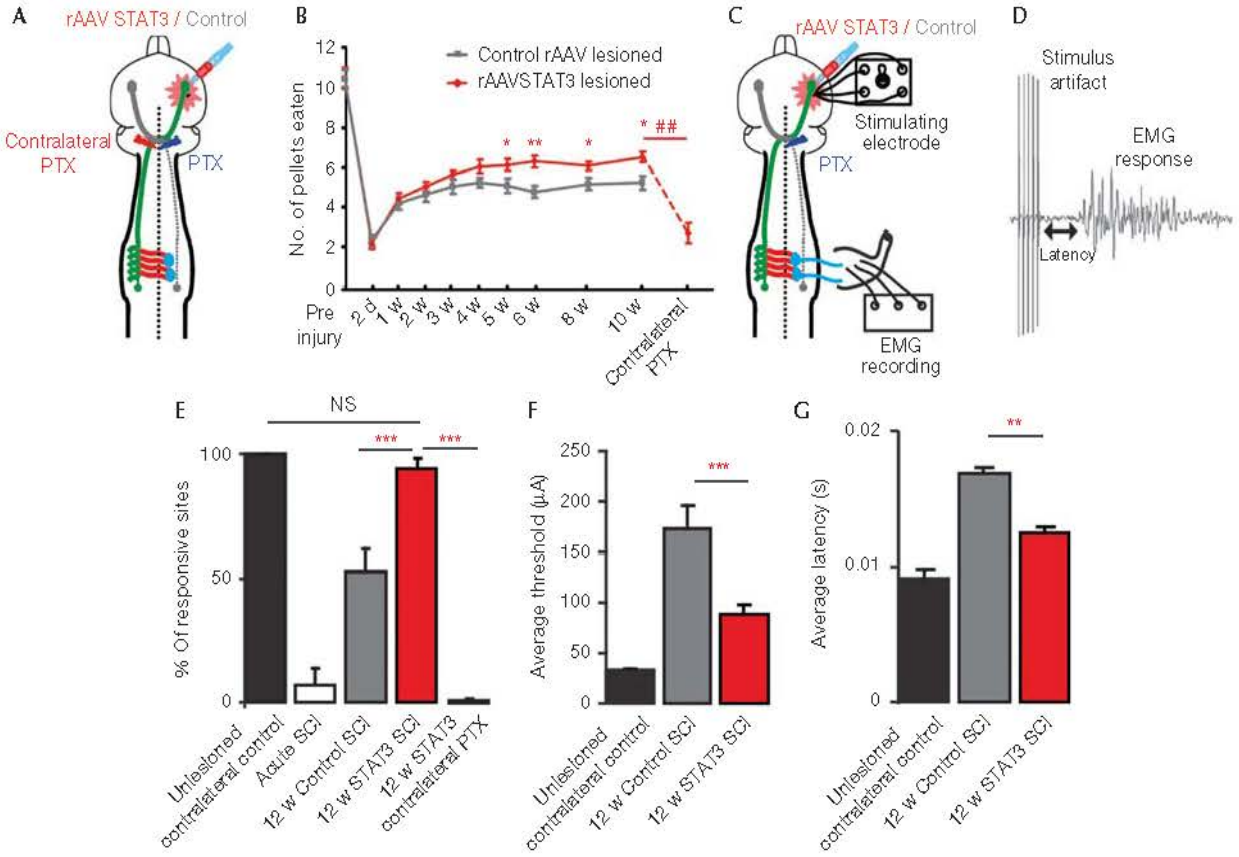

Fig 4 | Sustained STAT3 expression promotes functional recovery following pyramidotomy. (**A**) Schematic representation of the pyramidotomy paradigm used for assessing behavioural recovery. (**B**) Quantification of the number of pellets eaten by mice injected with Control rAAV (grey line, $n=23$) or rAAV-STAT3 (red line, $n=28$) at different test intervals up to 10 w following pyramidotomy and at 3 days following lesion of the contralateral CST tract (contralateral PTX, $n=13$). (**C**) Schematic representation of the cortical stimulations and EMG recordings that we used to quantify circuit reconnection after pyramidotomy. (**D**) Trace of a forelimb EMG recording after cortical stimulation. (**E**) Quantification of the percentage of responsive sites contralateral to the lesion in unlesioned mice (black bar, $n=6$ mice) and ipsilateral to the lesion acutely following pyramidotomy (white bar) and 12 w following pyramidotomy in mice injected with Control rAAV (grey bar) or rAAV-STAT3 (red bar, $n=6$–8 mice per group). A contralateral pyramidotomy 12 w following the initial lesion and injection of rAAV-STAT3 abolishes the ipsilateral responses (red bar, contralateral PTX; $n=5$ mice). (**F**,**G**) Quantification of the stimulation thresholds (F) and latencies (G) of the forelimb responses in unlesioned mice (black bars, contralateral to lesion) in mice injected with Control rAAV (grey bars, ipsilateral to the lesion) or rAAV-STAT3 (red bars, ipsilateral to the lesion) at 12 w following pyramidotomy ($n=5$–8 mice per group). All bars and error bars in this figure represent mean ± s.e.m. Statistical analysis was performed using a repeated one-way ANOVA followed by Tukey test in B and a one-way ANOVA followed by Tukey test in E, F, G. $^{*}P<0.05$; $^{**}P<0.01$; $^{***}P<0.001$. $^{\#\#}P<0.01$ 10 w re-lesion vs 10 w. ANOVA, analysis of variance; CST, corticospinal tract; EMG, electromyography; SCI, spinal cord injury; STAT3, signal transducer and activator of transcription 3.

example, by induction of sustained STAT3 expression, should thus be a promising complement to these strategies and help advance therapeutic concepts that improve functional recovery in neurological conditions in which trauma, inflammation or ischaemia cause permanent axon damage.

METHODS

Animals. To delete STAT3 expression in cortical projection neurons, we crossed $STAT3^{fl/fl}$ mice [13], in which deletion of the *STAT3* gene depends on Cre-mediated excision of loxP sites, and *Emx*-Cre mice [12], in which regulatory elements of the *Emx1* gene drive Cre expression in the forebrain starting at E12.5. Adult female mice homozygous for the floxed *STAT3* allele and either expressing Cre (STAT3-deficient group) or Cre-negative (STAT3-competent group) were used for experiments. For all other experiments, we used adult female C57/Bl6 mice (6–12 weeks old). All animal experiments were performed in accordance with regulations of the animal welfare act and protocols approved by the Regierung von Oberbayern. For further methods, see supplementary information online.

Supplementary information is available at EMBO *reports* online (http://www.emboreports.org).

ACKNOWLEDGEMENTS

We thank A. Schmalz and G. Heitmann for excellent technical assistance, D. Matzek for animal husbandry, S. McMullan for helpful advice on EMG recordings and S. Akira for providing the $STAT3^{fl/fl}$ mice. Work in F.M.B's lab is supported by the Deutsche Forschungsgemeinschaft (SFB 870) and by the Federal Ministry of Education and Research (BMBF, Independent Groups in the Neurosciences). Work in M.K.'s lab is supported by the DFG (SFB 870 and SFB-Tr 128), the BMBF (Competence Network Multiple Sclerosis), the European Research Council under the

European Union's Seventh Framework Program (FP/2007-2013; ERC Grant Agreement n. 310932), the Hertie Foundation and the Verein 'Therapieforschung für MS-Kranke e.V.'

Author contributions: M.K. and F.M.B. conceived the experiments. C.L. performed the analysis of axon growth, remodelling and behavioural recovery. C.L. and A.J. performed and evaluated immunohistochemistry experiments. P.M.B. conducted the electrophysiological analysis. C.L, P.M.B., M.K. and F.M.B. wrote the paper.

CONFLICT OF INTEREST

The authors declare that they have no conflict of interest.

REFERENCES

1. Dietz V, Wirz M, Colombo G, Curt A (1998) Locomotor capacity and recovery of spinal cord function in paraplegic patients: a clinical and electrophysiological evaluation. *Electroencephalogr Clin Neurophysiol* **109:** 140–153
2. Bareyre FM, Kerschensteiner M, Raineteau O, Mettenleiter TC, Weinmann O, Schwab ME (2004) The injured spinal cord spontaneously forms a new intraspinal circuit in adult rats. *Nat Neurosci* **7:** 269–277
3. Courtine G, Song B, Roy RR, Zhong H, Herrmann JE, Ao Y, Qi J, Edgerton VR, Sofroniew MV (2008) Recovery of supraspinal control of stepping via indirect propriospinal relay connections after spinal cord injury. *Nat Med* **14:** 69–74
4. Fouad K, Pedersen V, Schwab ME, Brösamle C (2001) Cervical sprouting of corticospinal fibers after thoracic spinal cord injury accompanies shifts in evoked motor responses. *Curr Biol* **11:** 1766–1770
5. Weidner N, Ner A, Salimi N, Tuszynski MH (2001) Spontaneous corticospinal axonal plasticity and functional recovery after adult central nervous system injury. *Proc Natl Acad Sci USA* **98:** 3513–3518
6. Lang C, Guo X, Kerschensteiner M, Bareyre FM (2012) Single collateral reconstructions reveal distinct phases of corticospinal remodeling after spinal cord injury. *PLoS One* **7:** e30461
7. Liu K, Tedeschi A, Park KK, He Z (2011) Neuronal intrinsic mechanisms of axon regeneration. *Annu Rev Neurosci* **34:** 131–152
8. Bareyre FM, Garzorz N, Lang C, Misgeld T, Büning H, Kerschensteiner M (2011) *In vivo* imaging reveals a phase-specific role of STAT3 during central and peripheral nervous system axon regeneration. *Proc Natl Acad Sci USA* **108:** 6282–6287
9. Shin JE, Cho Y, Beirowski B, Milbrandt J, Cavalli V, DiAntonio A (2012) Dual leucine zipper kinase is required for retrograde signalling and axonal regeneration. *Neuron* **74:** 1015–1022
10. Qiu J, Cafferty WBJ, McMahon SB, Thompson SWN (2005) Conditioning injury-induced spinal axon regeneration requires signal transducer and activator of transcription 3 activation. *J Neurosci* **25:** 1645–1653
11. Sun F *et al* (2011) Sustained axon regeneration induced by co-deletion of PTEN and SOCS3. *Nature* **480:** 372–375
12. Gorski JA, Talley T, Qiu M, Puelles L, Rubenstein JL, Jones KR (2002) Cortical excitatory neurons and glia, but not GABAergic neurons, are produced in the Emx1-expressing lineage. *J Neurosci* **22:** 6309–6314
13. Matsukawa A, Takeda K, Kudo S, Maeda T, Kagayama M, Akira S (2003) Aberrant inflammation and lethality to septic peritonitis in mice lacking STAT3 in macrophages and neutrophils. *J Immunol* **171:** 6198–6205
14. Yip PK, Wong LF, Sears TA, Yáñez-Muñoz RJ, McMahon SB (2010) Cortical overexpression of neuronal calcium sensor-1 induces functional plasticity in spinal cord following unilateral pyramidal tract injury in rat. *PLoS Biol* **8:** e1000399
15. Zhou L, Baumgartner BJ, Hill-Felberg SJ, McGowen LR, Shine HD (2003) Neurotrophin-3 expressed in situ induces axonal plasticity in the adult injured spinal cord. *J Neurosci* **23:** 1424–1431
16. Rosenzweig ES *et al* (2010) Extensive spontaneous plasticity of corticospinal projections after primate spinal cord injury. *Nat Neurosci* **13:** 1505–1510
17. Starkey ML, Barritt AW, Yip PK, Davies M, Hamers FPT, McMahon SB, Bradbury EJ (2005) Assessing behavioural function following a pyramidotomy lesion of the corticospinal tract in adult mice. *Exp Neurol* **195:** 524–539
18. Girgis J, Merrett D, Kirkland S, Metz GAS, Verge V, Fouad K (2007) Reaching training in rats with spinal cord injury promotes plasticity and task specific recovery. *Brain* **130:** 2993–3003
19. van den Brand R *et al* (2012) Restoring voluntary control of locomotion after paralyzing spinal cord injury. *Science* **336:** 1182–1185
20. Harkema S *et al* (2011) Effect of epidural stimulation of the lumbosacral spinal cord on voluntary movement, standing, and assisted stepping after motor complete paraplegia: a case study. *Lancet* **377:** 1938–1947

SUPPLEMENTARY INFORMATION

STAT3 promotes corticospinal remodeling and functional recovery after spinal cord injury

Claudia Lang[1], Peter M. Bradley[1], Anne Jacobi[1], Martin Kerschensteiner[1,2]* and Florence M. Bareyre[1,2]*

[1] Institute of Clinical Neuroimmunology, Ludwig-Maximilians Universität, Munich, Germany

[2] Munich Cluster for Systems Neurology (SyNergy), Munich, Germany

* equal contribution

SUPPLEMENTARY METHODS

Generation and production of AAV vectors

rAAV-STAT3 and Control rAAV were cloned and produced as previously described [1,2]. Briefly, for engineering pAAV-STAT3, the STAT3 gene was excised from pcDNA3 STAT3 (Addgene plasmid 8706) with BamHI and XhoI and cloned into the pAAV-MCS vector (Stratagene) at the HincII site. Control pAAV-ECFP was engineered by excising the ECFP gene from the pECFP N1 plasmid at BamHI and NotI and then it was cloned into the pAAV-MCS at the HincII site. Control pAAV-mbEYFP was constructed by excising the EYFP gene from an engineered pmbEYFP N1 plasmid at XhoI and NotI and then it was cloned into the pAAV-MCS at the BmgBI site.

Genomic titers were as follows: rAAV-STAT3, 9 $\times 10^{12}$ genome copies/ml; Control rAAV-ECFP, 9.2 $\times$ 10^{12} genome copies/ml; Control rAAV-mbEYFP, 1.7 x 10^{11} genome copies/ml. One microliter of undiluted rAAV solution was injected in all experiments.

Surgical procedures

Midthoracic hemisection, labeling of the hindlimb CST (hCST) fibers and long propriospinal neurons: Mice were anesthetized with a subcutaneous injection of ketamin/xylazine (ketamine 100 mg/kg, xylazine 13 mg/kg). After a laminectomy at thoracic level 8 (T8), a midthoracic dorsal hemisection, which results in a transection of the main dorsal and minor dorso-lateral CST component, was performed with fine iridectomy scissors. The lesion extent was assessed on spinal cord cross sections spanning the thoracic lesion site. Following staining with a fluorescent Nissl dye (NT435, dilution 1:500) the sections were scanned using an Olympus FV1000 confocal microscope. Image stacks were then processed with ImageJ and the lesion area, including both the cavity and surrounding damaged tissue, was outlined. To quantify the lesion volume, the measured lesion area of each section was multiplied by the section

thickness (50µm) and the results of consecutive sections spanning the entire lesion extension were summed up for each animal to provide a final estimation of the total lesion volume. Prior to and after surgery animals were administered Meloxicam (Metacam, Boehringer Ingelheim) once per day for 2 days. One week prior to the lesion, 1µl of rAAV-STAT3 or control rAAV-ECFP was pressure-injected into the hindlimb motor cortex using a finely pulled glass micropipette (coordinates from bregma: -1.0mm caudal; 0.8mm lateral; 0.6mm depth). The hindlimb CST was traced using 1µl of a 10% (in 0.1M PB) solution of biotinylated dextran amine (BDA, 10 000 MW, Life technologies) two weeks prior to sacrifice date using the coordinates: −1.3 mm posterior to bregma, 1 mm lateral to bregma, 0.6mm depth as previously described [3]. Long propriospinal neurons were then retrogradely traced by pressure injections of 1µl of 10% fluoroemerald (dextran, fluorescein, 10 000 MW, Life technologies) into each side of the spinal cord at thoracic level 12 as previously described for rats [4]. Mice were sacrificed 1, 3 or 12 weeks after dorsal hemisection.

Pyramidotomy, labeling of the forelimb CST fibers, short propriospinal neurons and motoneurons: A unilateral lesion of the CST at the level of the pyramidal decussation was performed using a ventral approach as previously described for rats [5]. Briefly, the left medullary pyramid was exposed through an opening of the occipital bone. A unilateral lesion of the left CST rostral to the decussation was made with a fine (tungsten) metal wire using the basilar artery as a landmark for the midline. The extent of the lesion was verified in all cases by histological analysis of the lesion site in Nissl-stained tissue sections. Mice were left to recover on a warming blanket until they regained consciousness. Prior to and after surgery animals were administered meloxicam (Metacam, Boehringer Ingelheim) once per day for 2 days. One week prior to the lesion, 1µl of rAAV-STAT3 or rAAV-mbYFP was injected into the right forelimb motor cortex using a fine pulled glass micropipette (coordinates from

bregma: -0.6mm caudal, 1mm lateral, 0.7mm depth). One µl of a 10% (in 0.1M PB) solution of biotinylated dextran amine (BDA, 10 000 MW, Life technologies) was used to trace the right intact CST one week prior to sacrifice date (coordinates from bregma: -0.6mm caudal, 1mm lateral, 0.7mm depth). Short propriospinal neurons were then retrogradely traced by pressure injections of 1µl fluoroemerald into each side of the spinal cord at thoracic level 1/2 as previously described [4]. Motoneurons were retrogradely labeled from the forelimb muscles using 1µl Cholera Toxin Alexa Fluor 647 (Life technologies) injected with a Hamilton syringe. Mice were sacrificed 1, 3 or 12 weeks after pyramidotomy.

Tissue processing and histological analysis

Brains and spinal cords were dissected and postfixed overnight in PFA. The tissue was then cryoprotected in 30% sucrose (Sigma) for 3 days. Coronal sections (50µm thick) were cut on a cryostat. To visualize CST collaterals, BDA detection was performed as follows: Sections were incubated in ABC complex (Vector Laboratories) overnight at 4°C. After a 20 min tyramide amplication (Biotin-XX, TSA Kit #21, Life technologies) sections were incubated overnight with Streptravidin conjugated to Alexa Fluor 594 (1:500, Life technologies). For STAT3 immunohistochemistry, antigen retrieval with Tris-EDTA was performed prior to immunostaining. After blocking for 1 hour, an anti-STAT3 antibody (dilution 1:500; Cell Signaling) or anti p-STAT3 antibody (dilution 1:50; Cell Signaling) diluted in PBS containing 0.1% Triton X-100 (Sigma) and 2.5% goat serum serum (Life technologies) was added. Sections were then incubated at 4°C overnight. The following day, the appropriate secondary antibodies (goat anti rabbit antibodies conjugated with Alexa Fluor 594 or Alexa Fluor 488) were applied. Counterstaining was performed using NeuroTrace 435 (Invitrogen) and sections were mounted in Vectashield (Vector Laboratories). The percentage of p-STAT3 positive neurons was determined by counting the number of NeuroTrace positive neurons and the number of neurons that were p-STAT3 positive in layer V of ten consecutive sections (50µm

thick) surrounding the injection site (five before and five after the injection site; imaging field of 423µm x 423µm). A ratio was made by dividing the number of p-STAT3 positive neurons by the total number of NeuroTrace positive neurons in the imaging field. For the retrograde labeling of CST projection neurons, animals were injected with rAAV-STAT3 one week prior to the injury. Immediately following the midthoracic dorsal hemisection, 2µl of a retrograde tracer (dextran tetramethylrhodamine 3 000 MW, 10% in 0.1M PB, Life technologies) was injected into the spinal cord at the site of injury (0.3mm lateral from the midline, 0.3mm depth) using a finely pulled glass micropipette. Three weeks following lesion (and injection of dextran tetramethylrhodamine), mice were sacrificed and then processed as described above. Consecutive 50µm thick cross-sections of the motor cortex (-0.96 to -1.26mm from bregma, covering the entire area that contained retrogradely labeled neurons) were evaluated by two independent observers and averaged to determine the percentage of retrogradely-labelled neurons that express p-STAT3.

To assess the density of neurons, the motor cortex of *Emx*-Cre x $STAT3^{fl/fl}$ mice and their Cre negative littermates (perfused 3 weeks post spinal cord injury) were processed and stained overnight with an antibody against NeuN (dilution 1:500). Consecutive sections were evaluated and the density of NeuN positive neurons in Layer V of the motor cortex was quantified.

Quantification of CST growth

To determine the effect of sustained STAT3 expression or STAT3 deletion on the growth of CST fibers after a midthoracic dorsal hemisection, we analyzed consecutive longitudinal sections of the midthoracic spinal cord. Image stacks were recorded on an Olympus FV1000 confocal microscope with a x20/0.85 oil immersion objective. The number of BDA-labeled growing fibers in the dorsal funiculus that intersected with a dorso-ventral lines positioned every 100µm distal from the lesion site was counted. The lesion site was

identified visually and level 0 was positioned at the end of the retracting non growing fibers. The total number of growing fibers counted on 4-5 consecutive longitudinal 50μm thick sections was then normalized to the number of fibers in the main CST tract (obtained from the dorsal funiculus at cervical C5 level) and divided by the number of sections evaluated. The value obtained for a given distance is the number of CST fibers per labeled CST axons per section, the "fiber number index" [6]. To exclude a contribution from spared fibers, only fibers emerging from the dorsal main CST and extending in the dorsal funiculus were counted. To confirm that all dorsal main CST axons were cut by the lesion, we verified the absence of labeled dorsal fibers further distal from the site of the lesion (at thoracic level 11) in all animals used for the analysis of the effects of sustained STAT3 activation on axon growth (n=14 mice). To quantify axonal sprouting, we counted the number of collateral sprouts emerging from the transected axons and normalized this number to the number of traced CST fibers. All quantifications were performed by an observer blinded with respect to injury status and treatment.

Quantification of CST remodeling

To evaluate axonal remodeling following a midthoracic dorsal hemisection, traced CST collaterals entering the grey matter at cervical levels C4 were counted on 30 consecutive coronal sections per animal using a light microscope (Olympus IX471) with a x40/0.65 air objective. To correct for differences in inter-animal tracing efficiency, the number of collaterals was divided by the number of traced fibers in the main CST tract and expressed as the ratio of collaterals per main CST fiber [4]. To evaluate axonal remodeling following a unilateral pyramidotomy, we counted traced CST fibers crossing the midline on 30 sections per animal using a light microscope. Again numbers were normalized to the number of traced fibers in the main CST tract and expressed as the ratio of midline crossing fibers per main CST fiber [5]. To assess the projection pattern of these midline crossing CST fibers in the

denervated side of the spinal cord, we counted the number of CST collaterals invading laminae I to V and VI to IX of the spinal cord and related to the total number of fibers crossing the midline. To assess the extension of fibers into the denervated side, we counted the number of CST collaterals crossing lines spaced in 25µm intervals from the midline into the gray matter of the denervated side of the cord. Values obtained were normalized to the number of fibers in the main CST tract and expressed as the density of midline crossing fibers. All quantifications were performed by an observer blinded with respect to injury status and treatment.

Behavioral analysis

BMS: We used the Basso mouse scale [7] to assess recovery of hindlimb locomotion after a spinal lesion. Following the ranking system previously described [7] mice were given scores from 0-9, with a score of 0 indicating no ankle movement and a score of 9 indicating frequent or consistent plantar stepping, mostly coordinated stepping, paws parallel at initial contact and lift off, normal trunk stability and tail consistently up. For evaluation, the mice were placed in an open field for 4 min and assessed by two observers blinded to the genotype of the mice. Mice were assessed before and 2, 7, 14 and 21 days after lesion.

Rotarod: To assess balance, coordination and motor control after injury, mice were tested using the Rotarod performance test [8]. Prior to injury mice were habituated to the apparatus every 3 days over a 2 week period. For testing, mice are placed in one of the four lanes that have a motor driven rod. The system records the velocity of the rod and the time at which the mouse falls from the rod onto the beam below. The performance of the mice was evaluated using two different paradigms: rotarod rotation at a fixed speed (20 rpm) and accelerating rotarod rotations (4-40 rpm). For accelerating rotarod rotations, the speed of the rotation and latency up to the fall were recorded. For each mouse the best performance after

three trials (with 15min intervals) was used. Rotarod performance was assessed before and 2, 7, 14 and 21 days after injury.

Food pellet grasping: To assess the recovery of forelimb function after pyramidotomy we used the food pellet staircase reaching test as previously described [9,10]. Mice were first accustomed to retrieve sucrose pellets (Bio-Serv) from a baited double staircase (Campden Instruments) two weeks before baseline recordings were taken. After unilateral pyramidotomy, mice were then tested starting at 2 days post-lesion and then weekly for up to 10 weeks after lesion. Prior to testing, mice were food deprived for 12 hours. Sessions lasted 15 min and the number of pellets eaten, displaced as well as the lowest step at which no pellet remained was recorded. For re-lesion experiments the contra-lateral (unlesioned) CST of mice treated with rAAV-STAT3 was cut on the level of the pyramids at 10 weeks after the initial pyramidotomy and the mice were tested 3 days after the contralateral pyramidotomy (n = 13 mice).

Electrophysiology

Determination of optimal coordinates for stimulation of forelimb motor cortex: From preliminary mapping experiments we determined the spatial centre of the motor cortex region that controlled forelimb movements to be around +0.4mm from bregma and 1.2mm lateral from the midline, which is consistent with previous studies [4,11]. We observed that forelimb responses to cortical stimulation were strongest in the more posterior areas of the forelimb region, corresponding to the region -0.2 to +0.1mm from bregma. In addition, we also obtained the greatest amount of forelimb-projecting CST labeling when tracers or viruses were introduced in this area. Therefore we injected rAAV expressing either membraneYFP or STAT3 at -0.4mm from bregma, 1mm lateral, and 0.6mm depth, corresponding to cortical layer V of the caudal border of the forelimb region. We injected the viruses slightly caudal of

the target region as we previously observed that diffusion of injected viruses or tracers into motor cortex is biased in the anterior direction.

Electrophysiological recordings: Animals were anaesthetized with an intraperitoneal injection of ketamine/xylazine (ketamine, 100mg/kg; xylazine, 13 mg/kg), and then supplemented with subdermal injections of ketamine alone (33mg/kg) as needed by assessment of the breathing rate and hindpaw pinch response. A craniotomy was made that extended approximately 0.8mm anterior to 0.8mm posterior from bregma and from 0.5 to 1.5mm lateral of midline, over the sensorimotor cortex of the right hemisphere. The dura was removed and the exposed brain was kept moist with saline. Unipolar stimulation of the right motor cortex was performed using parylene insulated tungsten microelectrodes of 1MΩ impedance (TM33B10, WPI). A chlorinated silver wire was placed in contact with the brain at the anterior-lateral edge of the craniotomy and served as the return electrode. Differential EMG recording in the ipsilateral forelimb was performed using hook electrodes in bipolar configuration, made from 50μm Teflon-coated steel wire (A-M Systems Inc.), with the tips of the hooks exposed. The electrodes were inserted into the forelimb flexor muscle group using a 25-gauge needle which was then withdrawn. The forelimbs were then placed in an elevated position on foam pads to assist visualization of muscle movements and to maintain correct placement of the hook electrodes. Signals were amplified (5k), band-pass filtered (low 300Hz, high 3kHz, NPI electronics, Tamm) and digitized using a Micro 1401 data acquisition unit (CED Ltd; Cambridge Electronic Design, UK) and sent to a computer running Spike2 software (Cambridge Electronic Design, UK).

Stimulation protocol: Stimulations were performed at four sites in the anterior-posterior direction along the middle of the forelimb motor cortex region, starting at the centre of the region (+0.4mm from bregma, 1.2mm lateral) and then at three further evenly spaced

sites back to the rostral edge of the scar that had formed at the virus injection site (-0.2mm from bregma, 1.2mm lateral). If necessary, slight adjustments in the mediolateral direction were made to prevent the electrode from penetrating blood vessels. Monophasic cathodal pulses (10ms train duration at 300Hz, 0.2ms pulse duration) were applied through the electrode at an interval of 1s using an iso-flex stimulus isolator triggered by a Master 8 stimulator (both from A.M.P.I. Instruments). The electrode was lowered vertically into the cortex initially using a high stimulus current (60-90μA) until movement of the contralateral forelimb was detected (20 trials per site). Forelimb activation was classified as a movement of the digits, the distal or proximal joints and/or muscle twitch. To determine the threshold of ipsilateral forelimb activation, the depth of the electrode was first optimized to give maximal contralateral forelimb movement. At this point the current was reduced to zero, and then increased in increments of 10μA until EMG signal in the ipsilateral forelimb appeared. If no EMG signal was detected at 250μA the site was deemed unresponsive. In situations where no response was evident, it was confirmed that the hook electrodes were correctly positioned and functional by squeezing the ipsilateral paw. It should be noted that using our stimulation protocol ipsilateral forelimb responses were detected in all unlesioned animals (n=7 mice; average threshold 49.5μA, average latency 0.0137s) an observation which has been extensively documented by others [12-14]. These ipsilateral responses are likely due to inter-hemispheric connections that cross the midline above the level of the medulla oblongata and are thus removed by the initial pyramidotomy [14]. Latencies were also determined and measured to the onset of the EMG response. Further we averaged EMG traces (generally 10 cycles or more) and measured the duration and amplitude of the peak-to-peak response in unlesioned control mice (average duration=0.0163±0.0031s, average amplitude=0.1226±0.0549mV, n=6 mice) as well as in lesioned mice at 12 weeks after injection with Control rAAV (average duration=0.0068±0.0007s, average

amplitude=0.0439±0.0059mV, n=8 mice) or rAAV-STAT3 (average duration=0.0101±0.0013s, average amplitude=0.1020±0.051mV, n=8 mice).

Statistical evaluation

Data were analyzed by the Student's t test in case of comparisons of two groups and one-way ANOVA with Tukey test or two-way ANOVA with Bonferroni test in case of multiple comparisons using Graphpad Prism 5.01 for Windows (GraphPad Software).

SUPPLEMENTARY REFERENCES

[1] Klugmann M, Symes CW, Leichtlein CB, Klaussner BK, Dunning J, Fong D, Young D, During MJ (2005) AAV-mediated hippocampal expression of short and long Homer 1 proteins differentially affect cognition and seizure activity in adult rats. *Mol Cell Neurosci*. **28**: 347–60

[2] Bareyre FM, Garzorz N, Lang C, Misgeld T, Büning H, Kerschensteiner M (2011) In vivo imaging reveals a phase-specific role of STAT3 during central and peripheral nervous system axon regeneration. *PNAS* **108**: 6282-7

[3] Lang C, Guo X, Kerschensteiner M, Bareyre FM (2012) Single collateral reconstructions reveal distinct phases of corticospinal remodeling after spinal cord injury. *PLoS ONE* 7: e30461

[4] Bareyre FM, Kerschensteiner M, Raineteau O, Mettenleiter TC, Weinmann O, Schwab ME (2004) The injured spinal cord spontaneously forms a new intraspinal circuit in adult rats. *Nat Neurosci* 7: 269-77

[5] Bareyre FM, Haudenschild B, Schwab ME (2002) Long-Lasting Sprouting and Gene Expression Changes Induced by the Monoclonal Antibody IN-1 in the Adult Spinal Cord. *J Neurosci* **22**: 7097-110

[6] Liu K *et al* (2010) PTEN deletion enhances the regenerative ability of adult corticospinal neurons. *Nat Neurosci* **13**: 1075-81

[7] Basso D, Fisher L, Anderson A, Jakeman L, McTigue D, Popovich P (2006) Basso Mouse Scale for locomotion detects differences in recovery after spinal cord injury in five common mouse strains. *J Neurotrauma* **23**: 635-59

[8] McGavern DB, Zoecklein L, Drescher KM, Rodriguez M (1999) Quantitative Assessment of neurologic deficits in a chronic progressive murine model of CNS demyelination. *Exp Neurol* **158**: 171-181

[9] Baird AL, Meldrum A, Dunnett SB (2001) The staircase test of skilled reaching in mice. *Brain Res Bull* **54**: 243-50

[10] Starkey ML, Barritt AW, Yip PK, Davies M, Hamers FPT, McMahon SB, Bradbury EJ (2005) Assessing behavioural function following a pyramidotomy lesion of the corticospinal tract in adult mice. *Exp Neurol* **195**: 524-539

[11] Tennant KA, Adkins DL, Donlan NA, Asay AL, Thomas N, Klein JA, Jones TA (2011) The organization of the forelimb representation of the C57BL/6 mouse motor cortex as defined by intracortical microstimulation and cytoarchitecture. *Cereb Cortex* **21**: 865-76

[12] Kartje-Tillotson G, Neafsey EJ, Castro AJ (1985) Electrophysiological analysis of motor cortical plasticity after cortical lesions in newborn rats. *Brain Res* **332**: 103-11

[13] Z'Graggen WJ, Fouad K, Raineteau O, Metz GA, Schwab ME, Kartje, GL (2000) Compensatory sprouting and impulse rerouting after unilateral pyramidal tract lesion in neonatal rats. *J Neurosci* **20**: 6561-9

[14] Brus-Ramer M, Carmel JB, Martin JH (2009) Motor cortex bilateral motor representation depends on subcortical and interhemispheric interactions. *J Neurosci* **29**: 6196-206

SUPPLEMENTARY FIGURES

Supplementary Figure S1: STAT3 expression in cortical neurons is transiently induced after spinal cord injury and can be conditionally deleted

(**A**,**B**) Confocal images illustrating the expression of STAT3 in layer V cortical neurons (green, NeuroTrace 435; red, STAT3) of an unlesioned mouse (**A**) or a mouse perfused 24hrs following a midthoracic hemisection (**B**). (**C**) Quantification of STAT3 expression in layer V cortical neurons in unlesioned mice (white bar) and mice perfused at different timepoints following a midthoracic hemisection (grey bars, n=4-6 mice per group). (**D**,**E**) Confocal images illustrating the expression of STAT3 in layer V cortical neurons (green, NeuroTrace 435; red, STAT3) in STAT3 competent (**D**) and conditional STAT3 deficient mice (**E**) perfused 3wks following a midthoracic hemisection. (**F**) Quantification of STAT3 expression in layer V cortical neurons of unlesioned mice (white bar, same as in **C**), STAT3 competent (grey bar) and conditional STAT3 deficient mice (blue bar) perfused 3wks following a midthoracic hemisection (n=5 mice per group). All bars and error bars in this figure represent mean±SEM. Statistical analysis was performed using a one-way ANOVA followed by Tukey test. *, $P<0.05$; **, $P<0.01$. Scale bars equal 50μm in **B** (also for **A**) and 100μm in **E** (also for **D**).

Supplementary Figure S2: Conditional deletion of STAT3 does not affect neuronal cell density in layer V of the motor cortex

(**A**-**D**) Confocal images of the motor cortex of STAT3 competent and STAT3 deficient mice that were immunostained with an anti NeuN antibody. (**E**) Quantification of the number of NeuN positive neurons in layer V of the motor cortex of STAT3 competent (grey bar) and STAT3 deficient (blue bar) mice (n=5 mice per group). All bars and error bars in this figure

represent mean±SEM. Statistical analysis was performed using a t-test. Scale bar equals 100 μm in **B** (also for **A**) and **D** (also for **C**).

Supplementary Figure S3: Conditional deletion of STAT3 does not affect CST growth early after spinal cord injury

(**A**) Schematic representation of the analysis of CST growth at the lesion site following spinal cord injury. (**B**,**C**) Quantification of the sprouting (**B**) and growth (**C**) of lesioned CST fibers in STAT3 competent (grey bars, n=5) and conditional STAT3 deficient mice (blue bars, n=5) at 1 wk after lesion. (**D**,**E**) Confocal images of longitudinal sections of the spinal cord (lesion indicated by asterisk) illustrating growth of the corticospinal tract (in red) in STAT3 competent mice (**D**) and conditional STAT3 deficient mice (**E**). The dotted lines in (**D**) represent the distances at which the growing axons were counted. (**F**) Schematic representation of the analysis of CST remodeling following spinal cord injury. (**G**,**H**) Confocal images of cervical hindlimb CST collaterals in lesioned STAT3 competent (**G**) and conditional STAT3 deficient (**H**) mice 1 wk following spinal cord injury. (**I**) Quantification of the number of collaterals exiting the hindlimb CST tract in the cervical spinal cord in STAT3 competent (grey bar, n=8) and conditional STAT3 deficient mice (blue bar, n=8) 1 wk following spinal cord injury. All bars and error bars in this figure represent mean±SEM. Statistical analysis was performed using a repeated one-way ANOVA followed by Tukey test in **C** and a t-test in **B**, **I**. Scale bars equal 100μm in **E** (also for **D**) and 50 μm in **H** (also for **G**).

Supplementary Figure S4: Conditional deletion of STAT3 in cortical projection neurons does not influence functional recovery following spinal cord injury

(**A**) Quantification of the BMS score before and up to 3 weeks following spinal cord injury in STAT3 competent (grey bars) and conditional STAT3 deficient (blue bars) mice (n=10-17 mice per group). (**B**) Quantification of the endurance time at a fixed rotorod speed before and up to 3 weeks following spinal cord injury in STAT3 competent (grey squares) and conditional STAT3 deficient (blue squares) mice (n=10-17 mice per group). (**C**) Quantification of the endurance time at an accelerated rotorod speed before and up to 3 weeks following spinal cord injury in STAT3 competent (grey squares) and conditional STAT3 deficient (blue squares) mice (n=10-17 mice per group). All bars and error bars in this figure represent mean±SEM. Statistical analysis were performed using a repeated one-way ANOVA followed by Tukey test. ***, $P<0.001$.

Supplementary Figure S5: Sustained expression of STAT3 increases growth of CST axons at the lesion site

(**A**) Schematic representation of the analysis of CST growth at the lesion site following spinal cord injury. (**B-E**) Confocal images of longitudinal sections of the spinal cord (asterisk, indicates lesion site) illustrating growth of the transected CST axons (BDA, white) in mice injected with rAAV-STAT3 (**B-D**) or Control rAAV (**E**). The dotted lines in (**E**) represent the distances at which growing CST axons were counted. Boxed areas in (**B**) are magnified 2-times in (**C**) and (**D**). (**F**,**G**) Quantification of axonal growth at different distances distal from the lesion site (**F**) and of axonal sprouting (**G**) at the site of the lesion in mice injected with Control rAAV (grey bars) and mice injected with rAAV-STAT3 (red bars) perfused 3 wks following midthoracic hemisection (n=7 mice per group). All bars and error bars in this figure represent mean±SEM. Statistical analysis was performed using a repeated one-way ANOVA

followed by Tukey test in **F** and a t-test in **G**. *, $P<0.05$; **, $P<0.01$. Scale bars equals 60μm in **E** (also for **B**).

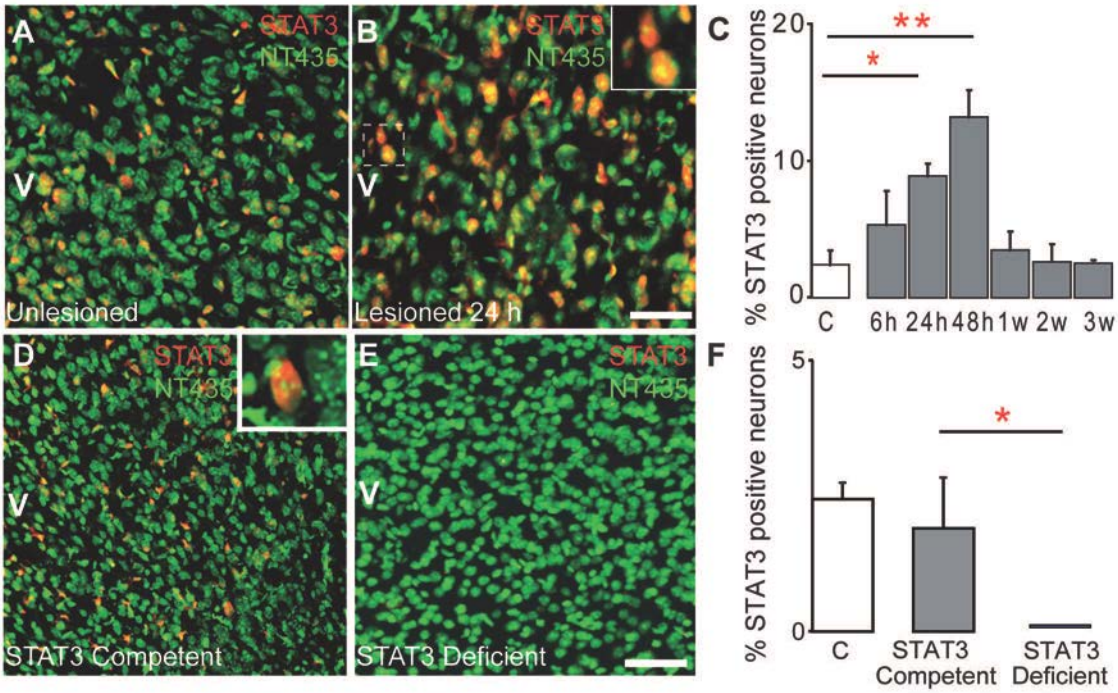

Lang et al., Supplementary Fig. S1

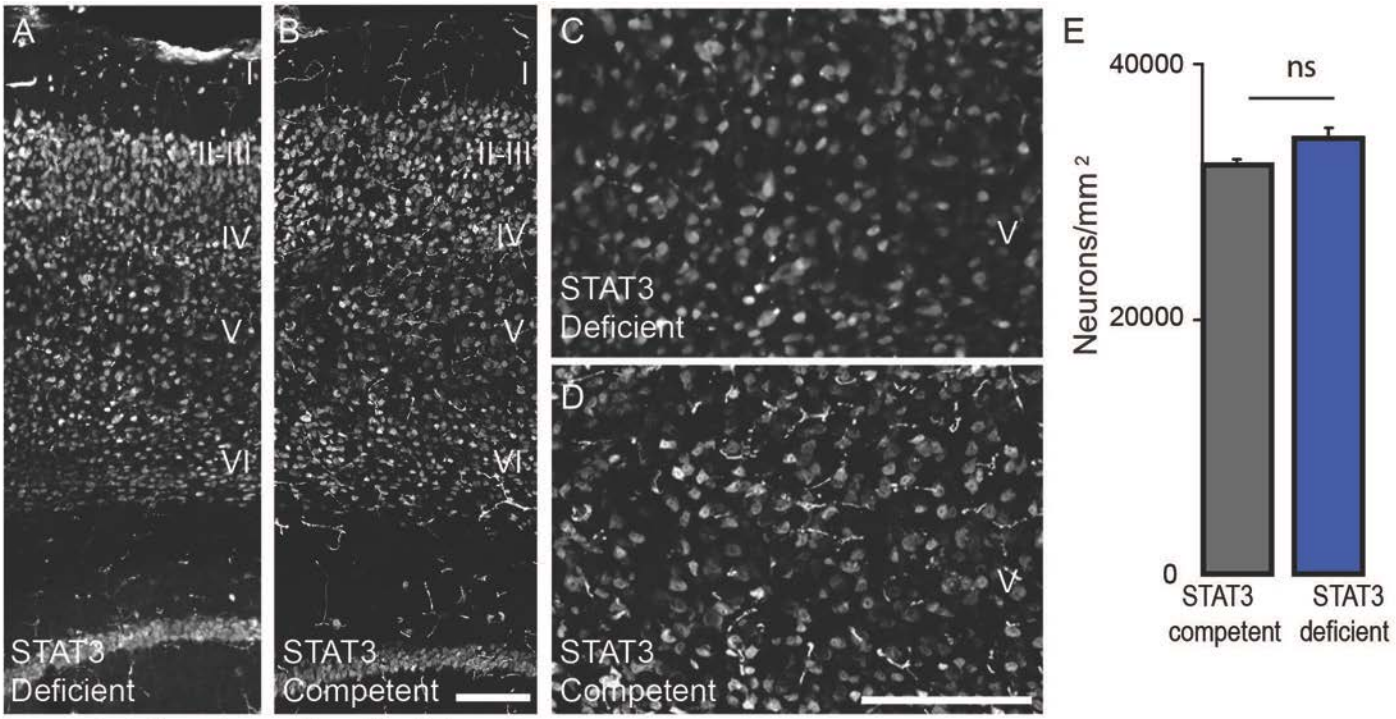

Lang et al., Supplementary Fig. S2

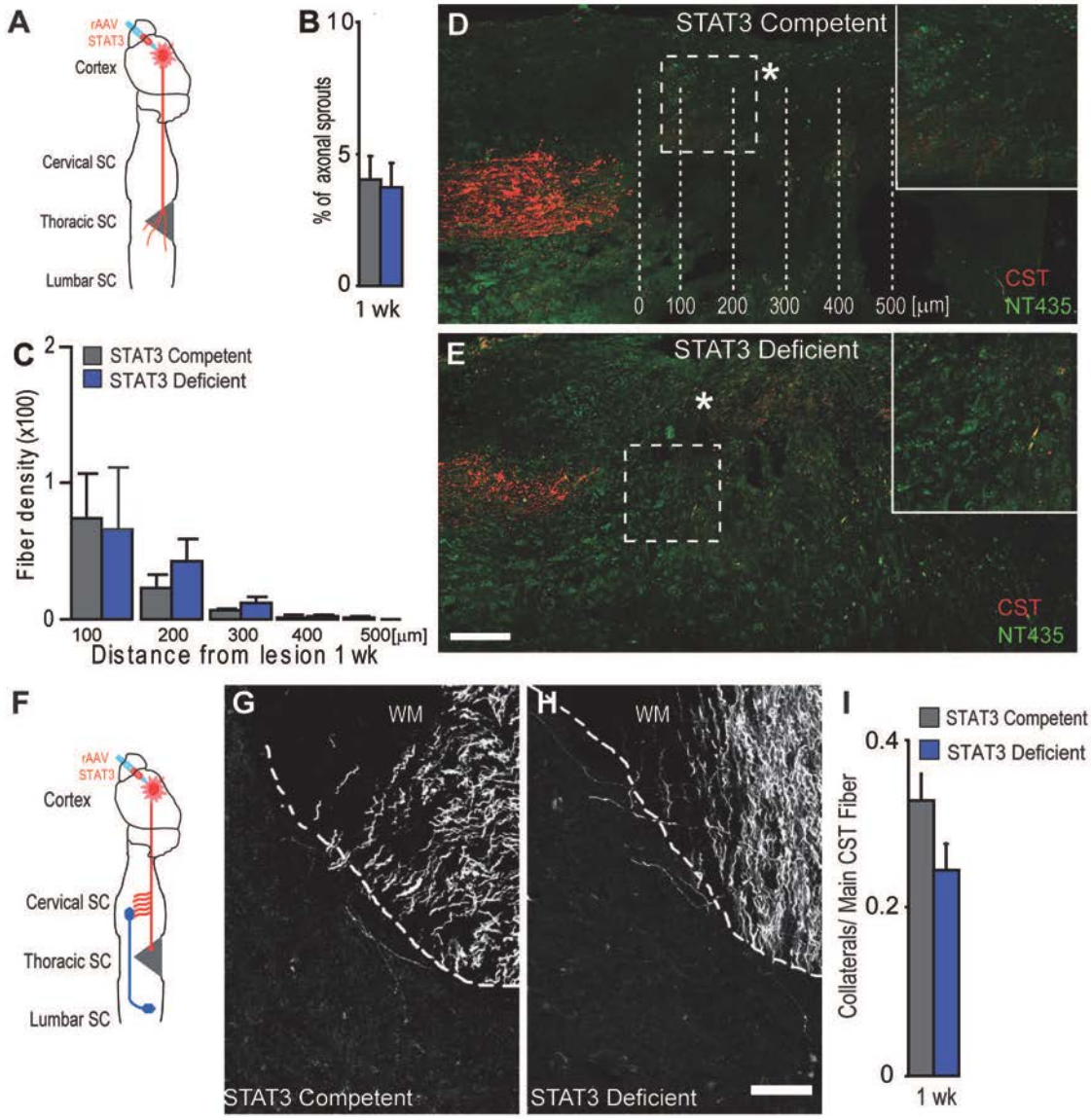

Lang et al., Supplementary Fig. S3

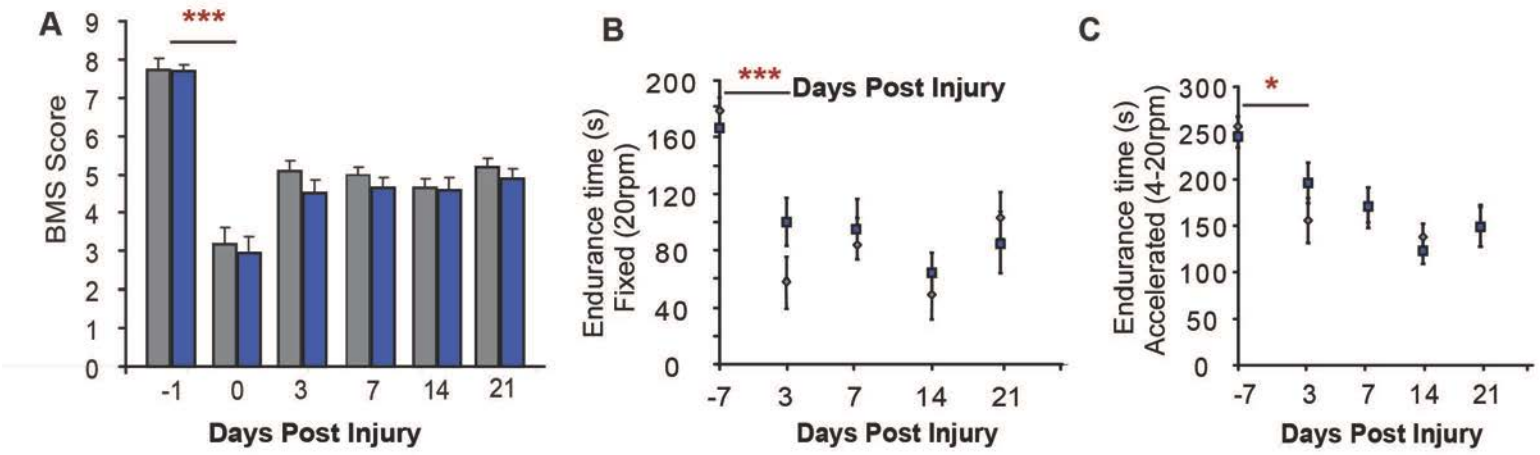

Lang et al., Supplementary Fig. S4

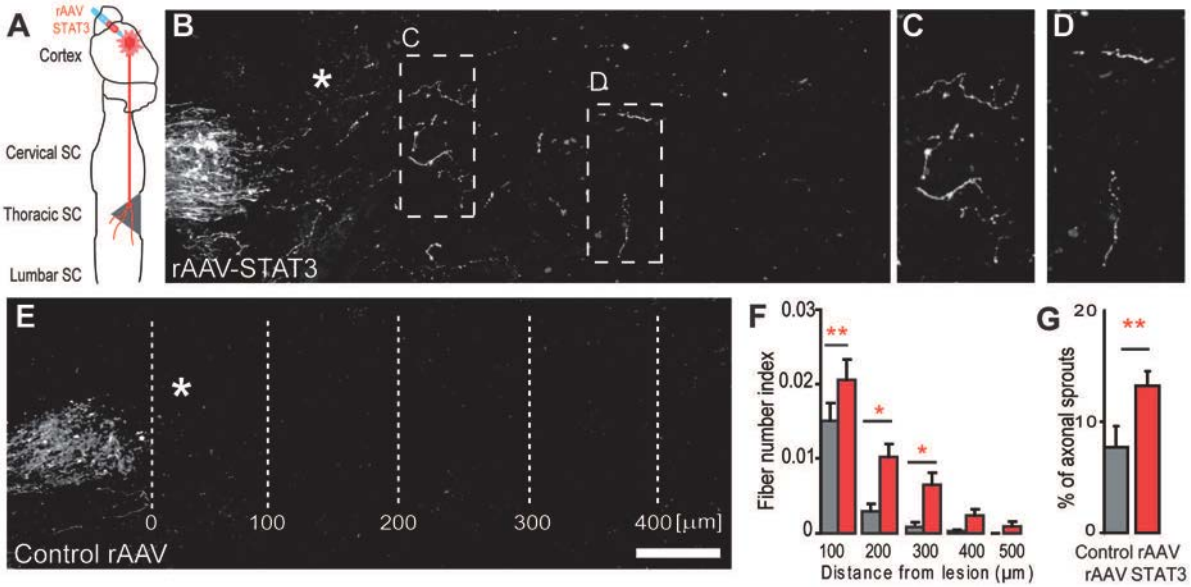

Lang et al., Supplementary Fig. S5

3.2

Abundant Expression of Guidance and Synaptogenic Molecules in the Injured Spinal Cord

Jacobi A, Schmalz AM and Bareyre FM.

An Article published in *PLoS One 2014 Feb 11;9(2):e88449*

OPEN ACCESS Freely available online

PLOS ONE

Abundant Expression of Guidance and Synaptogenic Molecules in the Injured Spinal Cord

Anne Jacobi[1], Anja Schmalz[1], Florence M. Bareyre[1,2]*

1 Institute of Clinical Neuroimmunology, Ludwig-Maximilians University Munich, Munich, Germany, **2** Munich Cluster for Systems Neurology (SyNergy), Munich, Germany

Abstract

Background: Spinal interneurons have emerged as crucial targets of supraspinal input during post-injury axonal remodelling. For example, lesioned corticospinal projections use propriospinal neurons as relay stations to form intraspinal detour circuits that circumvent the lesion site and contribute to functional recovery. While a number of the molecules that determine the formation of neuronal circuits in the developing nervous system have been identified, it is much less understood which of these cues are also expressed in the injured spinal cord and can thus guide growing collaterals and initiate synaptogenesis during circuit remodelling.

Methodology/Principal Findings: To address this question we characterized the expression profile of a number of guidance and synaptogenic molecules in the cervical spinal cord of healthy and spinal cord-injured mice by *in situ* hybridization. To assign the expression of these molecules to distinct populations of interneurons we labeled short and long propriospinal neurons by retrograde tracing and glycinergic neurons using a transgenically expressed fluorescent protein. Interestingly, we found that most of the molecules studied including members of slit-, semaphorin-, synCAM-, neuroligin- and ephrin-families as well as their receptors are also present in the adult CNS. While many of these molecules were abundantly expressed in all interneurons examined, some molecules including slits, semaphorin 7a, synCAM4 and neuroligin 1 showed preferential expression in propriospinal interneurons. Overall the expression pattern of guidance and synaptogenic molecules in the cervical spinal cord appeared to be stable over time and was not substantially altered following a midthoracic spinal cord injury.

Conclusions: Taken together, our study indicates that many of the guidance and synaptogenic cues that regulate neuronal circuit formation in development are also present in the adult CNS and therefore likely contribute to the remodelling of axonal connections in the injured spinal cord.

Citation: Jacobi A, Schmalz A, Bareyre FM (2014) Abundant Expression of Guidance and Synaptogenic Molecules in the Injured Spinal Cord. PLoS ONE 9(2): e88449. doi:10.1371/journal.pone.0088449

Editor: Norbert Weidner, Heidelberg University Hospital, Germany

Received July 20, 2013; **Accepted** January 8, 2014; **Published** February 11, 2014

Funding: Work in F.M.B.'s lab is supported by grants from the Deutsche Forschungsgemeinschaft (DFG, SFB 870) and the German Federal Ministry of Education and Research (BMBF). The funders had no role in study design, data collection and analysis, decision to publish, or preparation of the manuscript.

Competing Interests: The authors have declared that no competing interests exist.

* E-mail: Florence.Bareyre@med.uni-muenchen.de

Introduction

For successful wiring of the nervous system axons need to navigate and establish synaptic contacts with their proper target cells. Work in the developing nervous system has established that this process is regulated by target derived guidance and synaptogenic cues (for review see [1], [2]). A number of the molecules that can guide growing axons in the developing nervous system have been identified and include among others netrins [3], semaphorins [4], slits [5] and ephrins [6]. Similarly, molecules that can facilitate pre- and postsynaptic differentiation following axon-target contact have been studied in neuronal development. Among these, synCAMs [7] and neuroligins [8], for example, can act as pre-synaptic organizers while neurexins [9], and ephrinBs [10] are postsynaptic organizers. To what extend these molecules also regulate pathfinding and synapse formation of re-growing axons in the damaged adult nervous system is so far only incompletely understood.

During the recent years, it has become increasingly clear that new axonal connections are not only formed during development but also following nervous system injury. For example, we and others have shown that the corticospinal tract (CST) undergoes extensive remodelling following spinal cord injury [11 14]. A key element of this remodelling process is the formation of intraspinal detour circuits [11,13]. For detour circuits to form, the hindlimb CST sprouts new collaterals in response to a midthoracic dorsal hemisection. These collaterals then enter the gray matter of the cervical spinal cord and contact different populations of spinal interneurons including C3 C4 short propriospinal neurons (SPSN) - which are important for visually-guided target reaching with the forelimb [15] - and C3 C5 long propriospinal neurons (LPSN) - which contribute to locomotion and in particular mediate the coupling of forelimbs and hindlimbs during walking [16]. Initially CST collaterals equally contact long and short propriospinal neurons, however over time contacts onto SPSN are partially removed while contacts onto LPSN are refined and maintained [11,13]. LPSN in turn increase their projections onto lumbar motoneurons and thereby complete an intraspinal detour circuit that can relay information from hindlimb motor cortex to the lumbar spinal cord. The importance of intraspinal detour circuits

has been further emphasized by a number of subsequent studies that demonstrate that similar detour circuits (i) mediate the recovery of the supraspinal control of stepping after spinal cord injury [12], (ii) also form in response to inflammatory insults to the spinal cord [17,18], and (iii) are the target of therapeutic strategies that can promote remarkable recovery of locomotor function in rodents [19,20]. While the importance of intraspinal detour circuits for functional recovery is thus well-established, it is unclear how the initiation and stabilization of the synaptic contacts that form the new circuits is regulated. To identify candidate cues that can guide the formation of intraspinal detour circuits we investigated the expression pattern of a number of membrane-bound guidance and synaptogenic molecules in the cervical spinal cord of healthy mice and spinal-cord injured mice by *in situ* hybridization. In particular we assessed the expression in the following populations of spinal interneurons: (i) C3 C4 SPSN, (ii) C3 C5 LPSN and (iii) glycinergic neurons which are located in similar spinal laminae as propriospinal neurons and served as control population. Our results show that members of the slit-, semaphorin-, synCAM-, neuroligin- and ephrinB- families are abundantly expressed in spinal interneurons both before and after spinal cord injury. While most of these molecules are equally expressed in the different interneuronal populations, some molecules like slits, semaphorin 7a and neuroligin 1 are present in many propriospinal neurons but in only few glycinergic interneurons. These results suggest that similar molecular mechanisms might regulate the initial formation of circuits in development and their re-formation after injury.

Materials and Methods

Ethics Statement

All animal experiments conformed to the institutional guidelines and were approved by the Animal Study Committee of the Regierung von Oberbayern. Approval ID: 55.2-1-54-2531-127-05.

Mice

Adult mice between 6 and 12wks of age were used in this study. C57/Bl6 mice (Janvier SAS) were used to study stereotactically labeled long and short propriospinal neurons. *GlyT2*- EGFP mice that express enhanced green fluorescent protein (EGFP; [21]) under the control of the GlyT2 promoter were used to label inhibitory glycinergic neurons.

Surgery procedure

For hemisection procedures mice were anesthetized by i.p. injections of ketamine/xylazine (ketamine 87 mg/kg, xylazine 13 mg/kg). The dorsal spinal cord was exposed by a laminectomy at thoracic level 8 (Th8) and a dorsal hemisection which completely interrupts the main dorsal and minor dorsolateral CST was made with fine iridectomy scissors as previously described [13]. After surgery the mice were kept on a heating pad (38°C) until fully awake and treated with Metacam (0.05 mg/kg, Boehringer Ingelheim) for two more days. Spinal cord and cortex that were used for further analysis were derived from the same mice.

Retrograde labelling of propriospinal neurons and cortical projection neurons

To co-localize the *in situ* hybridization (ISH) signal with propriospinal neurons, these neurons were retrogradely-labeled two weeks before sacrifice for all time points investigated. One µl of Fluoro-Emerald (10% in 1 x PBS, Life Technologies) was stereotactically injected with a glass capillary filled into the lower thoracic cord (Th12) to label LPSN and into the lower cervical cord (C8-Th1) to label SPSN on both sides of the spinal cord (±1.0 mm lateral from spinal midline, depth 1.0 mm). The micropipette remained in place for 2min after completing the injection. To co-localize the ISH signal with the cortical projection neurons of the transected CST, these neurons were retrogradely-labeled 7 days before sacrifice. Briefly, after laminectomy at thoracic level 8 of the spinal cord, 0,5 µl of TexasRed® (5% in 0.1 M PB, Life Technologies) was stereotactically injected rostrally to the lesion with a glass capillary into each side of the spinal cord (±0,2 mm lateral from spinal midline, depth 0.3 mm). The micropipette remained in place for two minutes after completing the injection to avoid backflow. After retrograde labelling mice were kept on a heating pad (38°C) until fully awake and treated with Metacam for 2 more days.

Tissue preparation

Animals were deeply anesthetized with isoflurane and perfused transcardialy with saline solution followed by 4% paraformaldehyde (PFA) in 0.1 M phosphate buffer (PBS). After post-fixation in 4% PFA at 4°C overnight the spinal cord and brains were dissected, incubated in 30% sucrose for 2 3 d, frozen and stored at 20° until use.

Immunohistochemistry (IHC). To assess the presence of the ISH signal in NeuN positive neurons, the cervical spinal cord was sectioned in coronal orientation (30 µm) with a cryostat (Leica CM1850) and sections were then washed three times for 10min in 1x PBS. All solutions used for the IHC contained DEPC to prevent degradation of target RNAs for later ISH. After washing the sections were blocked for 45min in 1x PBS containing 10% horse serum and 0.1% Triton. The primary antibody anti-NeuN (1:500; Millipore MAB377) was incubated in 1x PBS solution containing 0.1% Triton and 2.5% goat serum overnight at 4°. On day 2 the tissue was washed three times for 10min in 1x PBS before the application of the secondary antibody (1:500, Alexa-Fluor 488 goat anti-mouse; Life Technologies). After 3hrs of incubation the tissue was washed three times for 10min in 1x PBS and mounted in VectaShield.

In situ Hybridization (ISH)

Spinal cord tissue (cervical region C2 C5) and brain tissue (Bregma 1.06 till 1.70) were sectioned in coronal orientation (50 µm thick) with a cryostat (Leica CM1850) and washed two times for 10min in 2X SSC (from 20X stock solution containing 3M NaCl and 0,3M Na Citrate). All steps were carried out with DEPC treated solutions to prevent degradation of target RNAs. Before the prehybridization step, the sections were incubated in a 1:1 mixture of 2X SSC and hybridization buffer (50% Formamide, 5X SSC, 5X Denhardt's solution (Sigma-Aldrich D2532), 250 µg/ml yeast tRNA, 500 µg/ml salmon sperm DNA) for 15min at RT. Afterwards the sections were incubated for 1hr in hybridization buffer at the appropriate (pre-) hybridization temperatures for each probe (see Table 1). For hybridization, the probe (200 400 ng/ml in hybridization buffer) was heated for 10min at 80°C, applied to the tissue and incubated overnight in an oven (for temperatures see Table 1). Sections were then rinsed at RT in 2X SSC and washed in decreasing concentration of SSC (2X to 0.1X SSC at hybridization temperature) before applying an alkaline-phosphatase-conjugated sheep anti-digoxigenin antibody, Fab fragments (1:2000; Roche Diagnostics) in blocking buffer overnight at 4°C. Alkaline phosphatase activity was detected using nitroblue tetrazolium chloride (337.5 mg/ml) and 5-Bromo-4-chloro-3-indolyl phosphate (175 mg/ml) (Carl Roth). The sections

Table 1. Hybridization and pre-hybridization temperatures for the different probes used in the study.

	Origin of the probe	Prehybridization Temperature	Hybridization Temperature	Washing Temperature
Slit-1	rat	45°C	48°C	55°C
Slit-2	rat	45°C	48°C	55°C
Slit-3	rat	45°C	48°C	55°C
Robo-1	rat	50°C	54°C	60°C
Robo-2	rat	50°C	54°C	60°C
Robo-3	rat	50°C	58°C	65°C
Sema6A	mouse	50°C	50°C	60°C
Sema7A	rat	50°C	55°C	65°C
PlexinA2	mouse	48°C	48°C	55°C
PlexinC1	mouse	50°C	55°C	65°C
SynCAM1	mouse	55°C	60°C	65°C
SynCAM3	mouse	55°C	65°C	65°C
SynCAM4	mouse	55°C	60°C	65°C
NL1	mouse	55°C	55°C	55°C
NL4	mouse	55°C	55°C	55°C
EphB2	mouse	50°C	52°C	55°C
EphrinB1	mouse	50°C	55°C	55°C

doi:10.1371/journal.pone.0088449.t001

Table 2. Distribution and intensity of the ligands in the unlesioned cervical spinal cord of adult mice.

Area	Slit-1	Slit-2	Slit-3	Sema6a	Sema7a	SynCam1	SynCam3	SynCam4	NL1	NL4	EphB2	EphrinB1
Gray Matter												
Laminae I – IV	++	+++	+	+	++	++	+	++	+	++	+++	+
Laminae V	++	++++	++	+++	+++	++++	+++	+++	++	++	+++	++
Laminae VI – IX	+++	++++	++	++++	+++	+++	++++	+++	+++	++	+++	++
White Matter												
Dorsal Column	+	+	– .	–	+	–	–	+	–	–	+	+
Ventral Funiculus	+	+	–	–	+	–	–	+	–	–	–	+

Relative intensities were estimated by visual comparison with sense probe in situ hybridization slides: +: weak; ++: moderate; +++: strong; ++++: very strong; –: not detected.

doi:10.1371/journal.pone.0088449.t002

were washed in ddH_2O after the staining procedure. When applied, the fluorescent Nissl stain Neurotrace 435 was applied for 2h at RT, the sections were washed and mounted with Gel Mount (Sigma Aldrich).

Imaging and image processing

As the ISH procedure interferes with the fluorescent labels we analyzed fluorescence and ISH signals using a two-step approach. For visualizing the co-localization of ISH signals and NeuN

Table 3. Distribution and intensity of the receptors in the unlesioned adult mouse cortex.

Area	Robo1	Robo2	Robo3	PlexinA2	PlexinC1	SynCam1	SynCam3	SynCam4	EphB2	EphrinB1
LayerI	+	–	–	–	–	+	–	–	–	–
Layer II	+	+	+	+	+	++	++	++	++	++
Layer III	++	++	–	++	++	++	++	+	++	++
Layer IV	++	++	–	–	–	++	+	+++	–	–
Layer V	++++	+++	++	++	+++	++	++	++++	+++	+++
Layer VI	++	+	+	+	–	++	+	++	–	–

Relative intensities were estimated by visual comparison with sense probe in situ hybridization slides: +: weak; ++: moderate; +++: strong; ++++: very strong; –: not detected.

doi:10.1371/journal.pone.0088449.t003

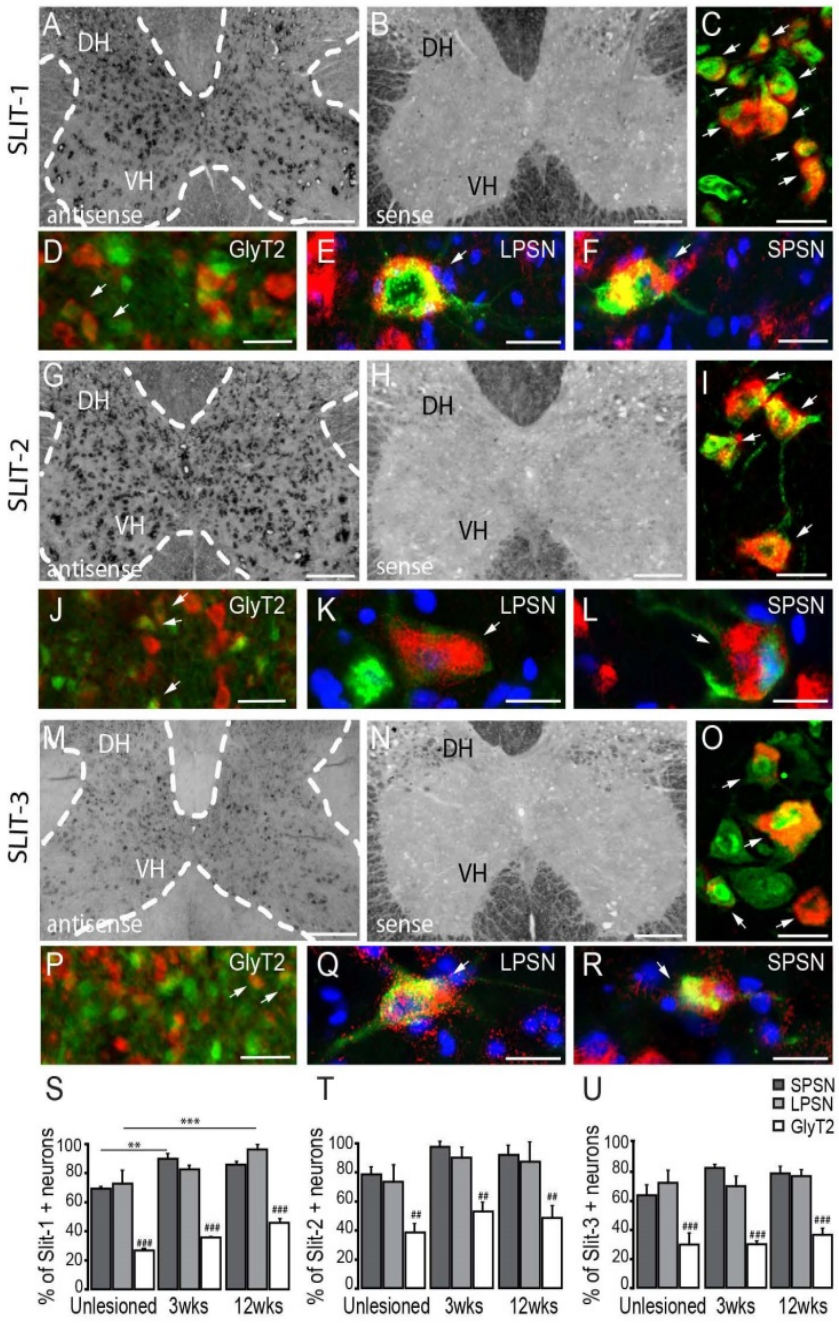

Figure 1. ***In Situ*** **hybridization pattern of Slit-1,-2,-3 in the cervical spinal cord.** *In situ* hybridization of slit-1 (A-F), slit-2 (G-L), slit-3 (M-R) mRNA in the unlesioned cervical spinal cord. Strong signals for slit-1 (A) and slit-2 (G) are detected with the anti-sense probe in cervical interneurons and motoneurons while slit-3 (M) shows a weaker signal. No signals are detected with the sense probes for slit-1 (B), slit-2 (H) or slit-3 (N). (C, I, O) Epifluorescence images of double-labeled neurons in the ventral horn (NeuN: green; *In situ* signal: red). (D-F) Co-localization of slit-1 mRNA in glycinergic neurons (D; GlyT2: green; slit-1: red), LPSN (E; LPSN: green; slit-1: red; NT435: blue) and SPSN (F; SPSN: green; slit-1: red; NT435: blue) in the cervical spinal cord. (J-L) Co-localization of slit-2 mRNA in glycinergic neurons (J; GlyT2: green; slit-2: red), LPSN (K; LPSN: green; slit-2: red; NT435: blue) and SPSN (L; SPSN: green; slit-2: red; NT435: blue) in the cervical spinal cord. (P-R) Co-localization of slit-3 mRNA in glycinergic neurons (P; GlyT2: green; slit-3: red), LPSN (Q; LPSN: green; slit-3: red; NT435: blue) and SPSN (R; SPSN: green; slit-3: red; NT435: blue) in the cervical spinal cord. (S-U) Quantification of the proportion of glycinergic neurons, LPSN and SPSN expressing slit-1 (S), slit-2 (T) and slit-3 (U) in the unlesioned and lesioned cervical spinal cord. Scale bars in A,B,G,H,M,N, 250 μm; Scale bars in C,I,O, 25 μm; Scale bars in D-F,J-K,P-R, 25 μm.
doi:10.1371/journal.pone.0088449.g001

immunolabelling, we first imaged sections immunostained for NeuN using a confocal microscope (FV1000, Olympus). The sections were then unmounted, ISH was performed as described above before the same sections were then re-imaged with a confocal microscope using bright field illumination. Both images (that were acquired with the same magnification) were overlaid in Photoshop (Adobe) and a number of anatomical landmarks including the central canal and the ventral and dorsal border between the gray and white matter were used as fiduciary marks to co-register the images and adjust for tissue shrinkage due to the ISH process. For imaging retrogradely-labeled CST neurons, we first imaged the fluorescence signals using a confocal microscope (FV1000, Olympus) using standard filter settings before we unmounted the sections, performed ISH and image alignment as described above. To assess the presence of ISH signals in transgenically-labeled glycinergic interneurons, we first imaged

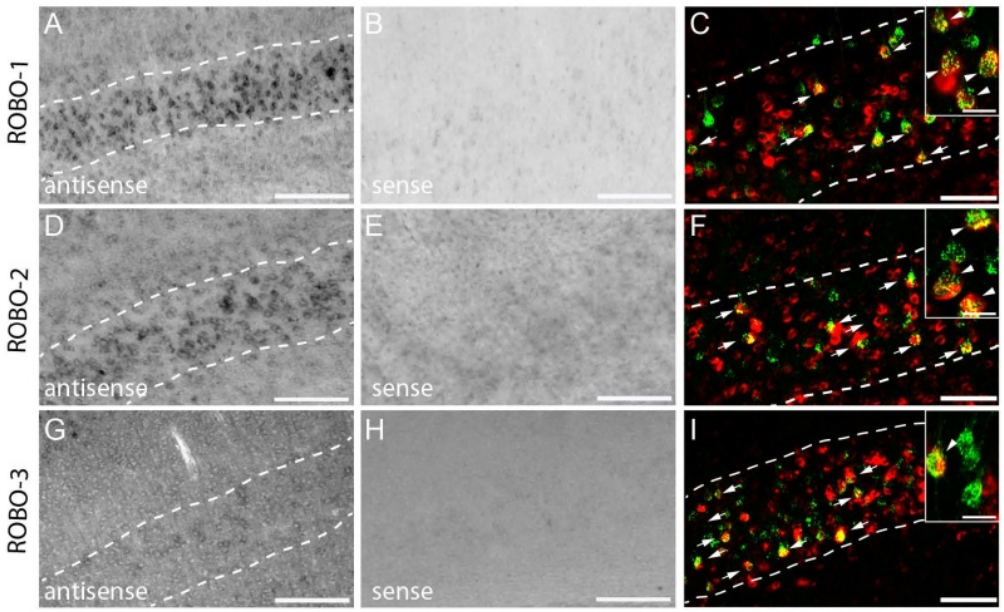

Figure 2. *In Situ* hybridization pattern of Robo-1,-2,-3 in the cortex. *In situ* hybridization of Robo-1 (A), Robo-2 (D) and Robo-3 (G) mRNA in the cortex. No signals are detected with the sense probes (B: Robo-1; E: Robo-2; H: Robo-3). Dotted lines in A, D, and G represent layer V. (C,F, I) Epifluorescence images of double-labeled neurons of layer V (Retrogradely-labeled CST neurons: green; *In situ* signal: red).Scale bars in A,B,D,E,G,H: 100 μm; Scale bars in C,F,I: 50 μm (25 μm in insets).
doi:10.1371/journal.pone.0088449.g002

the fluorescence signals using an epifluorescence Olympus IX71 microscope using standard filter settings before we unmounted the sections, performed ISH and image alignment as described above. Retrogradely-labeled propriospinal neurons were imaged using an epifluorescence Olympus IX71 concomitantly for fluoro-emerald and ISH signals as the ISH did not interfere with this fluorescent label.

Image analysis and cell counts

Retrogradely-labeled cortical projection neurons and propriospinal neurons were assessed under the fluorescent microscope by alternating between the fluorescence and the bright field. Glycinergic neurons were assessed on the acquired images.

To determine the proportion of cortical projection neurons that express a given molecule, we counted all retrogradely-labeled neurons on every third sections of the cortex (n = 3 mice). Sections were assessed from anterior to posterior and the analysis began with the first section in which retrogradely-labeled CST neurons appeared. To determine the proportion of glycinergic neurons that express a given molecule, three sections at C3/C4 and three sections at C5 were randomly selected. Then, all glycinergic neurons in lamina VI to IX (which are the laminae in which long and short propriospinal neurons are located) were assessed (n = 3 mice). To determine the proportion of long and short propriospinal neurons that express a given molecule, all retrogradely-labeled neurons located from C3 to C5 were counted until the number of cells reached 30 per animal (about 10 sections per animal, n = 3 mice) taking the first section as the section in which propriospinal neurons were first detected. Results were expressed as a ratio of the number of double-labeled neurons compared to the total number of assessed neurons. All counts were performed by an independent blinded-observer. To assess co-localization we used the following evaluation criteria: A cell was considered countable when the contour of its soma could be clearly identified either based in the retrograde label or based on the fluorescent transgenic label. ISH signals were considered to be overlaying when they followed the contour of the soma and did not extend beyond it.

For generating the rating in Table 2 and 3, we first defined the area for the analysis e.g. laminae VI to IX for the spinal cord or in the cortex at −1.3 from bregma starting at +/− 1 mm from the midline. To assess the expression in different cortical layers we used a box of 35 μm^2 that was overlaid on layer 1, or 2 or 3 or 4 or 5 or 6 of the cortex. We then set the threshold for detection and measured the grayscale intensity of the selected area with the ImageJ Measurement Tool. Values below 500 were defined as not detected; Values between 500 and 1500 were defined as +; Values between 1500 and 2500 were defined as ++; Values between 2500 and 3500 were defined as +++; Values above 3500 were defined as ++++.

Statistical analysis

Results are given as mean ± SEM unless indicated otherwise. Data were analyzed in GraphPad Prism5.01 software using a two-way ANOVA (factors: time and interneuron-type) followed by Bonferroni post hoc tests. Significance levels was taken with $p < 0.01$.

Results

Expression of the repulsive axon guidance cues slit-1, -2 and -3 and their receptors in the adult CNS

The process of axon pathfinding is mediated by a number of guidance molecules, among them slits (slit-1,-2,-3) and their receptors (robo-1,-2,-3), which have been shown to have a repulsive effect on axons during development [22–23] and have been proposed to restrict axonal growth at the lesion site following spinal cord injury [24]. To assess whether slits can also regulate axon growth during axonal remodelling distant from the lesion site we first investigated the expression of slit family members in the unlesioned mouse spinal cord by *in situ* hybridization. Hybridization with the anti-sense probe shows that slit-1, slit-2 and slit-3 mRNAs are detected in all laminae of the cervical gray matter (Fig. 1A,G,M) while hybridization with the sense probe showed no signal (Fig. 1B,H,N). In particular, slit-1 and slit-2 show high

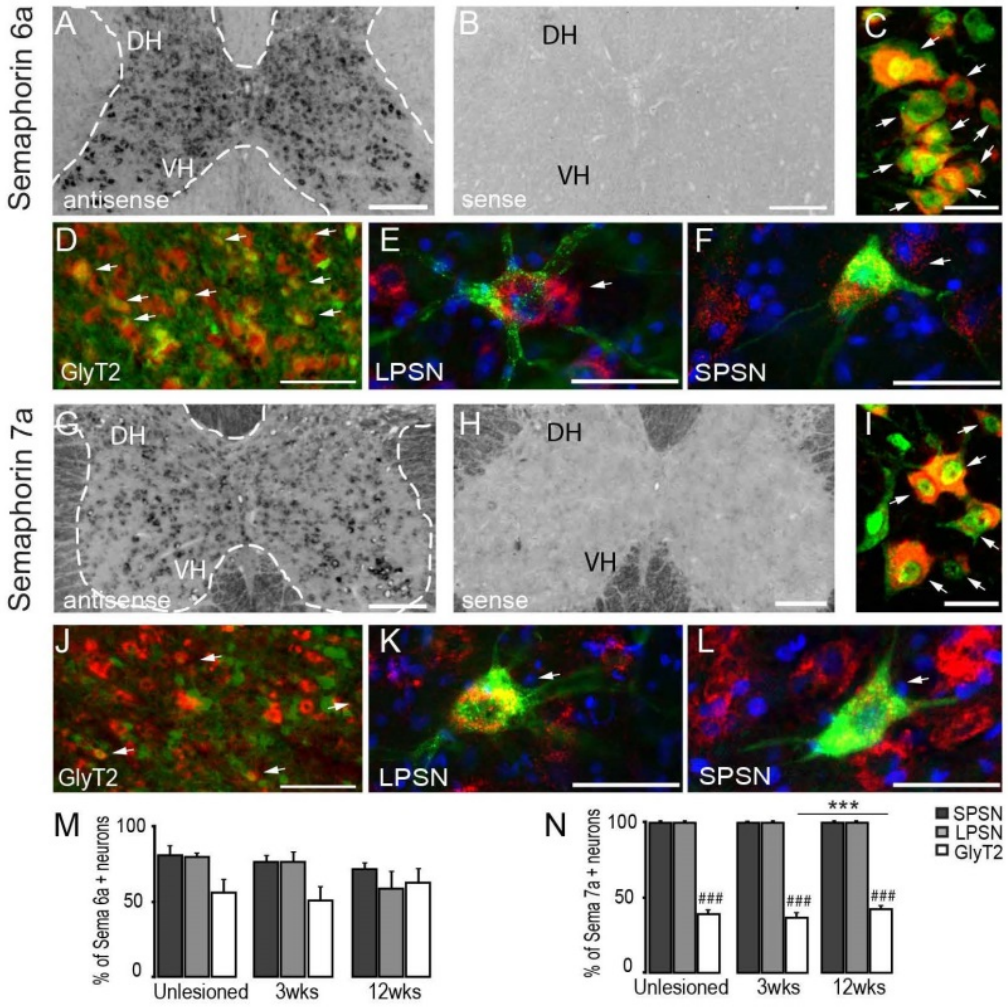

Figure 3. *In Situ* hybridization pattern of Semaphorin 6a and Semaphorin 7a in the cervical spinal cord. *In situ* hybridization of Semaphorin 6a (A) mRNA in the unlesioned cervical spinal cord. Strong signal for Semaphorin 6a (A) is detected with the anti-sense probe. No signal is detected with the sense probe (B). (C) Confocal picture of double-labeled neurons in the ventral horn (NeuN: green; Semaphorin 6a: red). (D-F) Co-localization of Semaphorin 6a mRNA in glycinergic neurons (D; GlyT2: green, Semaphorin6a: red), LPSN (E; LPSN: green, Semaphorin 6a: red, NT435: blue), and SPSN (F; SPSN: green, Semaphorin 6a: red, NT435: blue) in the cervical spinal cord. *In situ* hybridization of Semaphorin 7a (G) mRNA in the unlesioned cervical spinal cord. Moderate signals for semaphorin 7a in inter- and motoneurons for Semaphorin 7a (G) is detected with the anti-sense probe. No signal is detected with the sense probes (H). (I) Confocal image of double-labeled neurons in the ventral horn (NeuN : green; Semaphorin 7a: red). (J-L) Co-localization of Semaphorin 7a mRNA in glycinergic neurons (D; GlyT2: green, Semaphorin 7a: red), LPSN (E; LPSN: green, Semaphorin 7a: red, NT435: blue), and SPSN (F, SPSN: green, Semaphorin 7a: red, NT435: blue) in the cervical spinal cord. (M, N) Quantification of the number of GlyT2, LPSN and SPSN expressing Semaphorin 6a (M) and semaphorin 7a (N) in unlesioned and lesioned cervical spinal cord. DH: dorsal horn; VH: ventral horn. Arrows in D and J show double-labeled glycinergic neurons. Scale bars in A, B, G, H: 250 μm; Scale bars in C, I: 25 μm; Scale bars in E, F, K, L: 25 μm; Scale bars in D, J: 50 μm.
doi:10.1371/journal.pone.0088449.g003

expression levels throughout the spinal gray matter and in particular in the ventral horn (Table 2) while slit-3 mRNA seems to be expressed at a lower level. Analysis after counterstaining with NeuN suggests that slits are expressed by neurons including by interneurons and motoneurons (Fig. 1C,I,O). To better understand which populations of spinal interneurons express slit mRNA, we visualized glycinergic interneurons using a transgenic label (Fig. 1D,J,P) and LPSN (Fig. 1E,K,Q) and SPSN (Fig. 1F,L,R) using retrograde labelling . Our results show that, 60 to 80% of all propriospinal neurons but only about 30% of glycinergic interneurons express slit-1, -2 and -3 (Fig. 1S-U). While overall this expression pattern is rather unchanged in the cervical spinal cord of mice at 3 and 12 weeks after injury, there is a moderate but significant increase in the proportion of propriospinal neurons that expressed slit-1 or slit-3 after injury (Fig. 1 S-U).

To determine whether the corticospinal collaterals that enter the spinal gray matter can respond to slits expressed by spinal interneurons we examined the expression of the corresponding slit-receptors (robo-1, -2, -3) in the mouse cortex by *in situ* hybridization . In the cortex, robo-1 can be detected in layer I to VI, with its strongest expression in the cells of layer V (Table 3 and Fig. 2A). Robo-2 is expressed from layer II to VI in the cortex, with a slightly more intense labelling in layer V (Fig. 2D). Additionally, robo-3 mRNA is detectable in layer II, V and VI although the expression level is very low (Fig. 2G). Specificity of the staining was validated by hybridization of the tissue with the sense probe which showed no signals (Fig. 2 B,E,H). Retrograde labelling with Texas Red® revealed that 90,2±3,4% of CST projection neurons in layer V express robo-1, 55,2±5,2% of CST projection neurons express robo-2 and that 26,4±1,9% of CST projection neurons express robo-3 (Fig. 2 C,F,I).

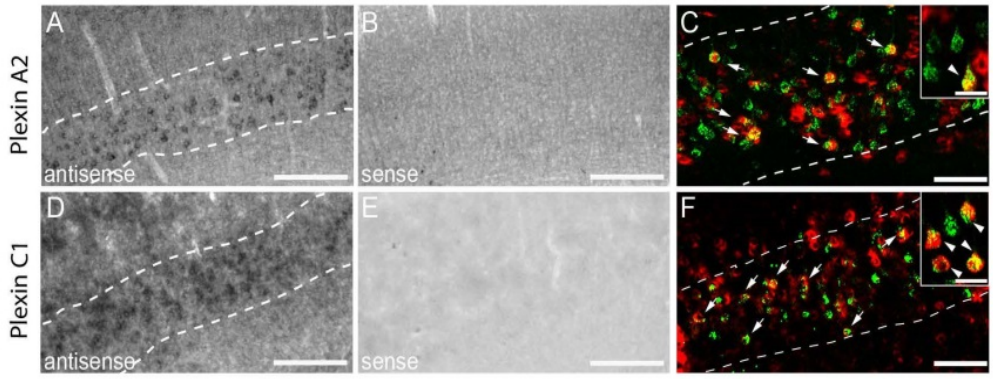

Figure 4. *In Situ* hybridization pattern of plexin A2 and plexin C1 in the cortex. *In situ* hybridization of PlexinA2 in the cortex (A). No signal is detected with the Sema6a sense probe (B). Dotted lines in A represent layer V of the cortex. (C) Confocal image of double-labeled neurons of layer V (retrogradely-labeled CST projection neurons, green; plexin A2, red). *In situ* hybridization of PlexinC1 in the cortex (D). No signal is detected with the Sema7a sense probes (E). Dotted lines in D represent layer V of the cortex. (F) Confocal picture of double-labeled CST projection neurons identified by retrograde tracing (retrogradely-labeled CST projection neurons, green; plexin C1, red). Scale bars in A,B,D,E: 100 μm; Scale bars in C, F: 50 μm (25 μm in insets).
doi:10.1371/journal.pone.0088449.g004

Expression of the guidance cues semaphorin 6a (Sema6a) and semaphorin 7a (Sema7a) and their receptors plexin A2 and plexin C1 in the adult CNS

The repulsive membrane associated Sema6a has been shown to control axon guidance in different parts of the nervous system [25-27] and specifically to affect the growth of the developing CST at multiple choice points [28]. We now investigated the expression pattern of Sema6a in the cervical spinal cord of healthy mice by *in situ* hybridization. While Sema6a mRNA is specifically present throughout the spinal gray matter (Fig. 3A,B) the hybridization signals are more intense in the middle and ventral laminae (IV – IX) of the spinal cord than in the dorsal horn (Fig. 3A and Table 2). Morphology analysis after counterstaining with NeuN suggests that in the gray matter Sema6a is primarily expressed by neurons and in particular by interneurons (Fig. 3C). Sema6a mRNA is also present in cells in the dorsal and ventral white matter (Table 2), consistent with the reported expression of Sema6a in oligodendrocytes, [25].

Analysis of different interneuronal populations revealed that the majority of glycinergic interneurons as well as LPSN and SPSN contain Sema6a mRNA (Fig. 3D-F) both before and at 3 and 12 weeks after a thoracic spinal cord injury (Fig. 3M).

In contrast to Sema6a, semaphorin7a (Sema7a) is an attractive guidance cue that supports axonal growth [29]. In order to determine the expression pattern of Sema7a, we hybridized a Sema7a anti-sense probe to sections from the cervical spinal cord of healthy mice. We can show that Sema7a is specifically expressed in all laminae of the spinal cord (I – IX; Table 2 and Fig. 3G,H) with the strongest expression in ventral and intermediate laminae (Table 2). Cells that expressed Sema7a morphologically resembled interneurons (Fig. 3I) and further anaylsis revealed that all long and short propriospinal neurons but only about 40% of glycinergic interneurons expressed Sema7a both in the healthy spinal cord as well as 3 and 12 weeks after spinal cord injury (Fig. 3J-L, N).

To determine whether corticospinal axons can integrate attractive or repulsive signals from Sema6a or 7a, we detected the mRNA coding for the main receptor of Sema6a, plexinA2, and the receptor for Sema7a, plexinC1 in the mouse cortex by *in situ* hybridization. Our results show specific expression of plexinA2 in layers II-III and V-VI of the cortex (Fig. 4.A,B and Table 3) and specific expression of plexinC1 in in layers II-III and V (Fig. 4D,E and Table 3) Notably, both plexinA2 and plexinC1 are expressed in retrogradely-labeled CST projection neurons in layer V(plexinA2: 54,0±3,65%; plexinC1: 70,0±2,00%) (Fig. 4C,F).

Expression of the bidirectional synaptogenic cues SynCAM1, SynCAM3 and SynCAM4 in the adult CNS

Once the newly growing collaterals have been guided to their target cells, they need to make appropriate synaptic connections. During development this process is regulated by molecules like the synaptic cell adhesion molecules (SynCAM) that promote synapse formation and maturation [7]. In order to determine the expression pattern of these bidirectional synaptic cues we analysed the mRNA expression of SynCAM1, 3 and 4 in the cervical spinal cord. In adult healthy mice SynCAM1, 3, 4 expression appears to be limited to the gray matter with particular strong signals seen in the ventral horn (Fig. 5A,B,G,H,M, N and Table 2). Morphology analysis after counterstaining with NeuN indicates that SynCAMs are primarily expressed by neurons including by interneurons and motoneurons (Fig. 5C,I,O). Expression in motoneurons was confirmed by ChAT immunostaining (data not shown).

In line with these findings, mRNAs for SynCAM1, 3 and 4 can be detected in the majority of LPSN, SPSN and glycinergic interneurons (Fig. 5D-F,J-L,P-R,S-U). Mostly similar expression patterns were observed in the cervical spinal cord of healthy mice and the cervical cord of mice perfused at 3 or 12 weeks following a thoracic spinal cord injury (Fig. 5 S-U).

Further analysis showed that SynCAM1 and SynCAM4 and to a lesser extent SynCAM3 are also expressed in the cortex (Table 3 and Fig. 6A,B,D,E,G,H). In all cases expression seems to be strongest in layer V neurons. In particular, we show that 69,8±6,5% of retrogradely-labeled layer V CST projection neurons express SynCAM1; 73,1±7,3% SynCAM3 and 94,7±0,3% SynCAM4 (Fig. 6C,F,I).

Expression of pre-synaptic organizers neuroligin-1 (NL1) and neuroligin-4 (NL4) in the adult spinal cord

Neuroligins are postsynaptic adhesion proteins, which have been shown to promote synapse maturation and synaptic function [30]. Their receptors, the neurexins, have been shown to be widely expressed not only in development but also in the adult cortex and in particular in layer V where pyramidal cells reside [31]. We analyzed NL1 and NL4 expression in the cervical spinal cord of adult mice by *in situ* hybridization. Both NLs are strongly

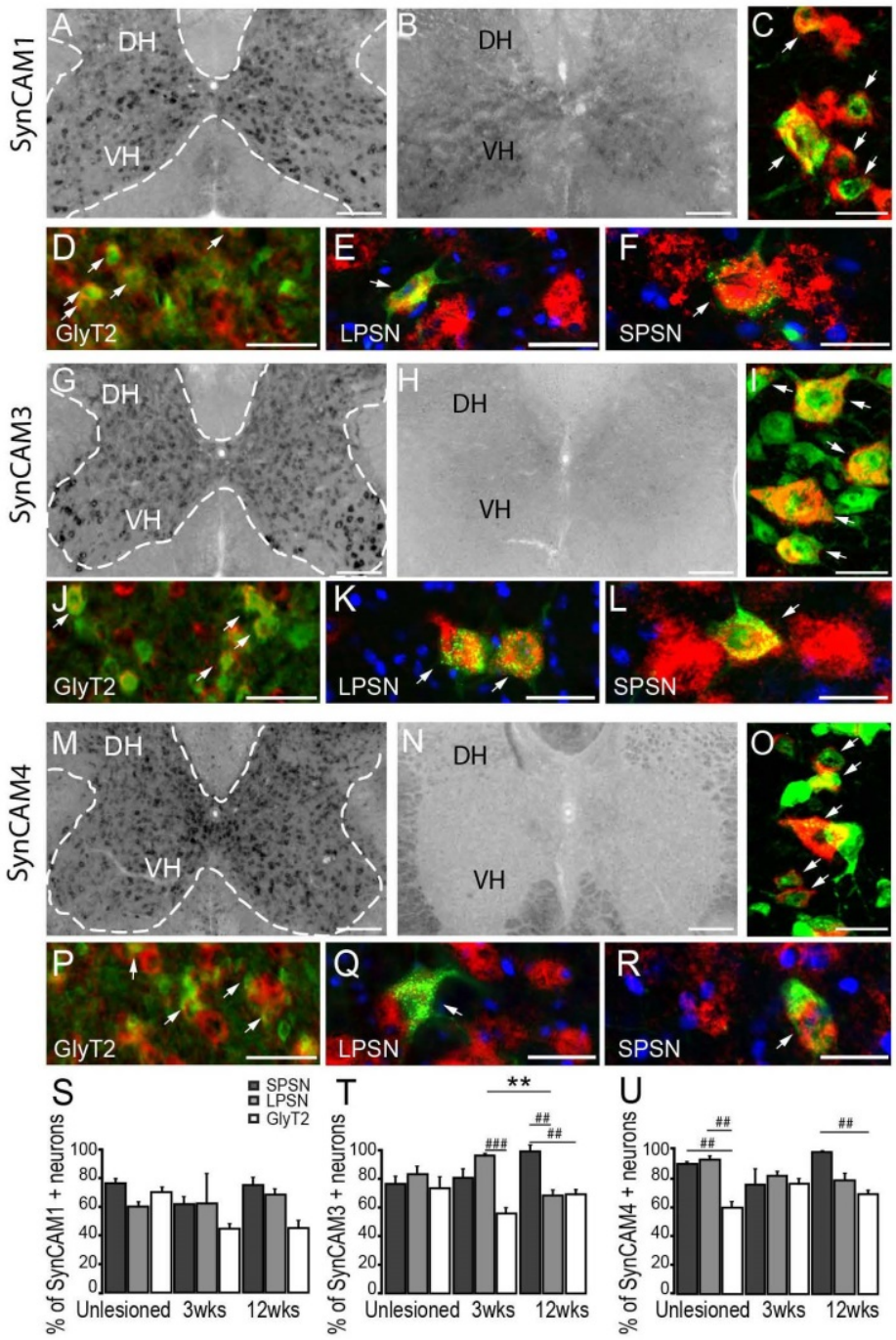

Figure 5. *In Situ* hybridization pattern of SynCAM1, SynCAM 3, SynCAM 4 in the cervical spinal cord. *In situ* hybridization of SynCAM1 (A) mRNA in the unlesioned spinal cord. Strong signal for SynCAM1 (A) is detected with the anti-sense probe. No signal is detected with the sense probe (B). (C) Epifluorescence picture of double-labeled neurons in the ventral horn (NeuN: green; SynCAM1: red). (D-F) Co-localization of SynCAM1mRNA in glycinergic neurons (D; GlyT2: green; SynCAM1: red), LPSN (E; LPSN: green; SynCAM1: red; NT435: blue) and SPSN (F; SPSN: green; SynCAM1: red; NT435: blue) in the cervical spinal cord. *In situ* hybridization of SynCAM3 (G) in the unlesioned spinal cord. Moderate signal for SynCAM3 (G) mRNA is detected with the anti-sense probe. No signal is detected with the sense probe (H). (I) Epifluorescence picture of double-labeled neurons in the ventral horn (NeuN: green; SynCAM3: red). (J-L) Co-localization of SynCAM3 in glycinergic neurons (J; GlyT2: green; SynCAM3: red), in LPSN (K; LPSN: green; SynCAM3: red; NT435: blue) and SPSN (L, SPSN, green; SynCAM3, red; NT435: blue) in the cervical spinal cord. *In situ* hybridization of SynCAM4 (M) in the unlesioned spinal cord. Strong signal for SynCAM4 (M) is detected with the anti-sense probe. No signal is detected with the sense probe (N). (O) Epifluorescence image of double-labeled neurons in the ventral horn (NeuN: green; SynCAM4: red). (P-R) Co-localization of SynCAM4 in glycinergic neurons (P; GlyT2: green; SynCAM4: red), in LPSN (Q; LPSN, green; SynCAM4, red; NT435: blue) and SPSN (R; SPSN, green; SynCAM4, red; NT435: blue) in the cervical spinal cord. (S-U) Quantification of the number of GlyT2 neurons, LPSN and SPSN expressing SynCAM1 (S), SynCAM3 (T) and SynCAM4 (U) in unlesioned and lesioned cervical spinal cord. DH: dorsal horn; VH: ventral horn. Arrows in D, J and P show double-labeled glycinergic neurons. Scale bar in A,B,G,H,M,N: 250 μm; Scale bar in C,I,O: 25 μm; Scale bars in D,J,P: 40 μm; Scale bars in E,F,K,L,Q,R: 25 μm.

doi:10.1371/journal.pone.0088449.g005

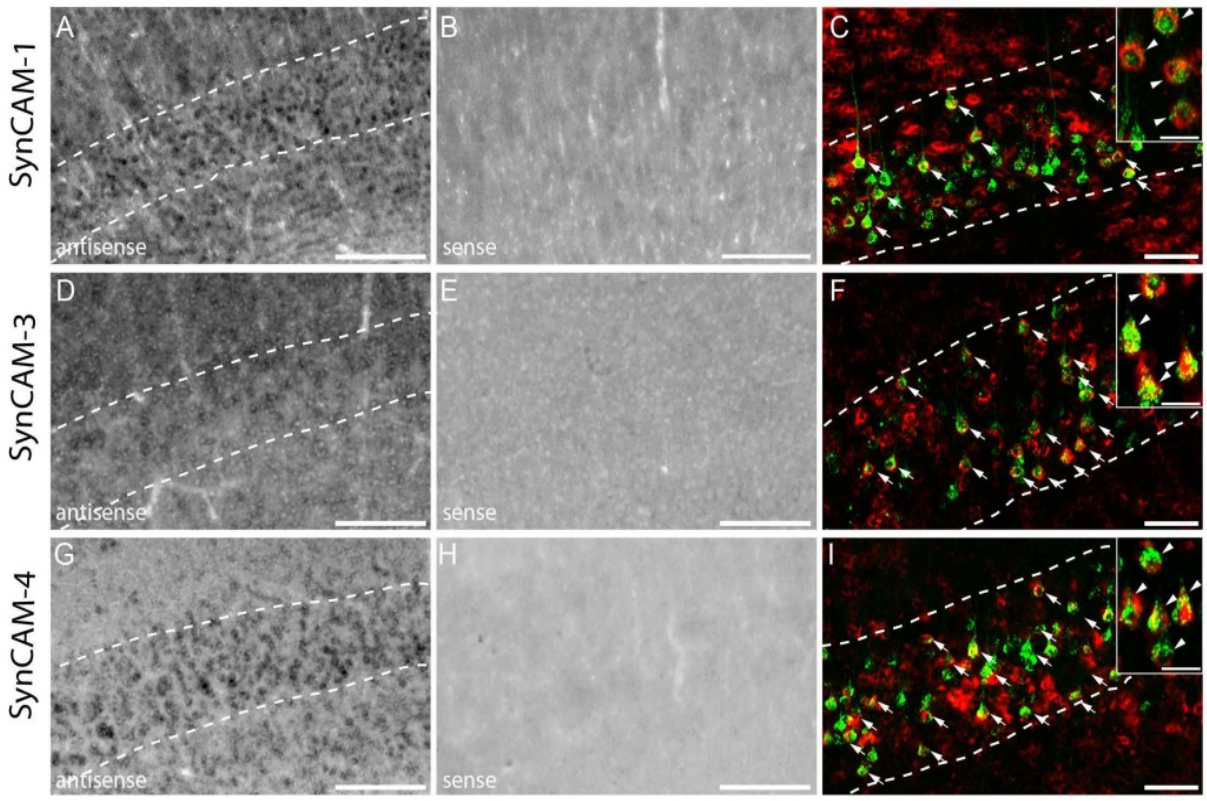

Figure 6. *In Situ* hybridization profile of SynCAM1, SynCAM 3, SynCAM 4 in the cortex. Profile of expression of SynCAM1 (A) mRNA in the cortex. No signal is detected with the SynCAM1 sense probe (B). Dotted lines in A represent layer V of the cortex. (C) Confocal image of double-labeled neurons of layer V (retrogradely-labeled CST neurons: green; SynCAM1: red). Profile of expression of SynCAM3 (D) mRNA in the cortex. No signal is detected with the sense SynCAM3 probe (E). Dotted lines in D represent layer V of the cortex. (F) Confocal image of CST projection neurons (retrogradely-labeled CST neurons: green, SynCAM3: red).). Profile of expression of SynCAM4 (G) mRNA in the cortex. No signal is detected with the sense SynCAM4 probe (H). Dotted lines in G represent layer V of the cortex. (I) Confocal image of double-labeled CST projection neurons (retrogradely-labeled CST projection neurons: green; SynCAM4: red). Scale bar in A, B, D, E, G, H: 100 μm; Scale bar in C,F,I: 50 μm (25 μm in insets).
doi:10.1371/journal.pone.0088449.g006

expressed throughout all laminae of the spinal gray matter (Table 2 and Fig. 7A,F). The analysis of different groups of spinal interneurons reveals that significantly higher percentage of long and short propriospinal neurons express NL1 compared to glycinergic neurons (Fig. 7B-E). In contrast no prominent differences in NL4 expression were observed between the different interneuronal populations studied (Fig. 7G-J). Further, the presence of a thoracic spinal cord injury did not change the expression pattern of either NL1 or NL4 in the cervical spinal cord (Fig. 7 I,J).

Expression of bidirectional guidance and synaptogenic cues ephrinB1 and ephB2 in the adult CNS

Ephrins and their receptors (Eph) are pleiotropic molecules involved in cell migration, axon guidance [32] and synapse formation [33] during nervous system development. Interestingly, eph-ephrin interactions can mediate both repulsive and attractive forces between cells [34]. EphB-ephrinB interaction has been shown to be important for proper ipsilateral targeting of CST and retinal axons [35–37]. *In situ* hybridization revealed that both ephB2 and ephrinB1mRNA are expressed throughout all laminae of the gray matter of the cervical spinal cord (Fig. 8A,B,G,H) with EphrinB1 having a dimmer expression in laminae I-IV (Table 2). Morphology analysis after counterstaining with NeuN suggests that both molecules are primarily expressed by neurons including by interneurons and at least in the case of EphB2 also motoneurons (Fig. 8C,I). Further characterization indeed showed that both EphB2 and Ephrin B1 are expressed in different interneuronal population located in the cervical spinal cord including LPSN, SPSN and glycinergic interneurons (Fig. 8D-F, J-L). While EphB2 mRNA is expressed by a similar proportion of these interneurons, Ephrin B1 was particularly prominently expressed in short propriospinal neurons in the healthy cervical spinal cord. Mostly, these expression patterns in the cervical spinal cord were not affected by the presence of a thoracic spinal cord injury (Fig. 8 M,N). The only exception is that the percentage of glycinergic interneurons expressing EphB2 was increased in the cervical spinal cord at 3 weeks post injury and decreased at 12 weeks after injury. Further expression analysis of cortical sections showed that both, Ephrin B1 and EphB2, were also expressed in layer II-III and layer V of the cortex (Fig. 9 A,B,D,E and Table 3). Retrograde labelling of layer V CST projection neurons revealed that 84, 6±3,5% of CST projection neurons express EphrinB1 and 74,1±2,2% EphB2 (Fig. 9 C,F).

Discussion

While a number of the cues that determine the formation of neuronal circuits during the development of the nervous system have been identified, it is currently unclear which molecular signals can attract growing axon collaterals and initiate the formation of synapses during the remodelling of circuits in the injured adult CNS. The aim of this work was to study the expression of chemotropic and synaptogenic factors in the cervical spinal cord of adult mice to determine which of these cues are presented by spinal interneurons in the mature CNS. We focused

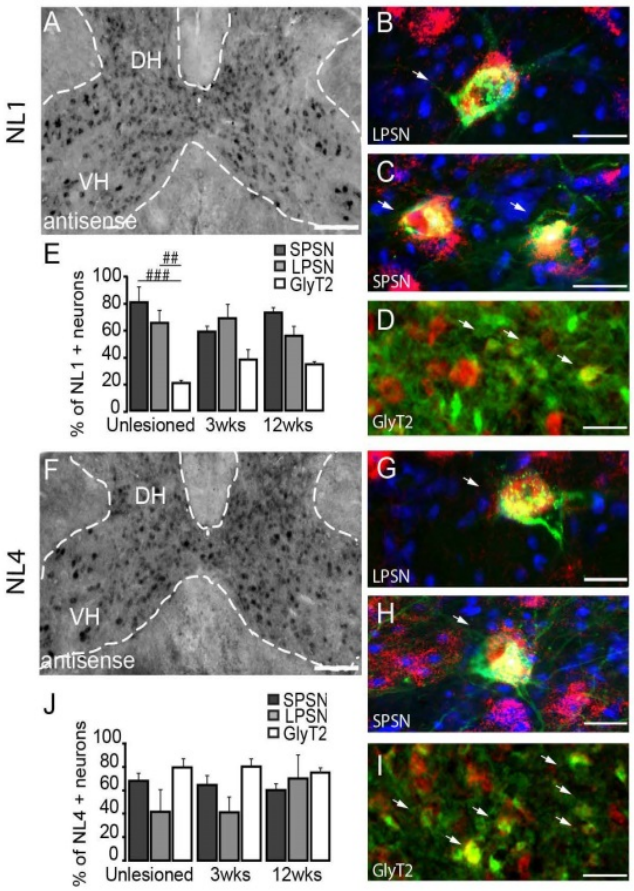

Figure 7. *In Situ* hybridization pattern of NL-1 and NL-4 in the cervical spinal cord. *In situ* hybridization of NL1 (A) and NL4 (F) mRNA in the unlesioned cervical spinal cord. Intense signals for NL1 (interneurons, A) and NL4 (inter- and motoneurons, F) are detected with the anti-sense probe. (B-D) Co-localization of NL1 in LPSN (B; LPSN: green; NL1: red; NT435: blue), SPSN (C; SPSN: green; NL1: red; NT435: blue) glycinergic neurons (D; GlyT2, green; NL1, red) in the cervical spinal cord. (E) Quantification of the number of GlyT2, LPSN and SPSN expressing NL1 in unlesioned and lesioned cervical spinal cord. (G-I) Co-localization of NL4 in LPSN (G; LPSN: green; NL4: red; NT435: blue), SPSN (H; SPSN: green; NL4: red; NT435: blue) glycinergic neurons (I; GlyT2: green; NL4: red) in the cervical spinal cord. (J) Quantification of the number of GlyT2, LPSN and SPSN expressing NL4 in normal and lesioned cervical spinal cord. DH: dorsal horn; VH: ventral horn. Arrows in D and I show double-labeled glycinergic neurons.Scale bar in A and F: 250 µm; Scale bar in B,C,G,H: 25 µm; Scale bar in D,I: 40 µm.
doi:10.1371/journal.pone.0088449.g007

our analysis on the cervical spinal cord – an area remote from the lesion site – as we and others have previously shown that new CST contacts with local cervical interneurons such as long propriospinal neurons play a key role during axonal remodelling following spinal cord injury [11–13]. While gene expression changes are certainly magnified at the lesion site [38–41], first reports indicate that a spinal lesion might also affect, although more moderately, gene expression changes more remote from the lesion site [38;41;42]. We mostly concentrated our efforts on membrane-bound molecules [7,26,43–47] as these are best suited to explain the attraction or repulsion of growing CST collaterals towards or from distinct spinal interneurons. To elucidate if and how the expression of these molecules in the cervical spinal cord changes following injury we analyzed the expression pattern at two time points following a midthoracic spinal cord injury. At 3 weeks after lesion when newly formed CST collaterals first initiate contact with spinal interneurons and 9 weeks later when these contacts have been refined [11,13]. Our study now shows that (i) all the guidance and synaptogenic cues studied were not only expressed in the developing CNS but also expressed in the adult nervous system. (ii) While we did not detect cues that were exclusively expressed in a subpopulation of spinal interneurons, some molecules studied e.g. slits, Sema7a, SynCAM4 and NL1 were preferentially expressed in propriospinal neurons compared to glycinergic neurons. (iii) The expression pattern of guidance and synaptogenic molecules appeared to be stable over time and was by large not affected by a thoracic hemisection. It is interesting to note that the individual cues appear to be quite uniformly expressed throughout the different laminae of the adult spinal cord. This expression pattern is distinct from the region-specific pattern observed during neuronal development. For example, Semaphorin 3 mRNA is expressed between E13 and E 17 in the entire ventral half of the spinal cord but not in the floor plate [48]. Conversely, Slits are essentially expressed in the floor plate during development [49,50]. Similarly it has been shown that expression of EphrinB ligands is confined to discrete regions of the spinal cord during development with for example EphrinB3 expression being localized to the floor plate around the ventral midline while EphrinB2 and B1 are primarily present in the dorsal spinal cord [51,52]. The different regional expression pattern observed in the developing and adult spinal cord also indicates that the role of guidance and synaptogenic molecules might evolve in adulthood - classical repulsive cues in development might indeed become attractive in adulthood or conversely. While the exact role of these molecules in adulthood thus still needs to be better defined, their abundant expression suggests that they also can influence the formation and stabilization of circuits in the adult spinal cord. This view is supported by our finding that all receptors for guidance and synaptogenic molecules that we probed for were expressed in the cell bodies of CST projection neurons that reside in lamina V of the cortex. While we can formally only show that mRNAs are expressed in the neuronal cell body we believe that it is highly likely that functional receptors are present on growing CST axons as numerous studies in development show that the guidance and synaptogenic molecules that bind to these receptors factors can influence the behavior of CST axons [28,35,53]. In the following paragraphs, we summarize the expression pattern of the different families of chemotropic and synaptogenic cues and discuss their potential relevance in the context of the post-injury remodelling of axonal connections.

Slit and Robo family

The attractive or repulsive action of axonal guidance cues in the developing nervous system has been documented extensively (for reviews see [54,55]). One family of these guidance cues are the slit molecules (slit-1, slit-2 or slit-3) and their binding partners the Robo-receptors [56]. These molecules have, for example, been shown to prevent commissural neurons from re-crossing the midline in *Drosophila* [23]. More recently it has been suggested that slits are also expressed after spinal cord injury and can contribute to the failure of axon regeneration at the lesion site in the adult CNS [24]. We can show that slits are not only expressed at the lesion site [24,56] but also in the cervical spinal cord of unlesioned animals. Their receptors in particular robo-1 and robo-2 are expressed throughout the forebrain while robo-3 is more sparsely expressed. This wide-spread expression of slits and robos in the adult CNS has previously been reported and suggests that these molecules also play an important role in the adult nervous system [57]. It is interesting to note that the slits were preferentially expressed by propriospinal neurons compared to glycinergic neurons. As propriospinal neurons are efficiently contacted by

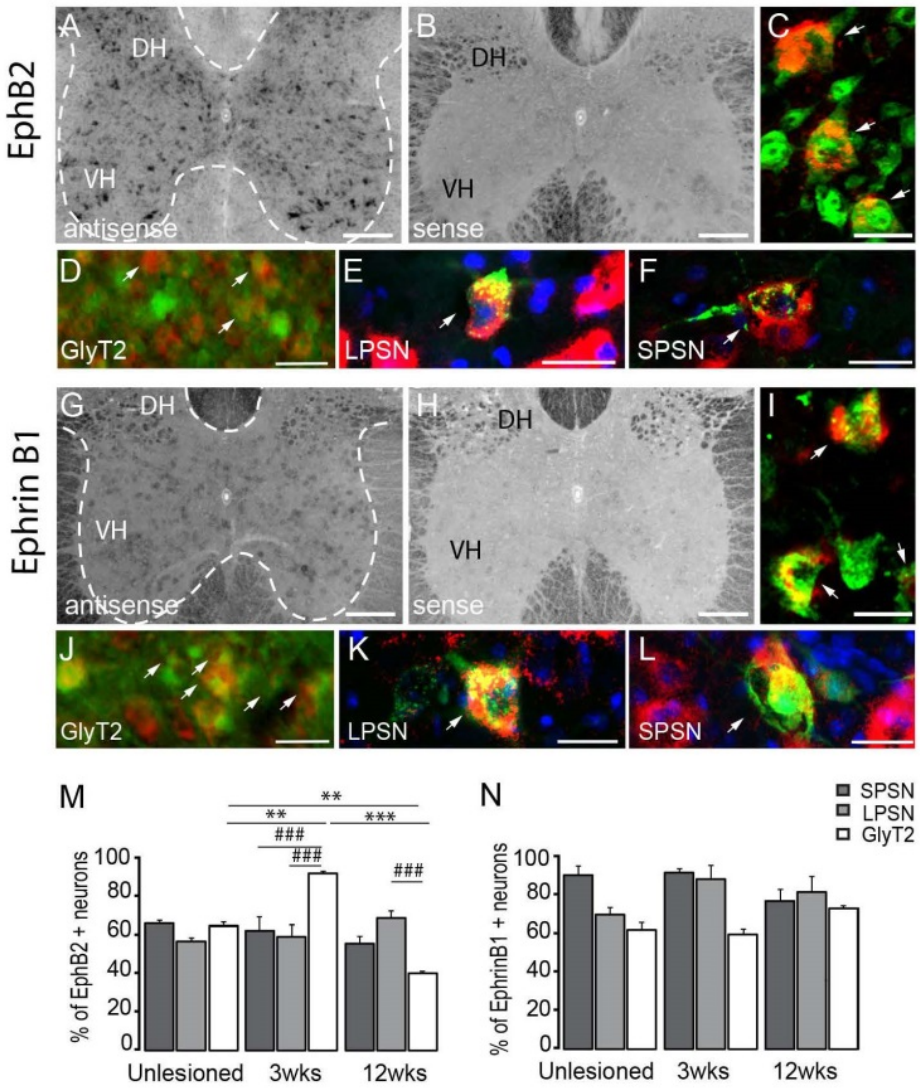

Figure 8. *In Situ* hybridization pattern of EphB2 and EphrinB1 in the cervical spinal cord. *In situ* hybridization of EphB2 (A), mRNA in the unlesioned cervical spinal cord. Intense signals for EphB2 is detected in inter- and motoneurons with the anti-sense (A). No signal is detected with the sense probe (B). (C) Confocal picture of double-labeled neurons in the ventral horn (NeuN, green; EphB2, red). (D-F) Co-localization of EphB2 in glycinergic neurons (D; GlyT2, green; EphB2, red), in LPSN (E; LPSN: green; EphB2: red; NT435: blue) and SPSN (F; SPSN, green; EphB2, red; NT435: blue) in the cervical spinal cord. *In situ* hybridization of EphrinB1 (G), mRNA in the unlesioned cervical spinal cord. Moderate signal for EphrinB1 is detected in inter- and motoneurons with the anti-sense probe (G). No signal is detected with the sense probe (H). (I) Confocal picture of double-labeled neurons in the ventral horn (NeuN: green; EphrinB1: red). (J-L) Co-localization of EphrinB1 in glycinergic neurons (J; GlyT2: green; EphrinB1: red), in LPSN (K; LPSN, green; EphrinB1, red; Neurotrace, blue) and SPSN (L; SPSN: green; EphrinB1: red; NT435: blue) in the cervical spinal cord. DH: dorsal horn; VH: ventral horn. Arrows in D and J show double-labeled glycinergic neurons.Scale bars in A, B,G,H: 250 μm; Scale bar in C,I: 25 μm; Scale bars in D,J: 40 μm; Scale bars in E,F,K,L: 25 μm.
doi:10.1371/journal.pone.0088449.g008

growing CST collaterals this might indicate that, in adulthood after injury, slit expression preferentially triggers neurite growth and arborisation rather than neurite repulsion as it has been shown for cortical interneurons during corticogenesis [58,59].

Semaphorin 6a and 7a and PlexinA2 and C1

Similarly to slits and robos, semaphorins and their receptors, the plexins [4,28,29,60] have been implicated in the control of multiple aspects of neural development, including cell migration and axon guidance [61,62]. In particular the transmembrane class 6 and 7 semaphorins, have been shown to be crucial regulators of axon growth, guidance and cell migration in many different parts of the brain [26–29,62]. In this study we observed that Sema6a and Sema7a are expressed throughout the cervical gray matter. As previously reported, we found that plexinA2 and plexinC1, the respective receptors of Sema6a and Sema7a are expressed in the cortex in particular layer V where the cell bodies of the corticospinal tract resides [63,64]. Interestingly, Sema7a is expressed by all propriospinal neurons but only some glycinergic neurons. As Sema7a is an attractive cue [63] that has been shown to promote axon growth [29] its expression might help to direct growing corticospinal collaterals towards propriospinal neurons during post-injury remodelling. A thoracic hemisection did not change the expression of semaphorin 6a and 7a in the cervical cord. This is in contrast to changes at the site of injury where Sema7a expression is increased in neurons, endothelial cells and components of the glial scar [65].

SynCAMs

For circuits to remodel successfully growing collaterals not only need to reach their appropriate target cells but also form new synaptic connection. The formation of synapses requires the

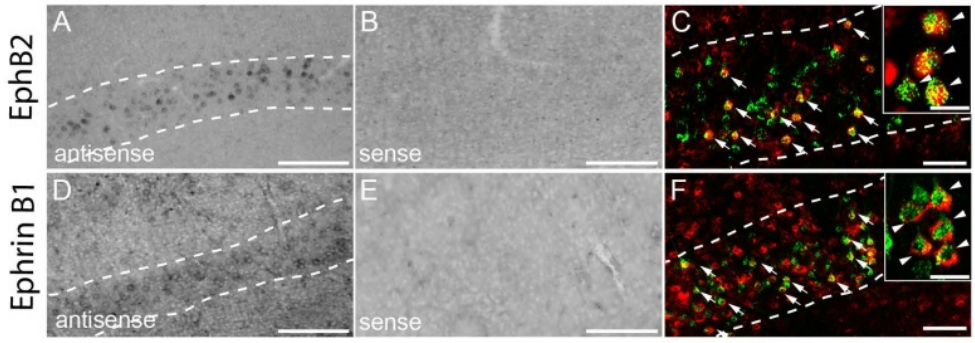

Figure 9. *In Situ* hybridization profile of EphB2 and EphrinB1 in cervical interneurons. *In situ* hybridization of EphB2 (A), EphrinB1 (B) mRNA in the cortex. No signal is detected with the sense probes for EphB2 (B) and EphrinB1 (E). Dotted lines in A and B represent layer V of the cortex. (C, F) Confocal images of double-labeled CST projection neurons (C; retrogradely-labeled CST projection neurons: green; EphB2: red and F; retrogradely-labeled CST projection neurons: green; EphrinB1: red). Scale bars in A, B, D, E: 100 μm; Scale bars C,F: 50 μm (25 μm in insets).
doi:10.1371/journal.pone.0088449.g009

involvement of trans-synaptic adhesion molecules which span the synaptic cleft [66]. How the tight and precise alignment of the pre- and postsynaptic sites is achieved is currently under close investigation. In vertebrates this process is thought to be mediated via synaptic adhesion molecules. Synaptic Cell Adhesion Molecules (SynCAMs) comprise a group of four immunoglobulin (Ig) superfamily members that are crucial for the establishment of new synapses during development [66]. Interestingly these molecules are also prominently expressed in the adult brain [7,66] and spinal cord [67,68]. In line with these findings we detected the expression of SynCAM1, 3 and 4 throughout the cortex with a prominent expression in layer V of the cortex. SynCAMs are also present in interneurons and motoneurons in the spinal gray matter. In addition we detected SynCAM expression in the white matter which is consistent with expression in oligodendrocytes that has been reported by Thomas and colleagues [67]. While SynCAM1 and SynCAM3 were similarly expressed in all interneurons studied, SynCAM4 is preferentially expressed in propriospinal neurons. The latter is reminiscent of the differential presence of SynCAMs in excitatory and inhibitory neurons has been reported previously in the hippocampus [67]. Overall however the abundant expression of SynCAMs in the spinal cord suggests that while they might contribute to formation of synaptic contacts between CST collaterals and spinal interneurons [68] they are unlikely to explain the differential targeting and stabilization of contacts observed during intra-spinal remodelling.

Neuroligins

Neuroligins [46,47] and their presynaptic partners, the neurexins [69,70], are another family of molecules that have been shown to regulate the maturation of functional synapses [30,71,72]. The expression of neurexins in the adult murine cortex has been previously documented [31]. In this study we now show that NL1 and NL4 are expressed throughout the cervical gray matter in both interneurons and in particular in the case of NL1 also in motoneurons. This is consistent with studies showing expression of NL2 and NL3 in spinal motoneurons [73]. Interestingly, NL1 was prominently expressed by propriospinal interneurons. As NL1 is known to be important for excitatory synapse formation [74] it might contribute to the establishment of mature synapses between CST collaterals and propriospinal neurons. Overall neuroligin expression in the neurons located distant from the lesion site in the cervical spinal cord did not changes substantially in response to a thoracic spinal cord injury while a downregulation of neuroligin mRNA expression has been previously reported to occur in transected neurons [73].

Ephrin B1 and EphB2

Ephrins and their receptors (Eph) regulate synaptic function and eph-ephrin interactions can activate both repulsive and attractive forces between cells [32]. As a result these interactions can influence crucial aspects of nervous system development including cell migration, axon guidance, and topographic mapping [32]. Interestingly ephB-ephrinB interaction has been shown to control proper ipsilateral targeting in the visual system and in the developmental CST [35–37]. We now find that ephrinB1 and ephB2 are expressed in neurons throughout the spinal gray matter as well as in parts of the white matter. While expression of ephrinB1 and ephB2 in spinal interneurons has not been reported so far, expression in the white matter has already been shown to occur following SCI and expression of ephB2 has been reported in meningeal cells and of ephrinB1 and ephBs in astrocytes [75]. We also show that both ligands are expressed in layer II-III and V of the cortex consistent with previous reports of ephB2 expression in the brain [76,77]. EphrinB1 and ephB2 were expressed in a large proportion of all interneurons studied both before and after spinal cord injury indicating that, similar to SynCAMs, ephrinB1-ephB2 interactions might contribute to the establishment of functional synapses but are unlikely to explain the differential stabilization of synaptic contacts during post-injury remodelling.

In summary, our systematic characterization of the expression pattern of guidance and synaptogenic molecules in the adult cervical spinal cord demonstrates that a large proportion of the cues that regulate developmental circuit formation are also present during the remodelling of circuits after injury. This suggests that many of the mechanistic insights gained by studying the developing nervous system might also help to better understand how the adult nervous system reacts to injury. Clearly, further studies are warranted to define the roles that each of these molecules play during the formation and maturation of new circuits after injury and ultimately to provide new avenues for the therapeutic support of axonal remodelling.

Acknowledgments

We would like to thank Dana Matzek for excellent animal husbandry, Martin Adrian for excellent technical help and Martin Kerschensteiner for critical reading of the manuscript. Additionally we would like to thank J. Pasterkamp, University of Utrecht; R. Klein, Max-Plank-Institute Munich; J. Burré, Stanford University, Palo Alto; F. Suto, Tohoku University,

Sendai; T. Biederer, Yale University, New Haven and I. Dusart, Paris University, Paris for the generous gift of plasmids.

Author Contributions

Conceived and designed the experiments: AJ FMB. Performed the experiments: AJ AS. Analyzed the data: AJ AS. Wrote the paper: AJ FMB.

References

1. Kolodkin AL, Tessier-Lavigne M (2011) Mechanisms and molecules of neuronal wiring: a primer. Cold Spring Harb Perspect Biol 3(6).
2. Fox MA, Umemori H (2006) Seeking long-term relationship: axon and target communicate to organize synaptic differentiation. J Neurochem 97(5): 1215 1231.
3. Kennedy TE, Wang H, Marshall W, Tessier-Lavigne M (2006) Axon guidance by diffusible chemoattractants: a gradient of netrin protein in the developing spinal cord. J Neurosci 26(34): 8866 8874.
4. Behar O, Golden JA, Mashimo H, Schoen FJ, Fishman MC (1996) Semaphorin III is needed for normal patterning and growth of nerves, bones and heart. Nature 383(6600): 525 528.
5. López-Bendito G, Flames N, Ma L, Fouquet C, Di Meglio T, et al. (2007) Robo1 and Robo2 cooperate to control the guidance of major axonal tracts in the mammalian forebrain. J Neurosci 27(13): 3395 3407.
6. Eberhart J, Swartz M, Koblar SA, Pasquale EB, Tanaka H, et al. (2000) Expression of EphA4, ephrin-A2 and ephrin-A5 during axon outgrowth to the hindlimb indicates potential roles in pathfinding. Dev Neurosci 22(3): 237 250.
7. Biederer T, Sara Y, Mozhayeva M, Atasoy D, Liu X, et al. (2002) SynCAM, a synaptic adhesion molecule that drives synapse assembly. Science 297(5586): 1525 1531.
8. Scheiffele P, Fan J, Choih J, Fetter R, Serafini T (2000) Neuroligin expressed in nonneuronal cells triggers presynaptic development in contacting axons. Cell 9; 101(6): 657 669.
9. Graf ER, Zhang X, Jin SX, Linhoff MW, Craig AM (2004) Neurexins induce differentiation of GABA and glutamate postsynaptic specializations via neuroligins. Cell 119(7): 1013 1026.
10. Henkemeyer M, Itkis OS, Ngo M, Hickmott PW, Ethell IM (2003) Multiple EphB receptor tyrosine kinases shape dendritic spines in the hippocampus. J Cell Biol 163(6): 1313 1326.
11. Bareyre FM, Kerschensteiner M, Raineteau O, Mettenleiter TC, Weinmann O, et al. (2004) The injured spinal cord spontaneously forms a new intraspinal circuit in adult rats. Nat Neurosci 7(3): 269 277.
12. Courtine G, Song B, Roy RR, Zhong H, Herrmann JE, et al. (2008) Recovery of supraspinal control of stepping via indirect propriospinal relay connections after spinal cord injury. Nat Med 14(1): 69 74.
13. Lang C, Guo X, Kerschensteiner M, Bareyre FM (2012) Single collateral reconstructions reveal distinct phases of corticospinal remodelling following spinal cord injury. PLoS ONE 7(1): e30461.
14. Weidner N, Ner A, Salimi N, Tuszynski MH (2001) Spontaneous corticospinal axonal plasticity and functional recovery after adult central nervous system injury. Proc Natl Acad Sci U S A 98(6):3513 3518.
15. Alstermark B, Gorska T, Lundberg A, Pettersson LG (1990) Integration in descending motor pathways controlling the forelimb in the cat. 16. Visually guided switching of target-reaching. Exp Brain Res 80(1): 1 11.
16. Alstermark B, Lundberg A, Pinter M, Sasaki S (1987) Subpopulations and functions of long C3-C5 propriospinal neurones. Brain Res 404(1 2): 395 400.
17. Kerschensteiner M, Bareyre FM, Buddeberg BS, Merkler D, Stadelmann C, et al. (2004) Remodelling of axonal connections contributes to recovery in an animal model of multiple sclerosis. J Exp Med 200(8): 1027 1038.
18. Muramatsu R, Takahashi C, Miyake S, Fujimura H, Mochizuki H, et al. (2012) Angiogenesis induced by CNS inflammation promotes neuronal remodelling through vessel-derived prostacyclin. Nat Med 18(11):1658 1664.
19. Dominici N, Keller U, Vallery H, Friedli L, van den Brand R, et al. (2012) Versatile robotic interface to evaluate, enable and train locomotion and balance after neuromotor disorders. Nat Med 18(7): 1142 1147.
20. van den Brand R, Heutschi J, Barraud Q, DiGiovanna J, Bartholdi K, et al. (2012) Restoring voluntary control of locomotion after paralyzing spinal cord injury. Science 336(6085): 1182 1185.
21. Zeilhofer HU, Studler B, Arabadzisz D, Schweizer C, Ahmadi S, et al. (2005) Glycinergic neurons expressing enhanced green fluorescent protein in bacterial artificial chromosome transgenic mice. J Comp Neurol 482(2): 123 141.
22. Brose K, Bland KS, Wang KH, Arnott D, Henzel W, et al. (1999) Slit proteins bind Robo receptors and have an evolutionarily conserved role in repulsive axon guidance. Cell 96(6): 795 806.
23. Kidd T, Brose K, Mitchell KJ, Fetter RD, Tessier-Lavigne M, et al. (1998) Roundabout controls axon-crossing of the CNS midline and defines a novel subfamily of evolutionarily conserved guidance receptors. Cell 92, 205 215.
24. Wehrle R, Camand E, Chedotal A, Sotelo C, Dusart I (2005) Expression of netrin-1, slit-1 and slit-3 but not of slit-2 after cerebellar and spinal cord lesions. Eur J Neurosci 22(9): 2134 2144.
25. Mauti O, Domanitskaya E, Andermatt I, Sadhu R, Stoeckli ET (2007) Semaphorin6A acts as a gate keeper between the central and peripheral nervous system. Neural Dev 2: 28.
26. Kerjan G, Dolan J, Haumaitre C, Schneider-Maunoury S, Fujisawa H, et al. (2005) The transmembrane semaphorin Sema6A controls cerebellar granule cell migration. Nat Neurosci 8: 1516 1524.
27. Suto F, Tsubio M, Kamiya H, Mizuno H, Kiyama Y, et al. (2007) Interactions between Plexin-A2, Plexin-A4, and Semaphorin6A controls lamina-restricted projection of hippocampal mossy fibers. Neuron 53: 535 547.
28. Rünker AE, Little GE, Suto F, Fujisawa H, Mitchell KJ (2008) Semaphorin-6A controls guidance of corticospinal tract axons at multiple choice points. Neural Dev 3: 34.
29. Pasterkamp RJ, Peschon JJ, Spriggs MK, Kolodkin AL (2003) Semaphorin 7A promotes axon outgrowth through integrins and MAPKs. Nature 424(6947): 398 405.
30. Varoqueaux F, Aramuni G, Rawson RL, Mohrmann R, Missler M, et al. (2006) Neuroligins determine synapse maturation and function. Neuron 51: 741 754.
31. Ullrich B, Ushkaryov YA, Südhof TC (1995) Cartography of neurexins: more than 1000 isoforms generated by alternative splicing and expressed in distinct subsets of neurons. Neuron 14(3): 497 507.
32. Klein R (2004) Eph/ephrin signaling in morphogenesis, neural development and plasticity. Curr Opin Cell Biol 16(5): 580 9.
33. Aoto J, Ting P, Maghsoodi B, Xu N, Henkemeyer M, et al. (2007) Postsynaptic ephrinB3 promotes shaft glutamatergic synapse formation. J Neurosci 27(28): 7508 7519.
34. Klein R (2001) Excitatory Eph receptors and adhesive ephrin ligands. Curr Opin Cell Biol 13(2): 196 203.
35. Yokoyama N, Romero MI, Cowan CA, Galvan P, Helmbacher F, et al. (2001) Forward signaling mediated by ephrin-B3 prevents contralateral corticospinal axons from recrossing the spinal cord midline. Neuron 29: 85 97.
36. Nakagawa S, Brennan C, Johnson KG, Shewan D, Harris WA, et al. (2000) Ephrin-B regulates the ipsilateral routing of retinal axons at the optic chiasm. Neuron 25: 599 610.
37. Williams SE, Mann F, Erskine L, Sakurai T, Wei S, et al. (2003) Ephrin-B2 and EphB1 mediate retinal axon divergence at the optic chiasm. Neuron 39, 919 935.
38. Aimone JB, Leasure JL, Perreau VM, Thallmair M, Christopher Reeve Paralysis Foundation Research Consortium (2004) Spatial and temporal gene expression profiling of the contused rat spinal cord. Exp Neurol 189(2):204 221.
39. Chamankhah M, Eftekharpour E, Karimi-Abdolrezaee S, Boutros PC, San-Marina S, et al. (2013) Genome-wide gene expression profiling of stress response in a spinal cord clip compression injury model. BMC Genomics 28; 14(1):583.
40. Di-Giovanni S, Knoblach SM, Brandoli C, Aden SA, Hoffman EP, et al. (2003) Gene profiling in spinal cord injury shows role of cell cycle in neuronal death. Ann Neurol 53(4):454 468.
41. De-Biase A, Knoblach SM, Di-Giovanni S, Fan C, Molon A, et al. (2005) Gene expression profiling of experimental traumatic spinal cord injury as a function of distance from impact site and injury severity. Physiol Genomics 22(3):368 381.
42. Bareyre FM, Haudenschild B, Schwab ME (2002) Long-lasting sprouting and gene expression changes induced by the monoclonal antibody IN-1 in the adult spinal cord. J Neurosci 22(16):7097 7110.
43. Xu X, Ng S, Wu ZL, Nguyen D, Homburger S, et al. (1998) Human semaphorin K1 is glycosylphosphatidylinositol-linked and defines a new subfamily of viral-related semaphorins. J Biol Chem 273: 22428 22434.
44. Pasquale EB (1997) The Eph family of receptors. Curr Opin Cell Biol 9(5): 608 15.
45. Flanagan JG, Vanderhaeghen P (1998) The ephrins and Eph receptors in neural development. Annu Rev Neurosci 21: 309 345.
46. Ichtchenko K, Hata Y, Nguyen T, Ullrich B, Missler M, et al. (1995) Neuroligin 1: a splice site-specific ligand for beta-neurexins. Cell 81: 435 443.
47. Boucard AA, Chubykin AA, Comoletti D, Taylor P, Sudhof TC (2005) A splice code for trans-synaptic cell adhesion mediated by binding of neuroligin 1 to alpha- and beta-neurexins. Neuron 48: 229 236.
48. Wright DE, White FA, Gerfen RW, Silos-Santiago I, Snider WD (1995) The guidance molecule semaphorin 3 is expressed in regions of spinal cord and periphery avoided by growing sensory axons. J Comp Neurol 361(2): 321 333.
49. Hammond R, Vivancos V, NaeemA, Chilton J, Mambetisaeva E, et al. (2005) Slit-mediated repulsion is a key regulator of motor axon pathfinding in the hindbrain. Dev 132(20): 4483 4495.
50. Philipp M, Niederkopfler V, Debrunner M, Alther T, Kunz B, et al. (2012) RabGDI controls axonal midline crossing by regulating Robo1 surface expression. Neural Dev 7:36
51. Jevince AR, Kadison SR, Pittman AJ, Chien CB, Kaprielian Z (2006) Distribution of EphB receptors and ephrin-B1 in the developing vertebrate spinal cord. J Comp Neurol 497(5):734 750.
52. Kadison SR, Murakami F, Matise MP, Kaprielian Z (2006) The role of floor plate contact in the elaboration of contralateral commissural projections within the embryonic mouse spinal cord. Dev Biol 296(2): 499 513.
53. Bagri A, Marín O, Plump AS, Mak J, Pleasure SJ, et al. (2002) Slit proteins prevent midline crossing and determine the dorsoventral position of major axonal pathways in the mammalian forebrain. Neuron 33(2):233 248.

54. Tessier-Lavigne M, Goodman CS (1996) The molecular biology of axon guidance. Science 274: 1123 1133.
55. Mueller BK (1999) Growth cone guidance: first steps towards a deeper understanding. Annu Rev Neurosci 22: 351 358.
56. Lu YJ, Xu NW, Yang WQ (2008) Immunofluorescence laser confocal expression and localization study of rat nerve growth guidance cues Netrin-1 and Slit2 after spinal cord injury. Chin J Traumatol 11(2): 98 103.
57. Marillat V, Cases O, Nguyen-Ba-Charvet KT, Tessier-Lavigne M, Sotelo C, et al. (2002) Spatiotemporal expression patterns of slit and robo genes in the rat brain. J Comp Neurol 442(2): 130 155.
58. Sang Q, Wu JY, Rao Y, Hsueh Y-P, Tan S-S (2002) Slit promotes branching and elongation of neurites of interneurons but not projection neurons from the developing telencephalon. Mol Cell Neurosci 21: 250 265.
59. Whitford KL, Marillat V, Stein E, Goodman CS, Tessier-Lavigne M, et al. (2002) Regulation of cortical dendrite development by slit robo interactions. Neuron 33: 47 61.
60. Kolodkin AL, Matthes D, Goodman CS (1993) The *semaphorin* genes encode a family of transmembrane and secreted growth cone guidance molecules. Cell 75(7): 1389 1399.
61. Muller B K, Bonhoeffer F, Drescher U (1996) Novel gene families involved in neural pathfinding. Curr Opin Genet Dev 6: 469 474.
62. Mann F, Chauvet S, Rougon G (2007) Semaphorins in development and adult brain: Implication for neurological diseases. Prog Neurobiol 82: 57 79.
63. Pasterkamp RJ, Kolk SM, Hellemons AJ, Kolodkin AL (2007) Expression patterns of semaphorin7A and plexinC1 during rat neural development suggest roles in axon guidance and neuronal migration. BMC Dev Biol 7: 98.
64. Shim SO, Cafferty WB, Schmidt EC, Kim BG, Fujisawa H, et al. (2012) PlexinA2 limits recovery from corticospinal axotomy by mediating oligodendrocyte-derived Sema6A growth inhibition. Mol Cell Neurosci 50(2): 193 200.
65. Kopp MA, Brommer B, Gatzemeier N, Schwab JM, Prüss H (2010) Spinal cord injury induces differential expression of the profibrotic semaphorin 7A in the developing and mature glial scar. Glia 58(14): 1748 1756.
66. Biederer T (2006) Hooking up new synapses. Nat Neurosci 9(10): 1203 1204.
67. Thomas LA, Akins MR, Biederer T (2008) Expression and adhesion profiles of SynCAM molecules indicate distinct neuronal functions. J Comp Neurol 510(1): 47 67.
68. Zelano J, Berg A, Thams S, Hailer NP, Cullheim S (2009) SynCAM1 expression correlates with restoration of central synapses on spinal motoneurons after two different models of peripheral nerve injury. J Comp Neurol 517(5): 670 682.
69. Ushkaryov YA, Petrenko AG, Geppert M, Südhof TC (1992) Neurexins: synaptic cell surface proteins related to the alpha- latrotoxin receptor and laminin. Science 257: 50 56.
70. Ushkaryov YA, Südhof TC (1993) Neurexin III alpha: extensive alternative splicing generates membrane-bound and soluble forms. Proc Natl Acad Sci USA 90: 6410 6414.
71. Scheiffele P, Fan J, Choih J, Fetter R, Serafini T (2000) Neuroligin expressed in nonneuronal cells triggers presynaptic development in contacting axons. Cell 101: 657 669.
72. Dean C, Scholl FG, Choih J, DeMaria S, Berger J, et al. (2003) Neurexin mediates the assembly of presynaptic terminals. Nat Neurosci 6: 708 716.
73. Zelano J, Wallquist W, Hailer NP, Cullheim S (2007) Down-regulation of mRNAs for synaptic adhesion molecules Neuroligin-2 and -3 and SynCAM1 in spinal motoneurons after axotomy. J Comp Neurol 503: 308 318.
74. Song JY, Ichtchenko K, Suedhof TC, Brose N (1999) Neuroligin 1 is a postsynaptic call-adhesion molecule of excitatory synapses. Proc Natl Acad Sci USA 96: 1100 1105.
75. Bundesen LQ, Scheel TA, Bregman BS, Kromer LF (2003) Ephrin-B2 and EphB2 regulation of astrocyte-meningeal fibroblast interactions in response to spinal cord lesions in adult rats. J Neurosci 23(21): 7789 800.
76. Moreno-Flores MT, Wandosell F (1999) Up-regulation of Eph tyrosine kinase receptors after excitotoxic injury in adult hippocampus. Neurosci 91(1): 193 201.
77. Wang Y, Ying GX, Liu X, Wang WY, Dong JH, et al. (2005) Induction of ephrin-B1 and EphB receptors during denervation-induced plasticity in the adult mouse hippocampus. Eur J Neurosci 21(9): 2336 46.

3.3

FGF22 signaling regulates synapse formation during post injury remodeling of the spinal cord

Anne Jacobi, Kristina Loy, Anja M Schmalz, Mikael Hellsten, Hisashi Umemori, Martin Kerschensteiner and Florence Bareyre

A manuscript to be submitted (2014)

FGF22 signaling regulates synapse formation during post injury remodeling of the spinal cord

Anne Jacobi[1], Kristina Loy[1], Anja M. Schmalz[1], Mikael Hellsten[1], Hisashi Umemori[2,3], Martin Kerschensteiner[1,4] and Florence M. Bareyre[1,4]

1. Institute of Clinical Neuroimmunology, Ludwig-Maximilians University Munich, Munich, Germany

2. Molecular and Behavioral Neuroscience Institute, University of Michigan Medical School, Ann Arbor, USA

3. Department of Biological Chemistry, University of Michigan Medical School, Ann Arbor, USA

4. Munich Cluster of Systems Neurology (SyNergy), Munich, Germany

Correspondence should be addressed to

F.M.B. (Florence.Bareyre@med.uni-muenchen.de)

Keywords: spinal cord injury, axonal remodeling, synapse formation, fibroblast growth factor, functional recovery

Words: 1135 Figures: 3 (+ 9 Suppl. Figures) References: 21

The remodeling of axonal circuits requires the formation of new synaptic contacts to enable functional recovery after injury. Here we show that depletion of FGF22 or its receptors FGFR1 and FGFR2 impairs formation of new synapses, delays synapse maturation and impedes functional recovery in a mouse model of spinal cord injury. Hence, FGF22 acts as a synaptogenic mediator in the adult CNS and is required for efficient post-injury remodeling.

Incomplete lesion of the spinal cord can be followed by substantial functional recovery in both human patients and rodent models. This recovery is mediated by the remodeling of spinal and supraspinal axonal circuits (Bareyre et al., 2004; Bareyre et al., 2005; Courtine et al., 2008; Courtine et al., 2009; Lang et al., 2011; Vander Brand et al., 2012; Beauparlant et al., 2013). The hindlimb corticospinal tract (CST), for example, responds to a thoracic transection with the de novo formation of intraspinal detour circuits that circumvent the lesion site and re-establish a functional connection between the motor cortex and the lumbar spinal cord (Bareyre et al., 2004; Kerschensteiner et al., 2004; Lang et al., 2011). The key step in the formation of this detour circuits is the establishment of new synaptic contacts between newly formed CST collaterals that enter the cervical gray matter and long propriospinal neurons that are located in the cervical cord and act as a relay to lumbar motor circuits. While the functional importance of this and similar detour circuits has been well established over the recent years (Bareyre et al., 2004; Courtine et al., 2008; Vander Brand et al., 2012; Beauparlant et al., 2013) it is currently unclear which mechanisms regulate the formation of these circuits. In particular, little is known about the molecular signals that can induce the formation of new synapses in the injured adult CNS.

In the developing nervous system however a number of synaptogenic molecules have been identified (Jessel and Sanes, 2000, Sanes and Lichtman, 2001). These include the family of the fibroblast growth factors and their receptors that have emerged as important regulators of presynaptic differentiation (Umemori et al., 2004; Terauchi et al., 2010; Stevens et al., 2010; Lee and Umemori, 2013; Singh et al., 2012). One member in particular, FGF22, is crucial for the establishment of excitatory synapses as shown for CA3 pyramidal cells in the developing hippocampus

(Terauchi et al., 2010). To investigate whether FGF22 signaling could also regulate synapse formation during post injury remodeling we first determined the expression and localization of FGF22 in the spinal cord of adult mice using in situ hybridization and single cell laser microdissection followed by quantitative PCR analysis (see Online Methods). Our results showed that FGF22 is expressed in spinal interneurons including a large proportion of long propriospinal neurons both constitutively as well as after spinal cord injury (Fig. 1a-d). To directly assess the role of spinal FGF22 expression we performed a T8 spinal cord injury in FGF22 deficient mice (Terauchi et al., 2010). Deletion of FGF22 reduced the formation of CST boutons (Fig. 1e, f) as well as the proportion of LPSN relay neurons that are contacted (Fig. 1 g, h) at 3 weeks after injury, while the sprouting and branching of CST collaterals was not affected (Supplementary Fig. 1). Deletion of FGF22 did not affect the normal development of mature CST projection in healthy mice (Supplementary Fig. 2). To better understand which receptors mediate FGF22 signaling to CST collaterals we first established that the two main FGF receptors, FGFR1 and FGFR2 (Umemori et al., 2004; Lee and Umemori, 2013) were expressed in the cortex of adult mice (Fig. 1 i-m) and then conditionally deleted them in the forebrain by crossing floxed mouse strains to EMX-Cre mice (Fox et al., 2007). While deletion of the receptors did not affect the development of a mature CST projection pattern in healthy mice (Supplementary Figure 3 and 4), the deletion of either FGR1 or FGR2 reduced the formation of synaptic bouton on newly formed CST collaterals. A similar reduction was observed in double-floxed mice, in which both FGFR1 and FGFR2 were selectively deleted in the hindlimb motor cortex by stereotactic injection of an rAAV-GFP-Ires- Cre (Fig.1 n,o) indicating that the effect of FGF22 on synapse formation requires the presence of both receptors on cortical projection neurons. Notably, reduced synapse formation was compensated by increased sprouting of CST collaterals if either FGFR1 or FGFR2 was deleted but not if both receptors were missing (Supplementary Figure 5) suggesting that FGF22 signaling via either receptor participates in the induction of compensatory CST sprouting. As a result only mice in which both FGFR1 and R2 were deleted showed impaired formation of detour circuits (Fig. 1p).

To evaluate whether FGF22 signaling not only regulates the formation of new synapses but also their molecular composition (as suggested by results in the developing hippocampus; Terauchi et al., 2012), we evaluated the expression of an

early (Bassoon, Lang et al., 2012) and late (Synapsin, Lang et al., 2012) marker of synapse maturation in newly formed hindlimb CST collaterals at different time points after injury by confocal microscopy and quantitative immunohistochemical analysis. We observed that deletion of either FGFR1 or FGFR2 alone led to a delay in synapse maturation that was most obvious at 3 weeks after injury whereas complete deletion of FGFR signaling either by conditional depletion of both receptors or by depletion of FGF22 enhanced the delay and induced synapse maturation defects that persisted for more than 12 weeks after injury (Fig. 2).

Finally we wanted to understand whether delayed synapse formation and maturation of newly formed CST collaterals would indeed affect the spontaneous recovery of CST function that follows an incomplete spinal cord injury. For this we performed T8 dorsal hemisection and followed the recovery of CST function using specific behavioral testing paradigms such as the “ladder rung test” (Metz and Wishaw, 2009) in FGF and FGFR competent control mice and in mice in which FGFR22 signaling was genetically interrupted by FGF22 deletion or the conditional ablation of FGFR1 and R2 receptors. Deletion of FGF22 or co-deletion of FGFR1 and R2 in the hindlimb motor cortex significantly delayed functional recovery in behavioral test paradigms (Fig. 3). Deletion of either FGFR1 or FGFR2 alone did not alter functional recovery likely due to the compensatory increase in CST sprouting that prevented deficits in detour circuit formation (Supplementary Figure 6).

Together, the targeted deletion of FGF22 and its receptors FGFR1 and FGFR2 thus identify an important contribution of FGF22-FGFR signaling to the formation new CST boutons, the maturation of synaptic contacts and the recovery of locomotor function after spinal cord injury. These results establish that FGF22 acts as a synaptogenic mediator in the adult nervous system and a crucial regulator of synapse formation and maturation during post-injury remodeling in the CNS.

Acknowledgments

We would like to thank Martin Adrian and Geraldine Heitmann, for excellent technical assistance, Dana Matzek for animal husbandry, Klaus Dornmair for his help with single cell laser microdissection and quantitative PCR and Alexander Gun for their help analyzing normal CST maturation in mutant mice. Work in F.M.B.'s lab is supported by grants from the Deutsche Forschungsgemeinschaft (DFG, SFB 870) and the German Federal Ministry of Education and Research (BMBF). Work in M.K.'s laboratory is financed through grants from the DFG (Transregio 128), the BMBF (Competence Network Multiple Sclerosis), the European Research Council under the European Union's Seventh Framework Program (FP/2007-2013; ERC Grant Agreement n. 310932), the Hertie-Foundation and the "Verein Therapieforschung für MS-Kranke e.V.". F.M.B. and M.K. are supported by the Munich Center for Systems Neurology (SyNergy; EXC 1010).

AUTHORS CONTRIBUTIONS

F.M.B., H.U. and M.K. conceived the experiments. A.J. performed spinal surgeries and tracing. A.J. and A.M.S. performed and analyzed in situ hybridizations and single cell PCR. A.J., K.L., A.M.S. and F.M.B. contributed to anatomical and immunohistochemical analysis. H.U. characterized mutant mouse strains. A.J. and K.L. performed and analyzed behavioral testing. F.M.B., A.J. and M.K. wrote the paper.

The authors declare no competing financial interests.

REFERENCES

1. Bareyre F.M. et al. Nat Neurosci 7, 269-277 (2004).

2. Bareyre FM, Kerschensteiner M, Misgeld T, Sanes JR. Nat Med 11 (12):1355-1360 (2005).

3. Courtine G, Song B, Roy RR, Zhong H, Herrmann JE, Ao Y, Qi J, Edgerton VR, Sofroniew MV. Nat Med 14 (1): 69-74 (2008).

4. Lang C, Guo X, Kerschensteiner M, Bareyre FM. Single collateral reconstructions reveal distinct phases of corticospinal remodeling following spinal cord injury. PLoS ONE 7 (1): e30461 (2012).

5. Weidner N, Ner A, Salimi N, Tuszynski MH. Proc Natl Acad Sci U S A 98 (6):3513-3518 (2001).

6. van den Brand R, Heutschi J, Barraud Q, DiGiovanna J, Bartholdi K, Huerlimann M, Friedli L, Vollenweider I, Moraud EM, Duis S, Dominici N, Micera S, Musienko P, Courtine G. Science 336 (6085): 1182-1185 (2012).

7. Beauparlant J, van den Brand R, Barraud Q, Friedli L, Musienko P, Dietz V, Courtine G. Brain 136 (Pt 11):3347-61 (2013).

8. Kerschensteiner M, Bareyre FM, Buddeberg BS, Merkler D, Stadelmann C, Brück W, Misgeld T, Schwab ME. J Exp Med 200(8): 1027-1038 (2004).

9. Terauchi A, Johnson-Venkatesh EM, Toth AB, Javed D, Sutton MA, Umemori H. Nature 465:783-787 (2010).

10. Jessell TM, Sanes JR. Development. The decade of the developing brain. Curr Opin Neurobiol. 10(5):599-611. (2000)

11. Sanes JR, Lichtman JW. Induction, assembly, maturation and maintenance of a postsynaptic apparatus. Nat Rev Neurosci. 2(11):791-805 (2001).

12. Umemori H, Linhoff MW, Ornitz DM, Sanes JR. Cell 118:257-270 (2004).

13. Stevens HE, Smith KM, Maragnoli ME, Fagel D, Borok E, Shanabrough M, Horvath TL, Vaccarina FM. J. Neurosci 30 (16): 5590-5602 (2010).

14. Lee CH, Umemori H. Front Cell Neurosci. 7:43. doi: 10.3389/fncel.2013.00043 (2013).

15. Singh R, Su J, Brooks J, Terauchi A, Umemori H, Fox MA. Front Mol Neurosci. 4:61. doi: 10.3389/fnmol.2011.00061 (2012).

16. Gorski, J.A. Cortical excitatory neurons and glia, but not GABAergic neurons, are produced in the Emx1-expressing lineage. J. Neurosci. 22, 6309-14 (2002).

17. Bareyre FM, Garzorz N, Lang C, Misgeld T, Büning H, Kerschensteiner M. Proc Natl Acad Sci U S A. 108(15):6282-7 (2011).

18. Lang C, Bradley PM, Jacobi A, Kerschensteiner M, Bareyre FM. EMBO Rep. 14(10):931-7 (2013).

19. Muramatsu R, Takahashi C, Miyake S, Fujimura H, Mochizuki H, Yamashita T. Nat Med 18(11):1658-1664 (2012).

20. Fox MA, Sanes JR, Borza DB, Eswarakumar VP, Fassler R, Hudson BG, John SW, Ninomiya Y, Pedchenko V, Pfaff SL, Rheault MN, Sado Y, Segal Y, Werle MJ, Umemori H. Cell 129(1):179-93 (2007).

21. Metz GA, Whishaw IQ. The ladder rung walking task: a scoring system and its practical application. Vis Exp. Jun 12;(28) (2009).

FIGURE LEGENDS

Figure 1. Deletion of FGF22 or its receptors impairs synapse formation and circuit remodeling after spinal cord injury. (a) In situ hybridization of FGF22 mRNA in the spinal cord of FGF22 competent and FGF22 deficient mice (right panel). (b) In situ hybridization showing localization of FGF22 signal in LPSN retrogradely labeled from T12 (LPSN: green; FGF22: red; Neurotrace 435: Blue). (c) Quantification of the percentage of LPSN showing FGF22 in situ signal in unlesioned mice ("Ctrl") and at 3 ("3w") and 12 ("12w") weeks after injury (n=5 in all groups). (d) Images illustrating single cell laser microdissection to perform quantitative single cell PCR. Top panel shows three long propriospinal neurons (LPSN) retrogradely labeled from T12 with Texas Red. Bottom panel shows the two remaining LPSN after one (asterisk) has been microdissected. (e) Quantification of single cell PCR analysis of FGF22 expression in LPSN in unlesioned mice ("Ctrl") and at 3 ("3w") and 12 ("12w") weeks after injury (n=5 in all groups). (f) Confocal images showing synaptic boutons on newly formed cervical hindlimb CST collateral 3 weeks following spinal cord injury (Left panel: FGF22 competent mouse; Right panel: FGF22 deficient mouse). (g) Quantification of boutons density on newly formed cervical hindlimb CST collaterals in FGF22 competent and deficient mice (n=8 per group). (h) Confocal image of putative synaptic contacts between CST collaterals (green) and LPSN (red). (i) Quantification of the percentage of LPSN contacted by CST collaterals in FGF22 competent and deficient mice (n=8 per group). (j, k) In situ hybridization of FGFR1 (top) and FGFR2 (bottom) mRNA in FGFR competent animals (j) and forebrain FGFR1 (k, top panel) and FGFR2 (k, bottom panel) deficient mice. (l) Retrograde labeling of CST neurons with Texas Red® (green) show that CST neurons express FGFR1 and FGFR2 (insets in k top and bottom are two-fold magnification of boxed areas). (m) Quantification of the percentage of CST neurons in layer V of the cortex expressing FGFR1 and FGFR2 (n=3 per group). (n) Quantification of the intensity of the in situ signal for FGFR1 in FGFR2 deficient mice and FGFR2 in FGFR1 deficient mice (n=3 per group). (o) Confocal images showing synaptic boutons on newly formed cervical hindlimb CST collateral 3 weeks following spinal cord injury (left panel: FGFR competent animal; Right panels: forebrain FGFR1, FGFR2 and FGFR1R2 deficient mice). (p) Quantification of the bouton density on newly formed cervical hindlimb CST collaterals in FGFR competent and forebrain FGFR deficient animals (n=8 for all group but FGFR1R2 co-deletion in which n=7). (q) Quantification

of the percentage of LPSN contacted by CST collaterals in FGFR competent and forebrain FGFR deficient mice (n=8 for all group but FGFR1R2 co-deletion in which n=7). Scale bars equal 200µm in a (10µm in inset); 20µm in b, 75µm in c, 20µm in f, 30µm in h, 200µm in j and k, 100µm in l (20µm in insets), 20µm in o. p value *p<0,05; **p value<0,01; *** p value< 0,001. Unpaired t-tests were used for two–column comparisons, ANOVA followed by Tukey tests were used in case of multiple group comparison.

Figure 2: Deletion of FGF22 or its receptors delays synapse maturation following spinal cord injury. (a) Confocal image of Bassoon immune reactivity (red) in synaptic contacts between a CST collateral (green) and a LPSN (blue). Right images are magnification (two-fold) of the area boxed on the left. (b) Quantification of the percentage of boutons on cervical hindlimb CST collaterals that are immunoreactive for Bassoon at 3 weeks (left panel) and 12 weeks (right panel) after spinal cord injury in FGF22 deficient and forebrain FGFR1, FGFR2 and FGFR1R2 deficient mice compared to FGF22 and FGFR competent mice ("Control"). (c) Confocal image of Synapsin immune reactivity (red) in synaptic contacts between a CST collateral (green) and a LPSN (blue). Right images are magnification (two-fold) of the area boxed on the left. Confocal image of a synaptic contact between CST collateral (green), a propriospinal neuron (blue). (d) Quantification of the percentage of boutons on cervical hindlimb CST collaterals that are immunoreactive for Synapsin at 3 weeks (left panel) and 12 weeks (right panel) after spinal cord injury in FGF22 deficient and forebrain FGFR1, FGFR2 and FGFR1R2 deficient mice compared to FGF22 and FGFR competent mice ("Control"). Scale bars equal 20µm in a; and 20µm in b. T-test was used for paired comparisons, ANOVA followed by Tukey tests were used in case of multiple group comparison.

Figure 3: Genetic disruption of FGF22 signaling impedes functional recovery following spinal cord injury. (a) Image of a spinal cord injured animal performing the ladder rung test that assesses recovery of CST function. (b) Quantification of the functional recovery in the ladder rung test (irregular walk, upper panel; regular walk, lower panel) in control (white bars), FGF22 deficient (red bars) and forebrain FGFR1

R2 deficient (blue bars) mice. Repetitive ANOVA followed by Tukey tests were used for multiple group comparison.

ONLINE METHODS

Animals: Adult mice from 6 to 12 weeks of age were used in the study. FGFR1fl/fl and FGFR2fl/fl mice (Yu et al., 2003; Pirvola et al., 2002), in which the FGFR1 or FGFR2 gene is flanked by loxed P sites have been used to study the importance of FGFR1 and FGFR2 to post-injury remodeling. Littermates have been used as controls. To delete FGFR1 or FGFR2specifically in the CST, we have crossed FGFR1fl/fl and FGFR2fl/fl mice to Emx1-Cre mice (Gorski et al., 2002; Bareyre et al., 2004) which trigger Cre expression in the forebrain as of embryonic day 10. For co-deletion of the two receptors in the CST, we did crossed FGFR1fl/fl and FGFR2fl/fl until obtaining double floxed offsprings. Then we injected adeno-associated viruses expressing the cre recombinase in layer V of the hindlimb motor cortex. To identify the role of FGF22 in the process of detour circuit formation after injury we used FGF22 knock-out mice (Terauchi et al., 2010). Normal wildtype C57Bl6j mice (Janvier, France) were used as control group for the FGF22 KO mice. All animal procedures were performed according to institutional guidelines and were approved by the Regierung von Oberbayern.

Generation and production of AAV vectors: pAAV- GFP-Ires-Cre was created by inserting an Ires sequence (from pIres2-DsRed2 (BD Bioscience) at the HincII site. The Cre coding sequence was excised from PBS185 (kind gift of Thomas Hughes, Montana State University) and inserted upstream to the Ires sequence at the site. Green Fluorescent protein (GFP) was excised from pEGFP-N1 and inserted downstream to the Ires sequence at. The Control pAAV-CMV-Ires2-GFP used was a kind gift of Hildegard Büning (Medical University of Cologne). pAAV-CMV-FGF22-Ires-GFP was created by excising FGF22 coding sequence from APtag5 (H. Umemori, Michigan University) with NheI, XhoI and ligating it into the pAAV –CMV-Ires-hrGFP vector (Stratagene) at the HincII site. The original pAAV-Ires-hrGFP

(Stratagene) for the above cloning was used as control. Production was done as indicated.

Genomic titers were as follows:

pAAV-GFP-Ires2-Cre, 1,2 x 10^12 genomes copies /ml

pAAV- Ires2-GFP, 2,4 x 10^12 genomes copies/ml

pAAV-FGF22-Ires-hrGFP, 2,06x10^13 genome copies/ml;

Control pAAV-Ires-hrGFP, 6,55x10^13 genome copies/ml;

Surgical procedures

Midthoracic dorsal hemisection. Mice were anesthetized with a subcutaneous injection of ketamin/xylazine (ketamine 100 mg/kg, xylazine 13 mg/kg). After a laminectomy to expose the dorsal spinal cord at thoracic level 8 (T8), a midthoracic dorsal hemisection, which results in a transection of the main dorsal and minor dorso-lateral CST component, was performed with fine iridectomy scissors as previously described (Lang et al., 2011; Lang et al., 2012). Prior to and after surgery animals were kept on a heating pad (38°C) until fully awake and treated with Metacam (Boehringer Ingelheim) twice per day for 48 hours.

Deletion of FGFR1 or FGFR2 and co-deletion of FGFR1 R2: To ablate FGFR1 or FGFR2 specifically in the CST, FGFR1fl/fl or FGFR2fl/fl were crossed to EMX1-Cre mice (Bareyre et al., 2005). For co-deletion of FGFR2 and FGFR1, FGFR1fl/fl were crossed to FGFR2fl/fl until obtaining homozygote double-floxed mice. Then, 0,7µl of rAAV-GFP-Ires2-Cre or control rAAV-Ires2-GFP were concentration-matched (to 0.6 x10^12 genomes copies /ml) and then pressure-injected 4 days prior to the lesion into the hindlimb motor cortex using a finely pulled glass micropipette (coordinates from bregma: -1.3mm caudal; 1.0mm lateral; 0.6mm depth).The micropipette remained in place for 3 minutes following the injection. This produced deletion of FGFR1R2 in the motor cortex and labeled the CST in these co-deleted mice. In order to verify that the virus remained confined to the hindlimb motor cortex and did not spread to the forelimb area, we amplified the GFP signal with an anti – GFP

antibody (rabbit polyclonal anti GFP; Invitrogen A11122), cut consecutive 50µm thick sections of the entire brain of all mice in order and determined the spread of the labeling of GFP labeled cells in layer V (Suppl. Fig. 7 a,b). Mice in which the labeling reached the forelimb motorcortex (coordinate from bregma: +0.5mm caudal) were excluded from the evaluation. To confirm that genetic FGFR deletion was similar to viral FGFR deletion, we virally deleted FGFR2 in the hindlimb cortex by injecting 0,7µl of AAV-GFP-Ires-Cre at the following coordinates (bregma: -1.3mm caudal; 1.0mm lateral; 0.6mm depth). No differences in boutons number, branchpoints and exiting CST collaterals could be seen between the genetic (see Fig. 1p,q) and the viral (Suppl. Fig. 8) FGFR2 deletion.

Labeling of the hindlimb CST (hCST) fibers: The hindlimb CST of FGFR1fl/fl or FGFR2 fl/fl crossed with the EMX-Cre mice (n= 8 per group) was traced by pressure injecting 1,5µl of a 10% (in 0.1M PB) solution of biotinylated dextran amine (BDA, 10 000 MW, Life Technologies) into the hindlimb motor cortex using a finely pulled glass micropipette two weeks prior to sacrifice using the following coordinates: −1.3 mm posterior to bregma, 1 mm lateral to bregma, 0.6mm depth. The micropipette remained in place 3 minutes following the injection.

Labeling of long propriospinal neurons: Long propriospinal neurons were retrogradely labeled by pressure injections of 0.5µl of 2.5% TexasRed (dextran, fluorescein, 3000 MW, Life technologies) or 0.25µl of 2% Fluoro–GoldTM (Santa Cruz Biotechnology; sc-358883). Briefly, a laminectomy was performed at thoracic level 12 as previously described (Lang et al., 2013) and the 0.5µl of 2.5% TexasRed or the 0.25µl of 2% Fluoro-GoldTM was injected into each side of the spinal cord using a thin glass capillary (coordinates from central vein: ± 0.6mm; depth: 0.9mm). The capillary was maintained in place for 3 minutes following the injection. Mice were sacrificed 3 or 12 weeks after dorsal hemisection.

Tissue processing and histological analysis: Mice were deeply anesthetized with isoflurane and perfused transcardialy with saline solution followed by 4% paraformaldehyde (PFA) in 0.1M phosphate buffer (PBS). Brains and spinal cords were dissected and post-fixed overnight in PFA. The tissue was then cryoprotected in 30% sucrose (Sigma) for at least 3 days. Coronal sections (50µm thick) were cut on

a cryostat. To visualize CST collaterals, BDA detection was performed as follows: Sections were incubated in ABC complex (Vector Laboratories) overnight at 4°C. After a 20 min tyramide amplification (Biotin-XX, TSA Kit #21, Life technologies) sections were incubated overnight with Streptravidin conjugated to FITC 488 (1:500, Life technologies). To visualize CST collaterals of the rAAV injected mice, an anti – GFP staining was performed to amplify the GFP signal. Anti – GFP antibody (dilution 1:500; Life Technologies A11122) diluted in PBS containing 0.1% Triton X-100 and 2.5% goat serum (Life Technologies) was thus applied and incubated over night at 4°C. On day 2, the corresponding secondary antibody was applied for at least 4 hours (goat anti rabbit conjugated with Alexa 488).

For synapse characterization, 20µm thick sections were cut and blocked for 1 hour with 5% GS (Life technologies) and 0.3% Triton X-100 diluted in 1 x PBS in which the hCST was labeled either with BDA or with the rAAV-CMV-GFP-Ires2-Cre. Sections were incubated with ABC (Vector Laboratories) and a primary polyclonal antibody reactive against synapsin I (Millipore AB1543; dilution 1:500) or a primary mouse monoclonal antibody reactive against bassoon (ENZO Life Science SAP7F407, dilution 1:200) in Tris buffer containing 0.3% Triton X-100 (Sigma) and 2.5% goat serum (Invitrogen) overnight at 4°C. The following day, after a 20 min tyramide amplification (Biotin-XX, TSA Kit #21, Invitrogen) to detect BDA, sections were then incubated together with Streptavidin-FITC 488 (1:500, Life technologies) and the appropriate secondary antibodies for the synaptic markers (donkey anti rabbit conjugated with Alexa Fluor 647 or goat anti rabbit conjugated with Alexa Fluor 635) incubated over night at 4°C. For rAAV-injected animals (FGFR1R2 co-deletion), the sections were first incubated with an anti – GFP antibody (see above) to amplify the GFP signal (Invitrogen, A11122) together with the primary antibodies against synapsin I or bassoon (concentrations as above) in 2.5% GS and 0.1% Triton X-100 in 1 x PBS over night at 4°C. On the next day the appropriate secondary antibodies for the GFP labeling (goat anti rabbit conjugated with Alexa Flour 488) and for synapse staining (donkey anti rabbit conjugated with Alexa Fluor 647 or goat anti rabbit conjugated with Alexa Fluor 635) were applied over night at 4°C. The counterstaining was performed with NeuroTrace 435 (Invitrogen) and sections were mounted in Vectashield (Vector Laboratories).

Quantification of synaptic markers: To determine the percentage of boutons that express the synaptic markers Synapsin I and Bassoon image stacks of about 20 sections spanning the C3 to C5 area of the spinal cord (20µm thickness, with every 5th section taken) were acquired with an Olympus FV1000 confocal microscope equipped with standard filter sets and a 660 (NA 1.45) oil immersion objective. Image stacks obtained with confocal microscopy were processed using ImageJ software to generate maximum intensity projections. On those, the percentage of Synapsin I or Bassoon positive boutons were determined by counting the number of Synapsin I or Bassoon positive boutons upon the following criteria's: A bouton was defined as a varicosity along the newly born collateral in the cervical spinal cord. Therefore this varicosity on the collateral is clearly distinguishable by its thickness from the thin arm of the collateral itself. To assess co-labeling of the boutons we used the following evaluation criteria: A bouton was considered Synapsin I or Bassoon positive when its contour was clearly overlaid with the synapse staining and did not extend beyond it. The number of boutons positive for Synapsin I or Bassoon was determined and expressed as a percentage of all boutons on the collaterals counted in the cervical spinal cord. A minimum of 100 boutons was counted. All quantifications were performed by an observer blinded with respect to injury status and treatment.

Quantification of CST remodeling: To evaluate axonal remodeling following a midthoracic dorsal hemisection, traced CST collaterals entering the grey matter at cervical levels C4 were counted on 30 consecutive coronal sections per animal using a light microscope (Olympus IX471) with a x40/0.65 air objective. To correct for differences in inter-animal tracing efficiency, the number of collaterals was divided by the number of traced fibers in the main CST tract and expressed as the ratio of collaterals per main CST fiber (Bareyre et al., 2004). All quantifications were performed by an observer blinded with respect to injury status and treatment.

Quantification of contacts onto LPSN: For quantifying the number of contacts formed onto LSPN a total amount of 30 sections was evaluated using a fluorescent microscope (Olympus IX471) with a x40/0.65 air objective. Collaterals were visualized as mentioned above (tyramide amplification or GFP amplification), the total number of LPSN labeled was counted and the total number of contacts onto those was examined. The number of LPSN was expressed as a ratio of all LPSN contacted

by collaterals over the total number of all LPSN. All quantifications were performed by an observer blinded with respect to injury status and treatment.

Quantification of the length of the collaterals: To determine the length of the collaterals 10 sections spanning the C3 to C5 area of the spinal cord (50µm thickness, sections randomly taken) were acquired with an Olympus FV1000 confocal microscope equipped with standard filter sets and a 660 (NA 1.45) oil immersion objective. Image stacks obtained with confocal microscopy were processed using ImageJ software to generate maximum intensity projections. The lengths of all collaterals in those sections were measured with the help of the measurement tool of ImageJ and a mean of the collaterals length per animal was acquired. All quantifications were performed by an observer blinded with respect to injury status and treatment.

Cortical neuronal density: To determine whether genetic deletion of FGFR1 or FGFR2 at embryonic day 10 or full deletion of FGF22 alters cortical lamination and cortical neuronal density, we cut 50µm brain sections and performed NeuN immunohistochemistry (Gt anti-NeuN, Millipore, dilution 1:500, 4°C overnight). Counterstaining was performed with Neurotrace500. The density of cells in layer V of the motorcortex and sensory – motorcortex was quantified by counting the number of NeuN positive cells in every third section all through the hindlimb cortex for a total of 10 sections per animal. All quantifications were performed by an observer blinded with respect to injury status and treatment.

Lesion volume and Regeneration at lesion site: We verified the extent of the spinal cord lesion in all animals, by performing analysis of lesion volume. Lesion volume was assessed on spinal cord longitudinal 50µm sections spanning the entire lesion extent at thoracic level. Following staining with a fluorescent Nissl dye (NT435, LifeTechnologies N-21479, dilution 1:500) the sections were scanned using an Olympus IX71 microscope. Images were then processed with ImageJ and the lesion area, including both the cavity and surrounding damaged tissue, was outlined. To quantify the lesion volume, the measured lesion area of each section was multiplied by the section thickness (50µm) and the results of all consecutive sections spanning the entire lesion extension were summed up for each animal to provide a final estimation of the total lesion volume (Suppl. Figure 9a).

To determine the effect of deletion of FGF22 on the growth of CST fibers after a midthoracic dorsal hemisection, we analyzed consecutive longitudinal sections of the midthoracic spinal cord. Image stacks were recorded on Olympus IX71 microscope. The number of BDA-labeled growing fibers in the dorsal funiculus that intersected with a dorso-ventral lines positioned every 100µm distal from the lesion site was counted. The lesion site was identified visually and level 0 was positioned at the end of the retracting non growing fibers. The total number of growing fibers counted on 4-5 consecutive longitudinal 50µm thick sections was then normalized to the number of fibers in the main CST tract (obtained from the dorsal funiculus at cervical C5 level) and divided by the number of sections evaluated. The value obtained for a given distance is the number of CST fibers per labeled CST axons per section, the “fiber number index”. To exclude a contribution from spared fibers, only fibers emerging from the dorsal main CST and extending in the dorsal funiculus were counted (Suppl. Figure 9b).

In situ Hybridization: Spinal cord tissue (cervical region C3-C5, 20µm thick) and brain tissue (Bregma -1.06 till -1.70, 30µm thick) were sectioned coronally using the cryostat (Leica CM1850) and processed as described previously (Jacobi et al., 2014). Briefly, all steps very carried out with DEPC treated solutions to prevent degradation of target RNAs. Sections were washed in 2X SSC (from 20X stock solution containing 3M NaCl and 0,3M Na Citrate) and before the prehybridization step, the sections were incubated in a 1:1 mixture of 2X SSC and hybridization buffer (50% Formamide, 5X SSC, 5X Denhardt’s solution (Sigma-Aldrich D2532), 250µg/ml yeast tRNA, 500µg/ml salmon sperm DNA) for 15min at RT. Sections were then incubated for 1hr in hybridization buffer at the appropriate (pre-) hybridization temperature (65°C). For hybridization, the probe (200-400ng/ml in hybridization buffer) was heated for 10min at 80°C, applied to the tissue and incubated overnight in an oven at 65°C. Sections were then rinsed at RT in 2X SSC and washed in decreasing concentration of SSC (2X to 0.1X SSC at hybridization temperature) before applying an alkaline-phosphatase-conjugated sheep anti-digoxigenin antibody, Fab fragments (1:2000; Roche Diagnostics) in blocking buffer overnight at 4°C. Alkaline phosphatase activity was detected using nitroblue tetrazolium chloride (337.5mg/ml) and 5-Bromo-4-chloro-3-indolyl phosphate (175mg/ml) (Carl Roth). The sections were washed in ddH2O after the staining procedure. The fluorescent Nissl

stain Neurotrace 435 was applied for 2h at RT; the sections were washed and mounted with Gel Mount (Sigma Aldrich).

Lasermicrodisection: Total RNA was isolated from LPSN in unlesioned animals and 3 weeks after lesion (n = 2 per timepoint). For this purpose 20µm thick fresh frozen coronal sections (C3-C5) were collected on Membrane Slides 1.0 PET (Zeiss). Sections were covered with n-propanol to prevent drying and to inhibit RNase activity, and immediately transferred to a PALM Microbeam-Z microscope. LPSN retrogradely labeled with TexasRed and located between layers 6 to 9 in C4 were marked electronically. After evaporation of the n-propanol, a total of 10 marked neurons were microdissected and laser pressure catapulted into a reaction tube (AdhesiveCap 200 clear PCR tubes, Zeiss) and directly put on dry ice. After microdissection, it was visually verified that all neurons were actually captured. For single cell, QPCR, we used the kit Lifetechnologies. Shortly, one single cell is lysed in 10µl Single Cell Lysis/Dnase I solution à 5 min RT. 1 µL of Stop Solution is added to lysis reaction -à2min RT and 4.5 µL of RT Mix is added à RT: Incubate for 10 min at 25 °C. Incubation is carried for 60 min at 42 °C and for 5 min at 85 °C. Then 11 µL of PreAmp Mix with Primers is added (FGF22 Forward primer 5'- ACT TTT TCC TGC GTG TGG AC -3', FGF22 Reverse primer 5'- TCA TGG CCA CAT AGA AGC CT -3'; GapDH Forward primer 5'-TCA ACG ACC CCT TCA TTG-3', GapDH Reverse primer 5'-ATG CAG GGA TGA TGT TCT G-3'). PreAmplification reaction is as follows: 95 °C 10 min; 14 cycles: 95 °C for 15 sec, 56 °C for 2 min, 60 °C for 2 min. Probes are diluted 1:10 in H2O. 5µl of the probe is used for qPCR in a total volume of 20µl. Then we use the 2xSsoAdvanced Universal SYBR Green Supermix (BioRad) for QPCR with the following protocol: 95°C 3min; 95°C 10sec; 56°C 10sec; (39 repeats).the melting curve is carried with 65°C to 95°C increments.

Behavioral Analysis: The following behavioral tests were used to assess locomotor recovery after spinal cord injury.

BMS: We used the Basso mouse scale to assess overall recovery of hindlimb locomotion after a spinal lesion. Following the ranking system previously described (Basso et al., 2006) mice were given scores from 0-9, with a score of 0 indicating no ankle movement and a score of 9 indicating frequent or consistent plantar stepping, mostly coordinated stepping, paws parallel at initial contact and lift off, normal trunk stability and tail consistently up. For evaluation, the mice (n = 12 per group) were

placed in an open field for 4 min and assessed by two observers blinded to the genotype of the mice. Mice were assessed before and 2, 7, 14 and 21 days after lesion. For overexpression experiments the mice were assessed until 8 weeks after lesion.

Ladder Rung: For more refined assessment of the CST function following spinal cord injury, we used the ladder rung test, or grid walk, which has been described previously (Metz and Whishaw, 2009). Animals were scored for their ability to cross accurately a 1 m long horizontal metal-rung runway with varying gaps of 1–2 cm between the rungs. All animals underwent a couple of familiarization sessions with the apparatus prior to pre-operative baseline testing. Following familiarization, sessions were videotaped and scored to determine baseline performance. Pre-operative score as well as post-operative performance on day 7, 14 and 21 post injury, and for the long term analysis of the mice were both receptors have been ablated (FGFR1fl/fl ;FGFR2fl/fl) at 8, 10 and 12 weeks after lesion, were collected. A hindlimb foot error was defined as a complete miss or slip from the rung at the moment of the placement of the paw onto the rung. Baseline and post-operative testing sessions consisted of 3 runway crossings. The total number of errors and steps by the hindlimbs in each session was counted.

REFERENCES (ONLINE METHODS)

Yu, K. et al. Conditional inactivation of the FGF receptor 2 reveals an essential role for FGF signaling in the regulation of osteoblast function and bone growth. Development 130, 3063-3074 (2003).

Pirvola, U. et al. FGFR1 is required for the development of the auditory sensory epithelium. Neuron 35, 671-680 (2002)

Terauchi A, Johnson-Venkatesh EM, Toth AB, Javed D, Sutton MA, Umemori H. Distinct FGFs promote differentiation of excitatory and inhibitory synapses. Nature. 465(7299):783-7 (2010).

Bareyre FM, Kerschensteiner M, Misgeld T, Sanes JR. Transgenic labeling of the corticospinal tract for monitoring axonal responses to spinal cord injury. Nat Med. 2005 Dec;11(12):1355-60 (2005).

Hofbauer M, Wiesener S, Babbe H, Roers A, Wekerle H, Dornmair K, Hohlfeld R, Goebels N. Clonal tracking of autoaggressive T cells in polymyositis by combining lasermicrodissection, single-cell PCR, and CDR3-spectratype analysis. Proc Natl Acad Sci U S A. 100(7):4090-5. (2003).

Seitz S, Schneider CK, Malotka J, Nong X, Engel AG, Wekerle H, Hohlfeld R,Dornmair K. Reconstitution of paired T cell receptor alpha- and beta-chains from microdissected single cells of human inflammatory tissues. Proc Natl Acad Sci U S A. 103(32):12057-62 (2006).

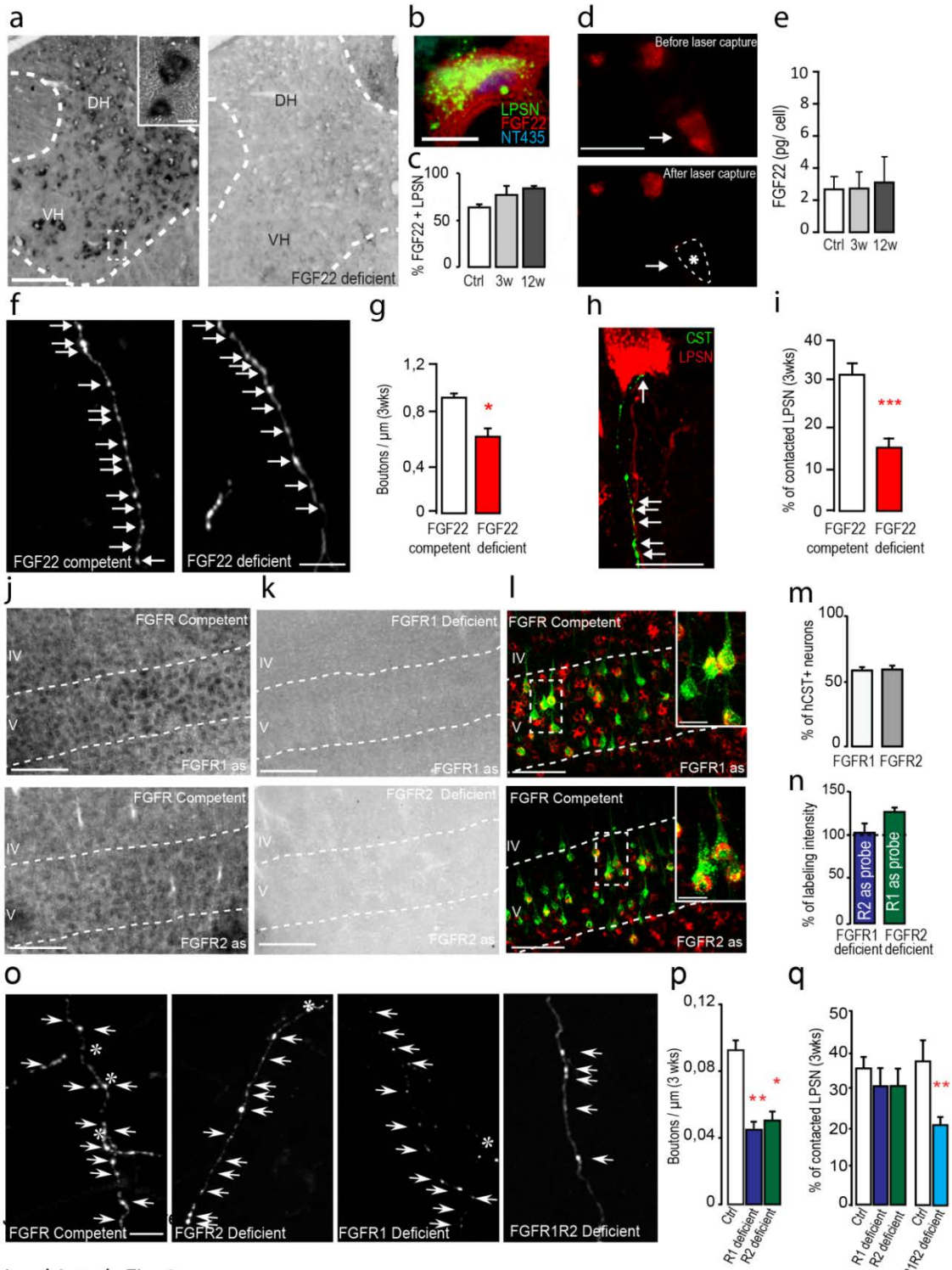

Jacobi et al., Fig. 1

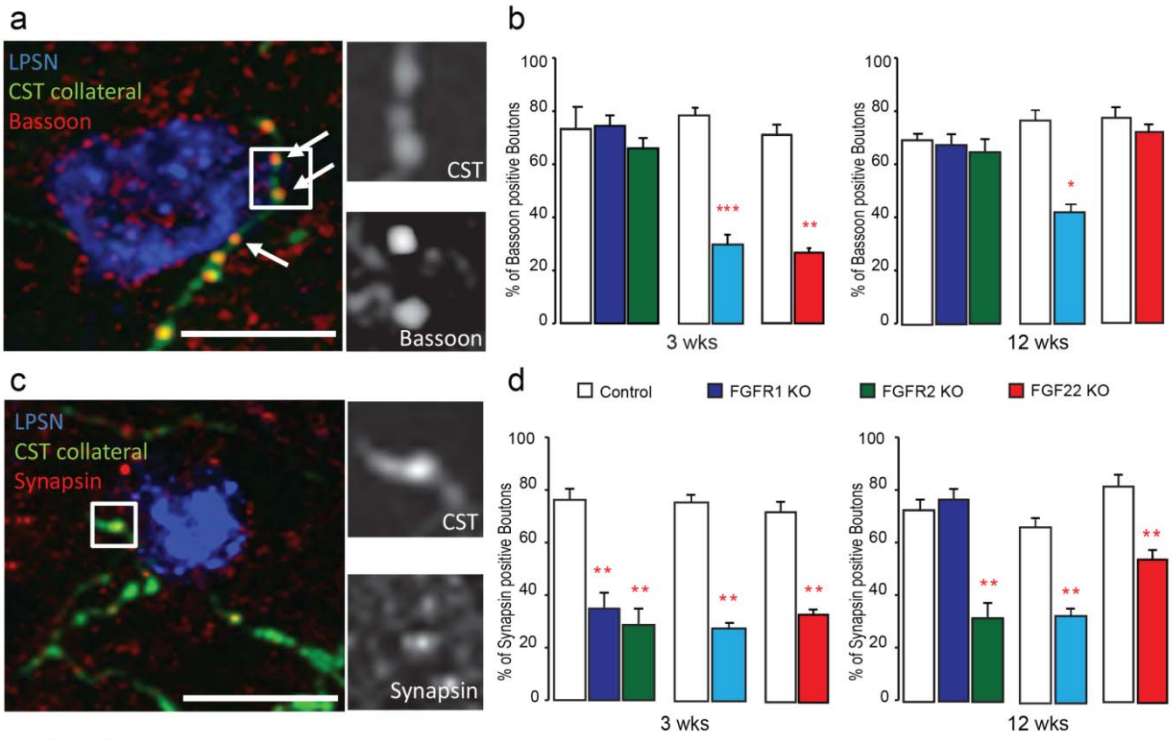

Jacobi et al., Fig.2

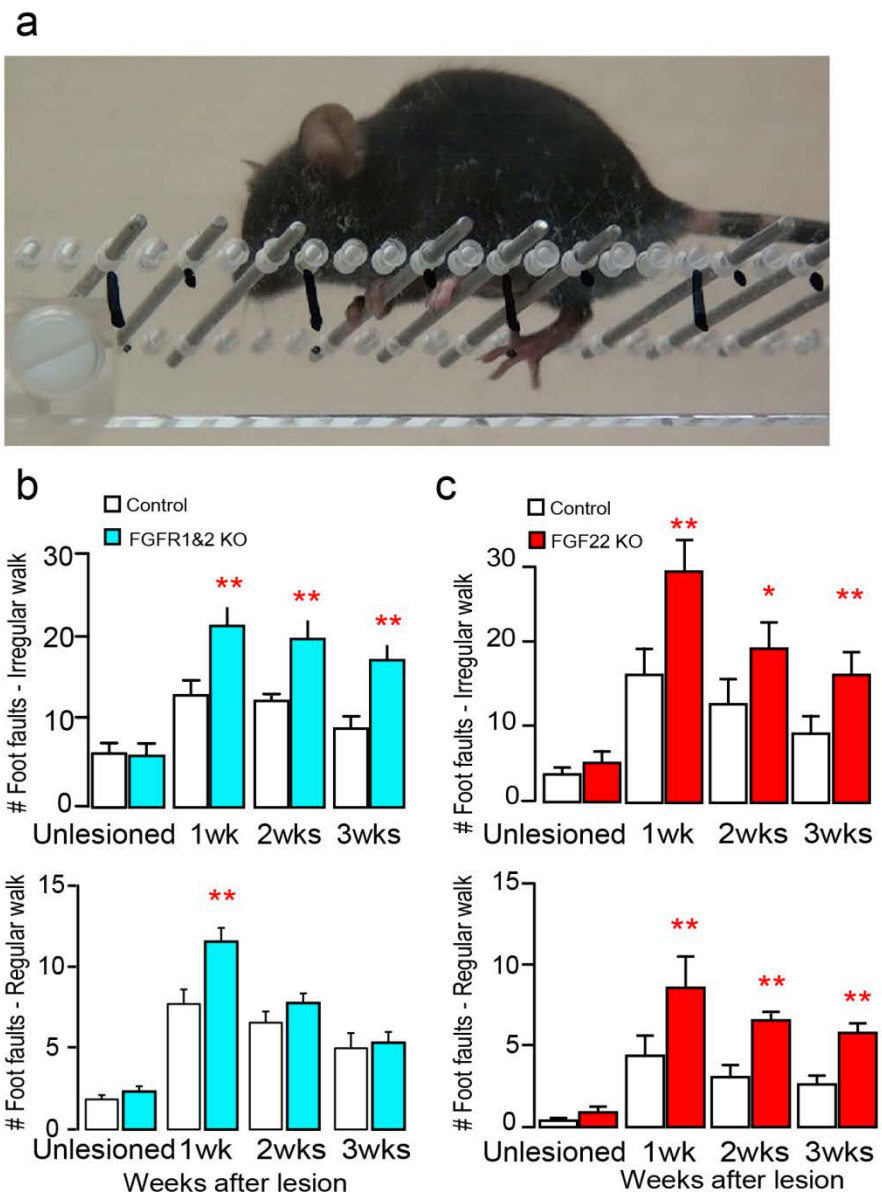

Jacobi et al., Fig. 3

FGF22 signaling regulates synapse formation during post injury remodeling of the spinal cord

– Supplementary Information –

Anne Jacobi[1], Kristina Loy[1], Anja M. Schmalz[1], Mikael Hellsten[1], Hisashi Umemori[2,3], Martin Kerschensteiner[1,4] and Florence M. Bareyre[1,4]

[1] Institute of Clinical Neuroimmunology, Ludwig-Maximilians University Munich, Munich, Germany

[2] Molecular and Behavioral Neuroscience Institute, University of Michigan Medical School, Ann Arbor, USA

[3] Department of Biological Chemistry, University of Michigan Medical School, Ann Arbor, USA

[4] Munich Cluster of Systems Neurology (SyNergy), Munich, Germany

Correspondence should be addressed to:

F.M.B. (Florence.Bareyre@med.uni-muenchen.de)

Keywords: spinal cord injury, axonal remodeling, synapse formation, fibroblast growth factor, functional recovery

SUPPLEMENTARY FIGURES and LEGENDS

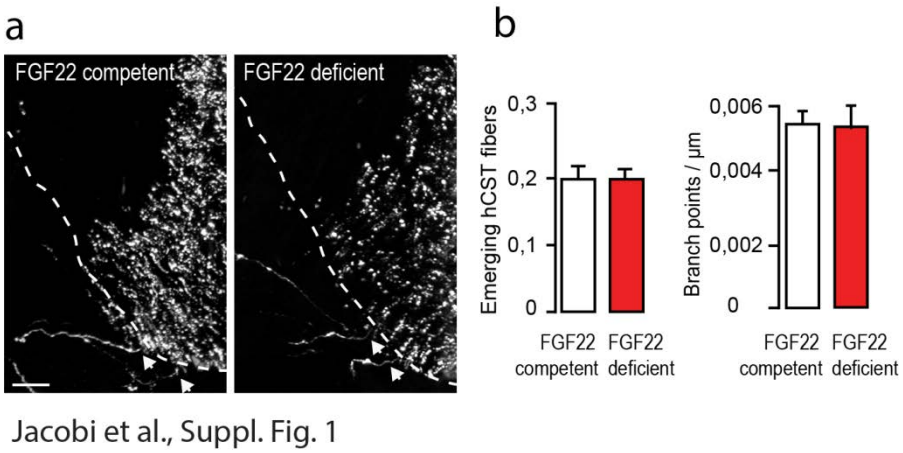

Jacobi et al., Suppl. Fig. 1

Supplementary Figure 1. FGF22 deletion does not change CST sprouting and CST branching following spinal cord injury. (a) Confocal images of exiting hindlimb CST collaterals in the cervical cord 3 weeks following T8 hemisection in FGF22 competent (left panel) and FGF22 deficient (right panel) mice. **(b)** Quantification of the number of exiting CST collaterals and of the number of hindlimb CST collateral branch points 3 weeks following T8 hemisection in FGF22 competent and deficient animals (n=8 per group; compared using unpaired *t*-test) . Scale bar in **a (both panels)**: 40 µm.

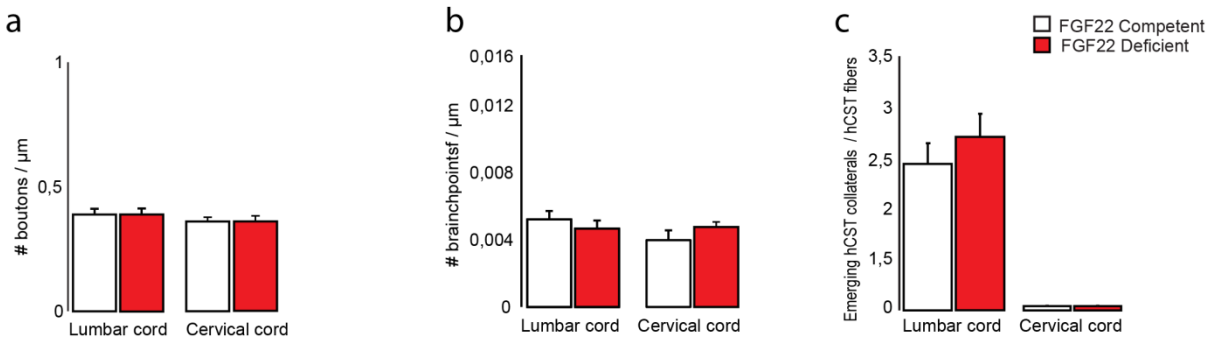

Jacobi et al., Suppl. Fig. 2

Supplementary Figure 2. Normal hindlimb CST maturation is not altered in forebrain FGF22 deficient mice. (a) Quantification of the number of boutons, **(b)** branchpoints and **(c)** of exiting CST collaterals in FGF22 competent and deficient mice (n=6 per group; compared using unpaired t-test).

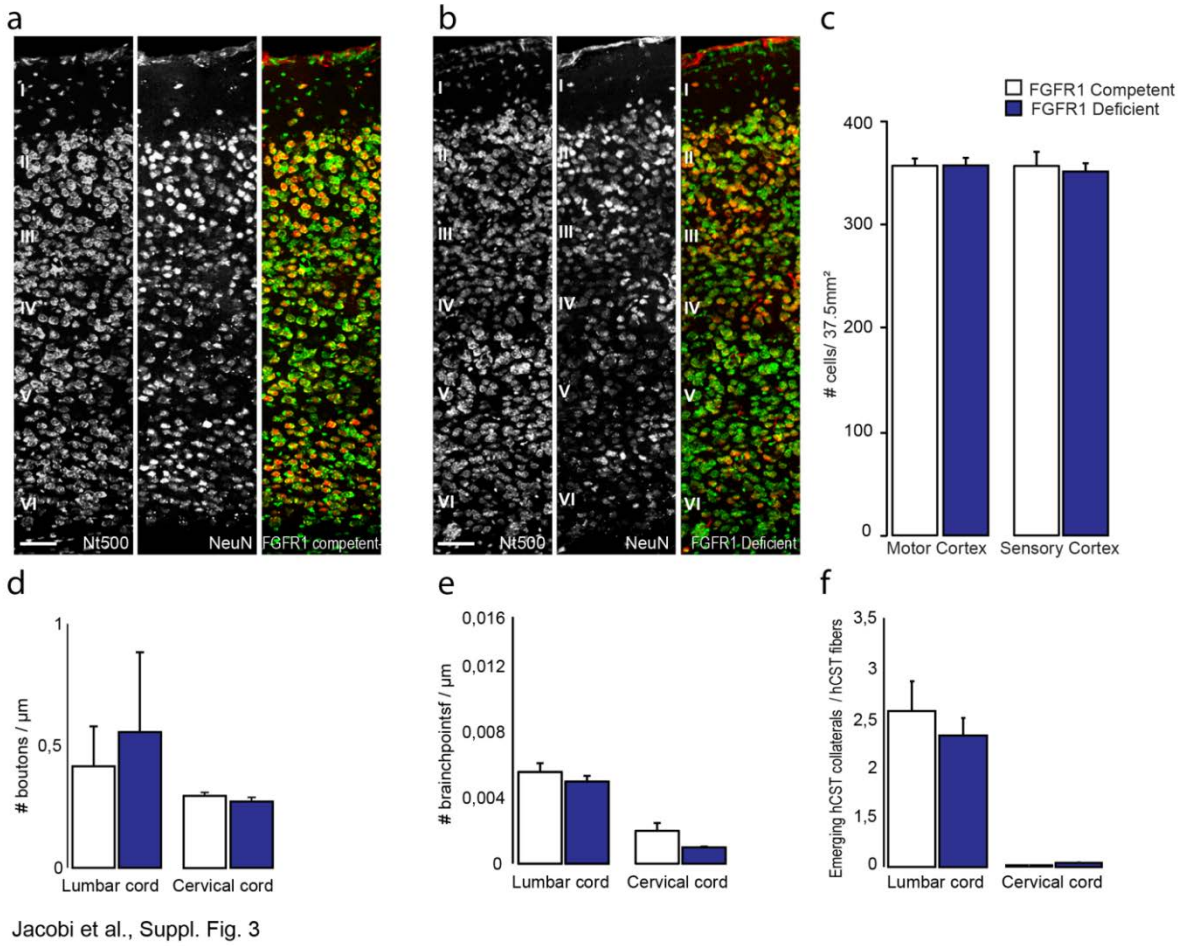

Supplementary Figure 3. Normal hindlimb CST maturation is not altered in forebrain FGFR1 deficient mice. (**a,b**) Confocal images of the cortex of FGFR1 competent (**a**) and forebrain FGFR1 deficient (**b**) mice. (**c**) Quantification of the number of neurons in layer V of the cortex in FGFR1 competent and forebrain FGFR1 deficient mice (n=3 per group; compared using unpaired *t*-test). (**d-f**) Quantification of the number of boutons (**d**) and branchpoints (**e**) per µm hindlimb CST collateral and the number of emerging hindlimb CST collaterals (**f**) in FGFR1 competent and forebrain FGFR1 deficient mice (n=6 per group; compared using unpaired *t*-test). Scale bar in **a, b**: 100 µm.

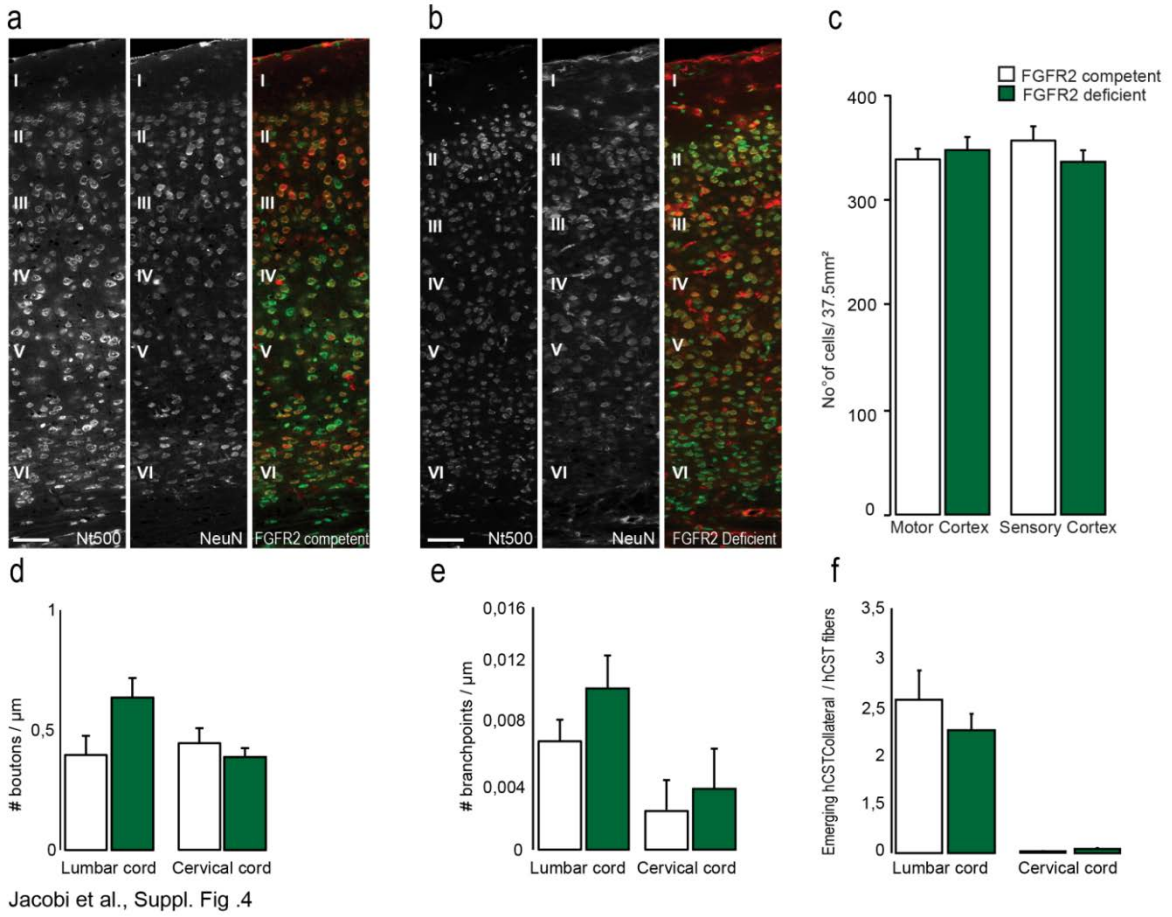

Supplementary Figure 4. Normal hindlimb CST maturation is not altered in forebrain FGFR2 deficient mice. (**a,b**) Confocal images of the cortex of FGFR2 competent (**a**) and forebrain FGFR2 deficient (**b**) mice. (**c**) Quantification of the number of neurons in layer V of the cortex in FGFR2 competent and deficient mice (n=3 per group; compared using unpaired *t*-test). (**d-f**) Quantification of the number of boutons (**d**) and branchpoints (**e**) per µm hindlimb CST collateral and the number of emerging hindlimb CST collaterals (**f**) in FGFR2 competent and forebrain FGFR2 deficient mice (n=6 per group; compared using unpaired *t*-test). Scale bar in **a, b**: 100 µm.

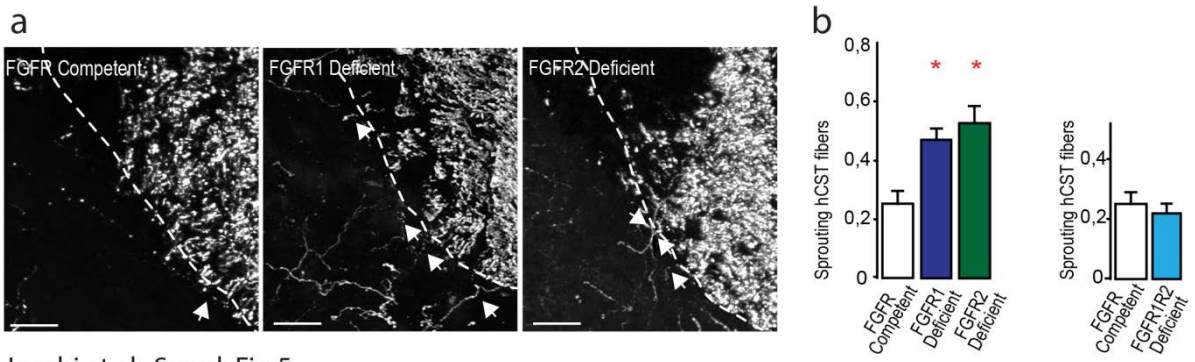

Jacobi et al., Suppl. Fig 5

Supplementary Figure 5. Deletion of either FGFR1 or FGFR2 but not deletion of both increases CST sprouting following spinal cord injury. (a) Confocal images of exiting CST collaterals in the cervical cord 3 weeks following T8 hemisection in FGFR competent (left panel) and forebrain FGFR1, FGFR2, FGFR1R2 deficient (right panels) mice. **(b)** Quantification of the number of exiting CST collaterals and of the number of CST collateral branch points 3 weeks following T8 hemisection in FGFR competent and forebrain FGFR deficient animals (n=8 per group except for FGFR1R2 deficient group in which n=7; compared using an ANOVA followed by Tukey test for the experiment with the single FGFR KO and with an unpaired *t*-test for the experiment using the double FGFR KO, * P <0,05). Scale bar in **a**: 40 μm.

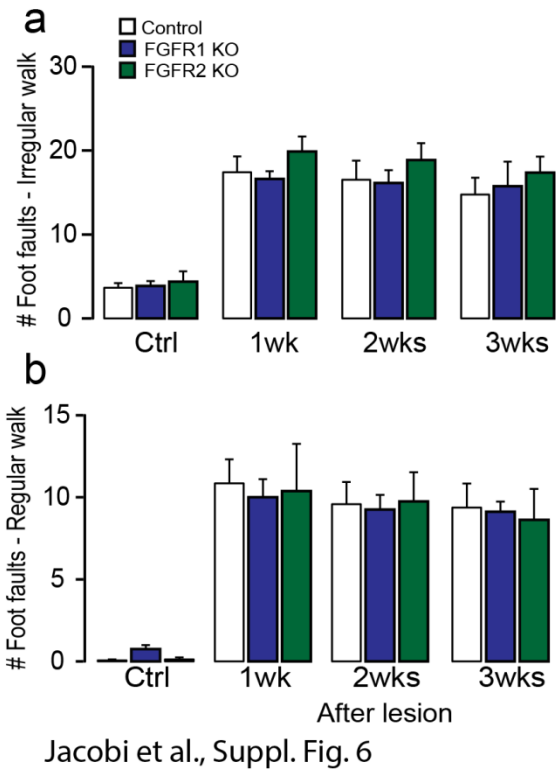

Supplementary Figure 6. Deletion of either FGFR1 or FGFR2 does not impair functional recovery after spinal cord injury. (**a**) Quantification of functional recovery in the ladder rung test (irregular walk) in control (white bars) and conditional FGFR1 (dark blue bars) or FGFR2 (green bars) deficient mice (n=8 per group; compared with a repeated ANOVA followed by post-hoc test). (**b**) Quantification of functional recovery in the ladder rung test (regular walk) in control (white bars) and conditional FGFR1 (dark blue bars) or FGFR2 (green bars) deficient mice (n=8 per group; compared with a repeated ANOVA followed by post-hoc test).

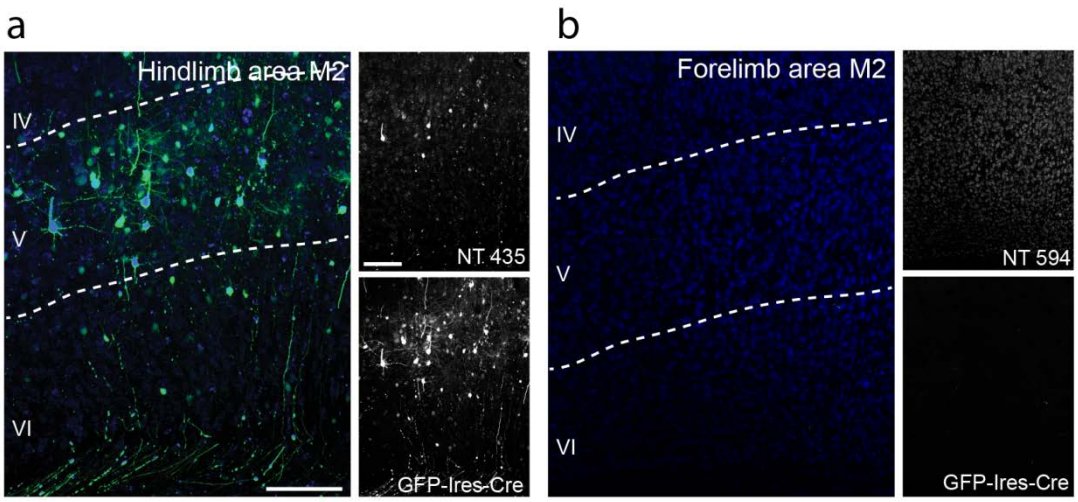

Jacobi et al., Suppl. Fig. 7

Supplementary Figure 7. Stereotactic injection of AAVs allows selective targeting of the hindlimb motor cortex. (**a**) Confocal image of the hindlimb motor cortex 3 weeks following injection of rAAV-GFP-Ires-Cre illustrating the presence of many transduced neurons (green) in layer V of the cortex (blue, counterstaining with Neurotrace 435). (**b**) No transduced neurons (green) are seen in the forelimb motor cortex of the same animals. Scale bar in **a, b**: 150 μm.

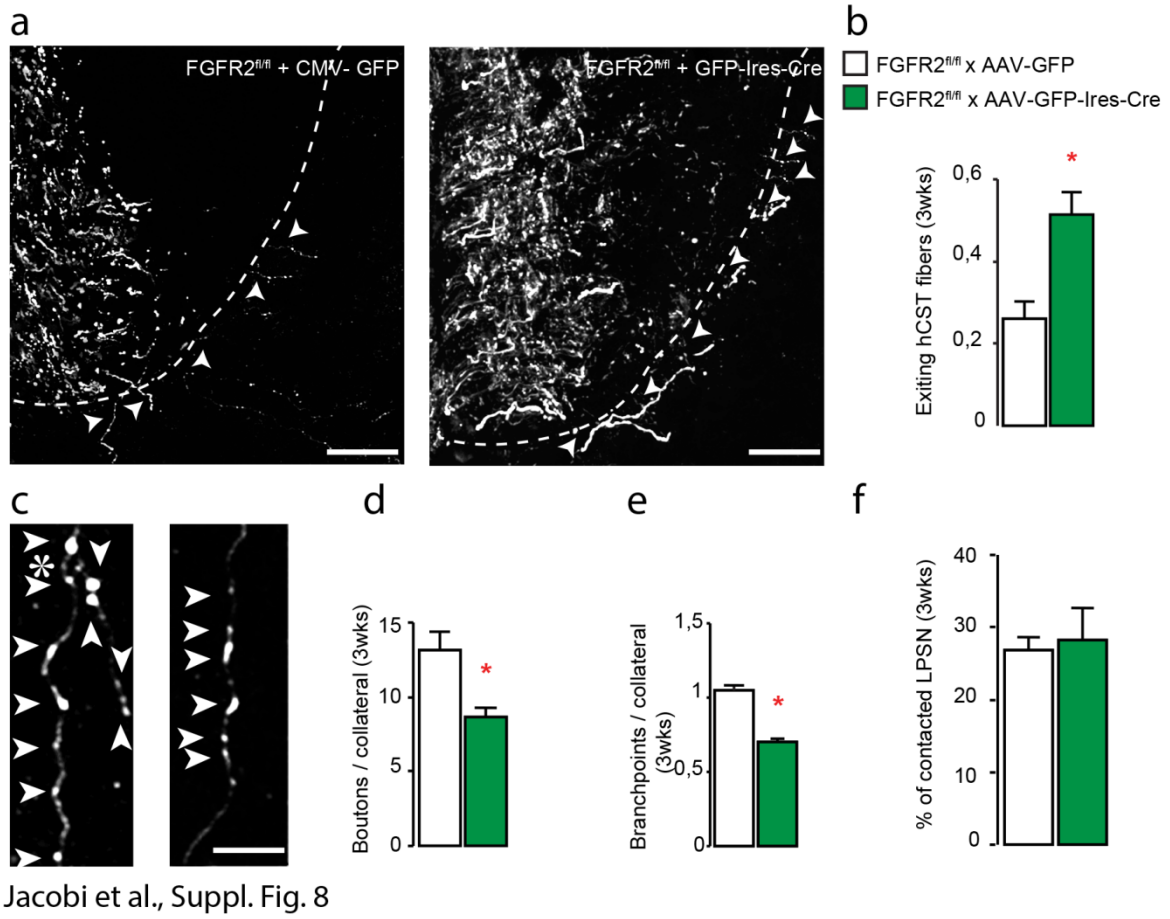

Supplementary Figure 8. Genetic and viral deletion of FGFR2 has similar effects on post-injury remodeling. (**a**) Confocal images of exiting hindlimb CST collaterals in the cervical grey matter 3 weeks following spinal cord injury in FGFR2 floxed mice after injection of either rAAV-GFP (left panel) or rAAV-GFP-ires-Cre (right panel) in the hindlimb motor cortex. (**b**) Quantification of the number of exiting hindlimb CST collaterals 3 weeks following spinal cord injury in FGFR2 floxed mice after injection of either rAAV-GFP or rAAV-GFP-ires-Cre in the hindlimb motor cortex. (n=8 per group; compared using unpaired t-test, * P value<0,05). The amplitude of the sprouting should be compared to Suppl. Fig. 5 when the deletion is performed by crossing $FGF22^{fl/fl}$ mice with EMX-Cre mice. (**c**) Confocal images of boutons on hindlimb CST collateral in FGFR2 floxed mice after injection of either rAAV-GFP (upper panel) or rAAV-GFP-ires-Cre (lower panel) in the hindlimb motor cortex. (**d-f**) Quantification of the number of boutons (**d**), branchpoints (**e**) per

hindlimb CST collateral as well as the percentage of contacted LPSN (**f**) 3 weeks after injury in FGFR2 floxed mice after injection of either rAAV-GFP or rAAV-GFP-Ires-Cre in the hindlimb motor cortex (n=8 per group, compared using unpaired t-test, * P value<0,05). Again the changes are similar to those obtained by crossing $FGF22^{fl/fl}$ mice with EMX-Cre mice (See Fig. 1). Scale bar in **a**, 40 μm; in **c**: 15 μm.

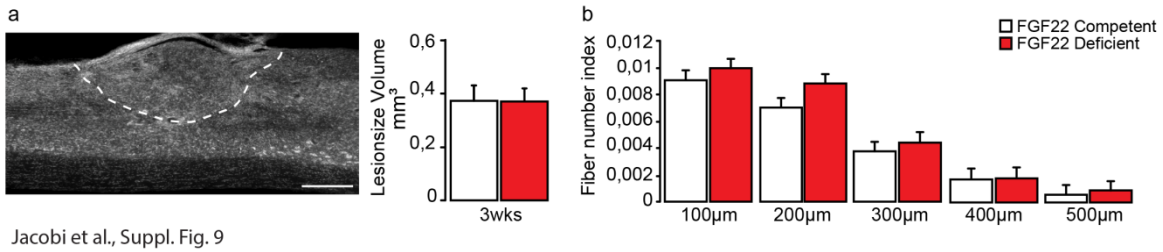

Supplementary Figure 9. Lesion volume and fiber number index of regenerative fibers in FGF22 KO mice following spinal cord injury. (a) Confocal picture (left panel) of a representative longitudinal section of spinal cord around T8 showing the extent of lesion size using NT435. Dash lines outline the lesion area. Quantification of lesion area (μm^3/ right panel) in FGF22 KO and control mice. **(b)** Fiber number index of regenerative fibers in FGF22 KO and control mice. Scale bar in a equals 250µm. Data were analyzed with student t-test in **(a)** and a repeated ANOVA followed by post-hoc test in **(b)**.

4. Discussion

The process of detour circuit formation after spinal cord injury is subdivided into different phases starting with (i) the growth of new CST collaterals, (ii) the navigation of those *de novo* collaterals toward their target area and (iii) the formation and refinement of synapses onto appropriate relay neurons (LPSN). My thesis was aiming at identifying some of the molecular mechanisms which govern these individual phases of post-injury axonal remodeling and the findings obtained during this time will be discussed in this chapter.

4.1 Molecular modulation of post-injury outgrowth of new CST collaterals.

The first aim of my thesis was the identification and manipulation of molecules that could influence axonal outgrowth during detour circuit formation following spinal cord injury. The work performed during this thesis has allowed the identification of a transcription factor STAT3 as a key regulator of axonal outgrowth following spinal cord injury. In the next paragraphs, I will discuss how STAT3 can induce sprouting of lesioned and unlesioned axons.

4.1.1 Activation of Intrinsic Growth Program: the Example of STAT3

CNS neurons axotomy can lead to the activation of the intrinsic growth program (Smith et al., 2011). However this process is thought to be very transient because of a simultaneous activation of inhibitory growth factors (Sun and He, 2010). Accordingly, we show a transient expression of STAT3 in cortical projection neurons after injury which is back to baseline levels one week after the injury (Lang et al., 2013). This could be due to a negative feedback loop with the

upregulation of SOCS3 upon STAT3 activation. As SOCS3 is a strong inhibitor of STAT3, this could lead to the quick down regulation of STAT3 following CNS injury (Crocker et al., 2008; Smith et al., 2009). In the CNS, the negative feedback loop could be regulated not only by SOCS3 but also by other factors. For example, a study in which the JAK-STAT pathway is inhibited via the infusion of a JAK2 kinase inhibitor (AG490, Qui et al., 2005), shows a significant reduction of dorsal column axonal regeneration after a pre-conditioning sciatic nerve transection. Similarly, genetically ablating the IL-6 pathway, in IL-6 deficient mice, leads to a failure in the regeneration processes after a conditioning lesion in the dorsal column neurons (Cafferty et al., 2001 and 2004). The inability of the injured neurons to regenerate in the CNS therefore might be due to the multi-level activation of feed-back loops triggering a failure of the timed upregulation of STAT3.Various studies could show that genetic deletion of SOCS3 is able to lead to sustained activation of STAT3 and thereby could promote axonal outgrowth and regeneration after a CNS lesion (Smith et al., 2009; Sun et al., 2011).

The results also show that the deletion of STAT3 in cortical projection neurons does not impair normal post-injury axonal sprouting and spinal remodeling after spinal cord injury (Lang et al., 2013). Indeed, the ability of the corticospinal tract to sprout spontaneously in the absence of STAT3 after injury (Lang et al., 2013), as well as the ability of the DRG neurons to induce the growth program albeit in a delayed fashion following PNS lesion (Bareyre et al. 2011), indicate that other growth factors can activate growth promoting pathways after injury. What are those factors that can initiate growth in the absence of STAT3 and may act as a backup system in case of absence of STAT3?

The intrinsic growth program has been in the focus of various studies in the last years and the identification of several regulators such as the members of the PTEN/ mTOR pathway (Park et al., 2008; Liu et al., 2010) has emerged. Liu et al., were able to show that the deletion of PTEN, a negative regulator for mTOR, leads to increased sprouting of CST neurons after SCI. Down regulation of PTEN also leads to the activation of Akt pathway (Park et al., 2010; Hassan et al., 2013) which in turn is known to be associated with enhanced neurite outgrowth in the DRG and in perinatal cortical neurons (Markus et al., 2002; Ozdinler and Macklis 2006). Other potential candidates could be the cyclic AMP (cAMP) pathway and its downstream mediators (Qiu et al., 2002; Deng et al., 2009). cAMP is known to regulate neurite outgrowth, i.e. administration of cAMP into the DRG can promote the regeneration of dorsal column axons (Neumann et al., 2002; Qiu et al., 2002).

In order to try to further promote the remodeling process, we aimed in exogenously inducing sustained STAT3 overexpression via viral gene transfer in order to investigate if this leads to improved spinal remodeling. We could show that if we overexpress STAT3 genetically in the neurons of the corticospinal tract this promotes axonal outgrowth after SCI (Lang et al., 2013). However, the increased CST sprouting does not lead to an increase in the number of contacts onto spinal relay neurons (LPSN). Why this is not the case might be due to the fact that the detour circuit is spontaneously formed at an optimal rate, at least in absence of additional manipulations which aim at inducing axonal guidance and synapse formation. Additionally we can show in our study, that long-lasting overexpression of STAT3 is able to induce outgrowth of non-injured axons. In particular, using the pyramidotomy lesion paradigm, in which only one

side of the CST is injured at the level of the medulla oblongata and the direct cortical input is unilaterally interrupted (Bareyre et al., 2002), we can show that the intact side is compensating for the loss of innervation by sending midline-sprouting collaterals to the denervated site. Those midline-crossing collaterals were in turn shown to contact spinal interneurons and motoneurons. Other manipulations have also been shown to induce remodeling after pyramidotomy. For example, neurotrophic factors (Zhou and Shine, 2003), or the inhibition of NOGO-A (Bareyre et al., 2002; Wiessner et al., 2003), a neurite outgrowth inhibitor, are able to induce sprouting of fibers across the midline. Also electrical stimulation has been shown to increase midline–crossing fibers (Brus-Ramer et al., 2007), or in combination with exercises improved behavioral outcome (Harel et al., 2013). Finally, manipulating the inhibitory milieu, i.e. degrading chrondrotin sulphate proteoglycans (CSPGs) via enzyme chrondrotinase ABC (ChABC), or overexpressing other proteins such as the neuronal calcium sensor1 (NCS1) have also promoted midline sprouting and supported functional recovery (Yip et al., 2010; Starkey et al., 2012).

4.1.2 STAT3 as a Therapeutic Agent: Risks and limitations

We have demonstrated that STAT3 is a potent mediator of neurite outgrowth. However, as STAT3 is a pleiotropic molecule embedded in a complex signaling cascade, its sustained expression might also induce unwanted side effects such as cancer or inflammation which are discussed in short below.

The effects of STAT3 for instance are not only restricted to neuronal cells. After a spinal cord injury, reactive astrocytes are migrating to the lesion site. Okada et al. (2006) could show that the

function of reactive astrocytes here are largely dependent on STAT3. Having astrocytes expressing STAT3 leads to the proper formation of the scar and prevents unorganized inflammation and reduces functional deficits (Okada et al., 2006; Herrmann et al., 2008). The critical point with STAT3 being applied in a non-selective way and over a longer time here could be the continuous activation of astrocytes that might be detrimental to axonal regeneration as this keeps the scar and its inhibitory environment intact. As the effects of STAT3 are on the transcriptional level, an upregulation can also lead to suppression of apoptosis because it activates genes, which in the case of an injury are pro regenerative (such as bcl-xl or bcl-2), but might lead to aberrant growth in other areas (Yu et al., 2009). This indicates that the use of STAT3 could have a high risk to induce cancer formation if not applied carefully.

A very promising application could be the use of viral gene therapy (recombinant adeno – associated viral vectors, rAAV). Not only that these tools have been used extensively in animal studies, but also they are very well characterized in terms of safety and restrictiveness to neuronal populations, depending on their capsid structure (Xiao et al., 2012). They have been used for gene therapy during clinical trials, i.e. for neurodegenerative diseases such as Alzheimer's disease (Lim et al., 2010) and cystric fibrosis (Moss et al., 2004; Moss et al., 2007). Limitations to overcome, so far are the reactions of the immune system, i.e. that transgene-expressing cells are eliminated by the cells of the immune system (Mingozzi et al., 2011; Rogers et al., 2011). Particularly in the case of spinal cord injury this could affect a stable expression of the rAVV. Here, the injury itself leads to a strong inflammatory response (Bareyre et al., 2003) which in addition could also "attack" the rAAVs and thereby eliminate transduced neuronal cells. However, efforts are taken to also overcome those difficulties. For example, studies are ongoing

in which the transduction efficacy of the vector is increased. This way, one can achieve the same expression levels, or higher, with a lower amount of transferred rAAV (Li et al., 2010; Bartel et al., 2011).

The identification of molecules such as STAT3, which induce growth during injury-induced axonal remodeling, is one key step in the aim of triggering the formation of the detour circuit after injury. Therefore, finding additional growth promoting cues, which could trigger growth or be combined with STAT3 for additive effects, is of great interest for the future.

4.2 Identification of the Expression of Guidance Molecules in the Injured Spinal Cord

Once the growth of the *de novo* collaterals is induced, the axons have to be guided into their proper target area and form contacts onto the target cells. The second aim of my thesis was the identification of potential candidate molecules which can guide the axons onto the proper target interneurons in the spinal cord during the remodeling process. To do so, we examined the expression of guidance molecules which determine the formation of neuronal circuits in the developing nervous system, within different groups of spinal interneurons during detour circuit formation following spinal cord injury.

4.2.1 Role of Guidance cues in the developing and in the Adult CNS

In the human developing CNS, each of over a trillion cells has to form connections with, on average, over a thousand target cells. The correct connection and wiring is essential for the proper

functioning of the nervous system. To achieve this, the newly growing axons are either guided via contact attraction, chemoattraction, contact repulsion or chemorepulsion. The contact mediated repulsion or attraction is used over short range guidance, whereas the chemoattraction or –repulsion is usually used during long range guidance (Figure 9; for review see Tessier-Lavigne and Goodman, 1996).

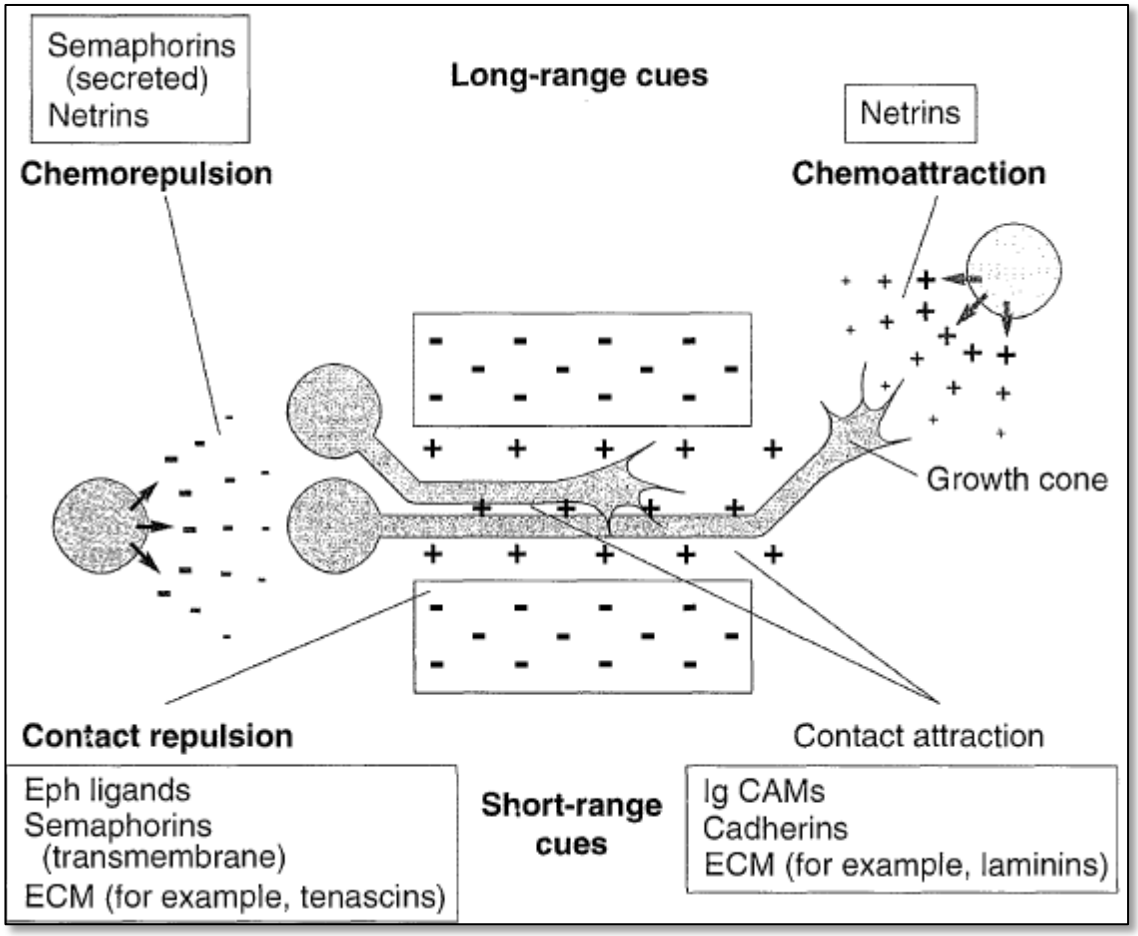

Figure 9: Guidance forces leading the growing axon through the developing tissue. Attraction or repulsion occurs either via long distance (such as secreted Semaphorines) or via contact mediation and thereby are defined as short-range cues (such as Ephrin ligands or transmembrane Semaphorines). (Adapted from Tessier – Lavigne and Goodman, 1996; Re-print permission from the American Association for the Advancement of Science)

In the last years, numerous cues important for axon guidance have been identified in the developing nervous system. Their expression usually is depending on the phase in which the axon is (growing, targeting or synapsing) or in which area it is growing to (Kolodkin and Tessier – Lavigne, 2011; Fox and Umemori, 2006). For instance, the guiding molecule semaphorin 6a is expressed in the developing corticospinal tract. It is shown to only be expressed in the area were the tip of the growing CST axons are located, such as at embryonic day E17.5 in the pons, and in the inferior olives just before the pyramidal decussation at P4 (Rünker et al., 2008). Other examples show spatially distinct expression patterns of the guidance cues. The Slits, repulsive guidance cues, are only located in the ventral half of the developing spinal cord, e.g. the floor plate (Hammond et al., 2005). Members of the Ephrin family, also part of the repulsive guidance cues, such as EphrinB3 is expressed in the floor plate, whereas EphrinB2 and B1 show expression only in the dorsal spinal cord (Jevince et al., 2006). In contrast, our study shows a very ubiquitous distribution of the individual cues investigated in the adult CNS (Jacobi et al., 2014). One potential explanation for the differences in the expression pattern between development and adult could be a change in the role of the guidance cues. Axon guidance cues could switch from a repulsive to an attractive cue and vice versa. The expression of these cues in the adult CNS indicates that they could influence the stabilization of neuronal circuits during adulthood and axonal remodeling following injury. Some of these cues have been shown to be expressed at the lesion site after injury (Wehrle et al., 2005; Kopp et al., 2010). So far, the exact roles of the different cues investigated during my thesis are not fully understood, but their potential role during adult neuronal circuit formation can be strengthened by the fact, that all their receptors are also expressed in the layer V neurons of the motorcortex that send their axons down to the spinal cord and form the CST tract. These receptors have also been shown to be

expressed in the developing CST tract (Rünker et al., 2008; Yokoyama et al. 2001; Bagri et al., 2002). More experiments are warranted in order to elucidate the role of these cues in adulthood and following injury.

4.2.2 Role of Axon Guidance Cues During Post-Injury Remodeling

As mentioned above, the attractive and repulsive guidance cues have been studied in great detail during the development (Tessier-Lavigne and Goodman, 1996; Mueller et al., 1999).

One group is the repulsive guidance cues of the s**lit / robo family** (Slit-1,-2 and -3, and their receptors Robo-1,-2 and -3). First hints of this family being a negative regulator in the adult CNS rose after it has been shown that the slits are expressed at the lesion site after spinal cord injury and thereby perhaps contribute to the failure of regeneration (Wehrle et al., 2005, Lu et al., 2008). In our study we can show that slits are also expressed in the cervical spinal cord, in unlesioned and lesioned animals, remote from the lesion site. As we also show their receptors being expressed by the neurons of the corticospinal tract, we can assume an important role in the nervous system and among others after injury. Interestingly, we do observe a specific expression of the slit ligands in excitatory propriospinal neurons compared to inhibitory glycinergic interneurons (Jacobi et al., 2014). As those are specifically contacted by regrowing CST collaterals after injury, this might indicate a change in their role from neurite repulsion in development (Sang et al., 2002) to neurite attraction in adulthood (as mentioned above).

Another group of guidance cues are the **semaphorins and their receptors** (Sema6a, -7a and their receptors PlexinA2 and –C1). Similarly to the slits, they have been implicated in the control of neuronal development (Suto et al., 2007; Rünker et al., 2008; Pasterkamp et al., 2003; Mann et al., 2007). Also here we can show the ubiquitous expression of the two

ligands, sema6a and sema7a, in the cervical gray matter. The two main receptors, PlexinA2 and PlexinC1 respectively, do also show expression in the adult cortex, as reported before (Shim et al., 2012; Kopp et al., 2010) and in particular in the lamina V of the motorcortex.

Sema7a is known to be a growth promoting cue (Pasterkamp et al., 2003). After injury this cue is expressed by all propriospinal neurons but in only a restricted subset of glycinergic interneurons, indicating that this cue might help the new collaterals to grow towards the propriospinal neurons. It is worth noting that the injury is not accompanied by a change in the expression pattern of Sema7a. This is in contrast to previous findings where Sema7a expression is increased in neurons and components of the glial scar (Kopp et al., 2010) at the site of the injury. This discrepancy is most likely due to the difference in location for the analysis. The study of Kopp et al is performed at the site of the lesion while our study is performed remote from the lesion site, at the level of axonal remodeling.

The axon guidance cues studied here have been shown to be expressed in the adult central nervous system, in the unlesioned and lesioned situation. The distinct expression of the ligands preferably on the propriospinal neurons might suggest a change in the signaling effect from development to adulthood for sema6a but a preserved transduction pathway for Sema7a.

Taken together, the expression of the slit's and Sema7a mainly on the excitatory spinal relay neurons (LPSN) but not on inhibitory, glycinergic interneurons, gives rise to a potential role in post-injury axonal remodeling. Further, more detailed investigations, i.e. via genetic manipulations (knock-out mice or viral mediated genetic overexpression), could help gaining a greater insight into their role in the adult CNS and after injury.

4.3 Identification and Molecular Modulation of Synaptogenesis during Injury Induced Remodeling

The last task of my thesis was to identify molecules that could be involved in regulating synapse formation during post-injury axonal remodeling. We first established an *in situ* screen to identify potential candidates and then continued by manipulating one particular synaptic organizer in our injury model. In this chapter I will explain which synaptogenic molecules we investigated and will discuss how the modulation of one of them, FGF22, interferes with detour circuit formation following spinal cord injury.

4.3.1 Role of Synaptogenic Cues During Post-Injury Remodeling

Once the axon has reached its target cell, a synapse has to be formed in order for neuronal transmission to be established. This usually is induced either pre-synapticaly or post-synapticaly (Gerrow and El-Husseini, 2006). The process of synapse formation has been studied extensively during development (Fox and Umemori, 2006; Biederer et al., 2006). It involves several molecules such as trans-synaptic adhesion molecules which span the synaptic cleft and are needed to precisely align pre- and postsynaptic sites.

We first focused on **Synaptic Cell Adhesion Molecules (SynCAMs)**, which are known to be crucial for the formation of new connections during development (Biederer et al., 2006). This family of molecules acts bi-directionally (Biederer and Stagli, 2008); therefore we analyzed their expression in the cortex, for the receptors, and in the spinal cord, for the ligands. We can detect expression of SynCAM1, 3 and 4 throughout the adult cortex (prominently in layer V) and the adult spinal cord which is in line with previous reports (Thomas et al., 2008; Zelano et al, 2009). We can show that, SynCAM1 and SynCAM3 do not show a preferential expression

in the different types of interneurons; however SynCAM4 is preferentially expressed in propriospinal neurons. The abundant expression of the SynCAMs in the spinal cord indicates a contribution of these molecules to the formation or maintenance of synapses in the adult CNS and might reveal a role in the formation of new contacts and synapses between the newly born CST collaterals and propriospinal interneurons after dorsal hemisection. As we did not detect any change in expression over time, it is unlikely that the SynCAMs, in particular SynCAM4 contribute to the pruning process or the maintenance and stabilization of synapses during injury-induced axonal remodeling.

Next to the SynCAMs, our studies focused on other inducers of presynaptic organization - the **neuroligins** (Scheiffele et al., 2000). They are located post-synapticaly and connect to the postsynaptic organizers neurexins which are located pre-synapticaly (Ushkaryov et al., 1992 and 1993). They are known to play a role in the concept of formation of new synapses during development of non-neuronal as well as neuronal tissue (Scheiffele eta al., 2000; Dean et al., 2003). We were able to show, that the neuroligins, NL1 and NL4, are present in interneurons and motoneurons throughout the cervical gray matter of the spinal cord, which is consistent with previous findings showing also NL2 and NL3 being localized to motoneurons (Varoqueaux et al., 2006). One interesting finding of our study is the distinct expression of NL1 mainly in excitatory propriospinal interneurons, whereas NL4 is strongly expressed in the inhibitory glycinergic interneurons. NL1 is known to be an initiator for excitatory synapse formation (Song et al., 1999) and therefore might contribute to the establishment of excitatory synapses between the newly growing CST collaterals and their target cells after spinal cord injury. This way NL1 might play a role in the remodeling processes after injury. In another study from Zelano and Colleagues (2007), it could also be shown, that neuronal transection leads to a downregulation of neuroligin mRNA in transected neuron. In our study we could

not show such a downregulation following the thoracic lesion. Again, the distance between the lesion site and the area of investigation, as well as the fact that these interneurons are not directly affected by the lesion itself might explain such differences.

The next group we investigated was the group of **Ephrins** and their receptors (**Ephs**). This family has been found to be involved in several developmental processes such as cell migration, axon guidance and the neuronal organization of the CNS (Klein, 2004). Their role in targeting has been shown in studies which investigated the development of the visual system and the development of the corticospinal tract (Nakagawa et al., 2000; Williams et al., 2003; Yokoyama et al., 2001). The first study revealing the role of ephrinB-ephB signaling in synapse formation was presented by Greenberg and Colleagues in 2000. Here they show that ephrinBs induce glutamate receptor clustering. Following studies showed, i.e. that hippocampal neurons, lacking ephB1-3, exhibit smaller postsynaptic components and smaller postsynaptic densities (Henkemeyer et al., 2003). In our study we were able to show for the first time the expression of ephrinB1 and its receptor ephB2 in spinal interneurons. So far, ephrinB1 and ephB2 have only been shown in the white matter, as well as in meningeal cells and astrocytes before and after SCI (Budensen et al., 2003). Similar to the SynCAMs, they are known to be bidirectional inducers of synapse formation and therefore we detected the receptors and ligands in the cortex, which is consistent with previous findings (Moreno-Flores et al., 1999; Wang et al., 2005). The abundant and constantly unaffected expression of ephrinB1 and ephB2 in interneurons of the cervical spinal cord before and after SCI indicates a similar role for those cues as for the SynCAMs. They might be important contributors of the establishment of functional synapses but are most probably not participating in the stabilization of those contacts.

4.3.2 Role of FGF Signaling during Development and Adulthood

The last group of synaptogenic molecules we focused on is the family of the fibroblast growth factors (FGFs). The FGF family is a very well-known group of secreted molecules, which are important in various organs during embryonic development (for review see Ornitz and Itoh, 2001), i.e. FGF10 has been shown to play a role in wound healing (Tagashira et al., 1997) or development of the limbs and lung (Martin, 1998; Bellusci et al., 1997). In 2004, Umemori et al. identified for the first time FGF22 and its close relatives, FGF7 and -10, as inducers of presynaptic differentiation via signaling through their main receptor FGFR2b, during neuronal development (Ornitz et al., 1996). The authors show that i.e. FGF22 is able to induce clustering of synaptic vesicles and neurite branching *in vitro* and *in vivo* (Umemori et al., 2004). This function is specific to FGFR2b but not the other main isoform of the FGF receptor, FGFR2c. Later it has been shown that FGFR1b also shows a specific binding affinity to FGF22, albeit not as strong as FGFR2b (Zhang et al., 2006). Another study in 2010 shows how FGF22 and FGF7 promote the organization of excitatory and inhibitory presynaptic terminals, respectively, during the development of CA3 hippocampal pyramidal neurons (Terauchi et al., 2010). The involvement of this FGF family in presynaptic differentiation has also been shown in the development of neuromuscular junctions in the mouse (Fox et al., 2007). However, the presence and role of FGF22 and its receptors in the adult CNS, also in the context of the detour circuit after injury, has not been investigated so far.

In our study we can show, that FGF22 and its receptors, FGFR1 and FGFR2, are also expressed in the adult CNS. FGF22 is expressed ubiquitously in the cells of the spinal cord, whereas the receptors show a distinct expression in the cortex, in particular in layer V of the

cortex. The fact that FGF22 and its receptors are expressed in the adult CNS indicates that they could play a role in adulthood and particularly during detour circuit formation. We also show that a lesion to the spinal cord does not alter the expression of the ligand, FGF22, distal to the lesion site. As with the synaptogenic cues investigated in our previous paper (Jacobi et al., 2014), we can assume, that the effect of the lesion onto the expression of the FGF22 ligand and its receptors might only be minimal because of the distance of the observed area to the lesion site. It is important to note that a conditional ablation of one of the receptors does not lead to compensation by an increased expression of the other receptor after injury. It might indicate that those two receptors have slightly different function.

4.3.3 Role of FGF Signaling following Injury

To identify an involvement of FGF22 and / or its receptors in the process of detour circuit formation, we took advantage of several approaches. First, we analyzed mice with a genetic ablation of FGF22 (FGF22 KO). Second, we genetically ablated either of the receptors in the cells of layer V of the cortex (origin of the CST) by crossing a floxed mouse line ($FGFR1^{fl/fl}$ or $FGFR2^{fl/fl}$) with an EMX1-*Cre* mouse line. Because the EMX1 promoter drives the expression of the *Cre* recombinase in the forebrain, this leads to the specific deletion of the FGF receptors in the forebrain and hence in the CST as of E10. Finally, we deleted each of the receptor separately or we co-deleted both receptors in the neurons of the hindlimbCST via gene-therapy using adeno-associated viruses expressing the Cre recombinase (See also Manuscript 3). We can show that the deletion of the ligand and the receptors leads to a drastic reduction of boutons on newly formed collaterals during injury-induced detour circuit formation. In mice deleted of one FGF22 receptors, we could also show that complexity of the new collaterals is reduced – an additional marker for neuronal plasticity (Shen and Cowan, 2010). A reduction in the number of boutons indicates that contact-induced

presynaptic differentiation is less efficient in these mice. Both, a deletion in the receptors or of the ligand, seem to inhibit synaptic bouton formation. This is in contrast to the study of Terauchi et al., 2010, who show that in the CA3 of the hippocampus the KO of FGF22 does not alter the number of asymmetric excitatory synapses but only the vesicle recruitment. However they also show, that already in the adjacent area, CA1, the FGF signaling mechanism is not required for synapse formation, thus indicating that the effect of FGF signaling can be very specific to the type of cells, the area and the time point.

The loss of either of the receptors, FGFR1 or FGFR2, also shows an interesting side effect. Knocking out the receptors as early as embryonic day E10, leads to an increased sprouting of the corticospinal tract after spinal cord injury. This suggests that FGF22 signaling via either receptor participates in the induction of compensatory CST sprouting. Co-deletion of the two FGF receptors and deletion of FGF22 before the injury did not lead to such an increased sprouting while the synapse formation and maturation was strongly reduced. One possible explanation could be that there is activation of a different signaling pathway via one or the other of the receptors (Guillemot and Zimmer, 2011). Also, it is not known if the different receptors are able to dimerize with each other and in this case, FGFR1-FGFR2 interaction could activate another pathway.

We also characterized the maturation of the boutons on *de novo* CST collaterals in the cervical spinal cord of our different mouse lines following spinal cord injury. We can show that markers for early and late synapse maturation, Bassoon and Synapsin respectively (Zhai et al., 2000; Lang et al., 2012), are differentially expressed at different time points. Bassoon expression, a marker for the active zone in the synapse (Schoch and Gundelfinger, 2006), is reduced in the boutons of CST collaterals of the FGF22 KO and FGFR co-deletion mice shortly after lesion and only goes back to baseline levels in the FGF22KO at the later time

point, when the detour circuit is fully established (12wks). In FGFR co-deleted mice, Bassoon labeling remained significantly below control even 12wks following the lesion. For Synapsin, a vesicle marker which stands for more mature boutons (Lang et al., 2012), the boutons in the different types of KO show a decreased labeling at early time points as well as at later time points, with an exception of the single KO of FGFR1.

These results indicate that inactivating FGF signaling prevents presynaptic differentiation by blocking active zone formation and vesicle clustering at early and late stages of detour circuit formation rather than just delaying it. This is in agreement with another study where this blockade is shown in the postnatal development of hippocampal CA3 neurons (Terauchi et al., 2010).

4.3.4 Impaired FGF Signaling Delays Functional Recovery after Injury: a Potential Therapeutic Target?

In our study we can show, that the co-deletion of both receptors, FGFR1 and FGFR2, or the ligand, FGF22, results in a drastic decrease of the contacts onto the LPSN. To test how this affects functional recovery, we performed various behavioral tests (Figure 10). The BMS test is an open field test, in which the mice are under observation while exploring a certain area. It is a gross locomotor test which is commonly used to observe the recovery of the animals following spinal cord lesion. The Ladder Rung Test is reflective of the thin locomotion abilities of the animal and is highly CST specific in particular when an irregular spacing of the bars is used. Indeed, it tests the ability of the mouse to place its hindlimbs onto the bars of the ladder and therefore is a very good behavioral assessment of CST related functional recovery and detour circuit formation after injury. We can see that control mice recover gradually some motor function over the course of 3 weeks. However, we found that

FGF22KO and FGFR1-R2 co-deleted mice could not recover as well as the control mice and remained impaired over the weeks following the injury. In particular in the irregular walk, in which the mice have to pass the ladder rung with altering bars and gaps between those, the FGF22 KO and the FGFR1-R2 co-deleted mice perform a lot worse than their controls.

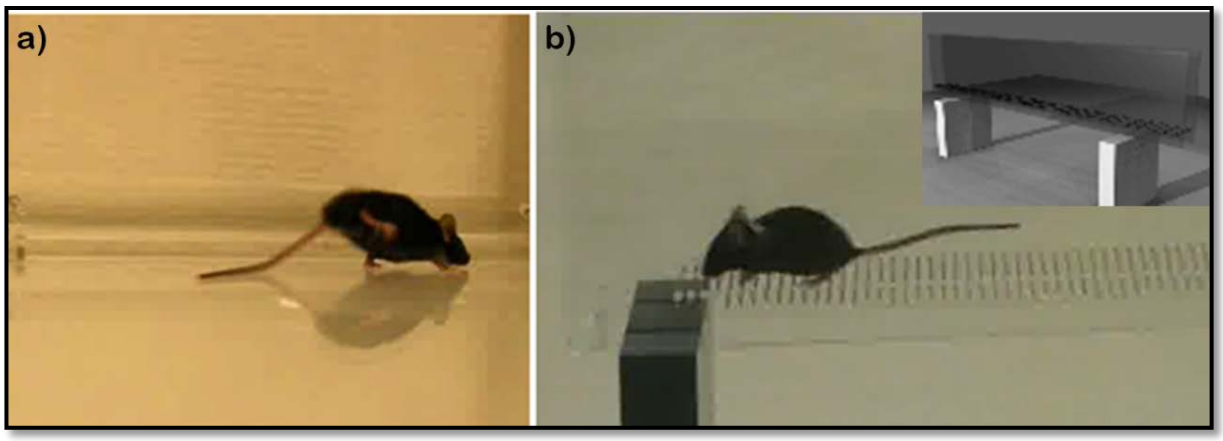

Figure 10; Behavioral Tests to record functional recovery after SCI. A) BMS (Basso Mouse Scale for locomotion, Basso et al., 2006)) is an open field test in which the mouse is scored under different points, i.e. limb movement, trunk support, tail movement, according to its performance after injury. B) Ladder Rung (Grid Walk; Metz and Whishaw, 2009) is a horizontal ladder which the mice have to pass. While doing so the number of foot falls is acquired and compared. The placement of the paws is a very CST specific function.

These results show a potential effect of a FGF22 overexpression on recovery after SCI in wildtype mice. Trying to overexpress FGF22 in the LPSN of the cervical spinal cord of normal wildtype mice could have a positive effect on recovery after injury and maybe also increase axonal remodeling. To test this, we now created a virus (rAAV) which carries the FGF22 sequence and inject this virus into C3-C5, the area in which the cell bodies of the LPSN are located (Alstermark et al., 1987). After an incomplete spinal cord injury, we would like to investigate if the establishment of the detour circuit is strengthened by additional contacts onto the LPSN, or fastened by a quicker formation of the full circuit, i.e. already after two weeks (with growth rate being the limiting factor here). Also the overexpression of FGF22 could lead to a quicker maturation of the synapses, as we show in our study that this

maturation is impaired in the FGF22 KO mice. These ongoing investigations will help us finding out if FGF22 can act as a potential therapeutic target after injury.

However, one also has to keep in mind that some FGF family members and their overexpression or activation-mutations have been shown to induce various kinds of tumors and cancer in humans (Turner and Grose, 2010; Brooks et al., 2012). The persistent and excessive activation of the FGFR signaling pathway for example can result in carcinogenic functions in the cells and thereby end in excessive proliferation and apoptosis (Greulich et al., 2012). Also in the CNS, the FGF family has been shown to lead to several types of tumors, i.e. gliomas and meningiomas (Takahashi et al., 1990) or astrocytomas (Morrison et al., 1994). Even though there is nothing known about FGF22 in CNS tumor development, one has to keep this strong proliferation potential in mind that is activated by overexpression of FGFs and has to be careful when performing experiments using FGF22 to increase axonal remodeling after injury.

More recently the FGFs have also been shown to play a role in a different disease – epilepsy (for review see, Paradiso et al., 2013). In particular, FGF22 has been shown to be a potential target of therapy for epilepsy (Lee and Umemori, 2013). The authors show in their study that the FGF22 KO mice exhibit resistance to kindling generated epileptic seizures. The mice don't show the typical pathological events such as increased neurogenesis, ectopic migration of dendate gyrus cells (DGC) or hilar cell death after a seizure. This suggests the possibility that inhibiting FGF22 signaling in the hippocampus might alleviate epileptogenesis.

The results obtained during my thesis suggest that i.e. STAT3 or FGF22 could be valuable therapeutic candidates for the induction of growth (STAT3) or the efficient establishment and maturation of synapses (FGF22), hence axonal remodeling following SCI.

The work carried out during my thesis also suggests that some other molecules, such as Sema7a (Jacobi et al., 2014) for example could be important for the correct targeting of detour circuits following injury.

5. Conclusions

Axonal remodeling after spinal cord injury is a key feature that contributes to functional recovery (Fouad et al., 2001; Bareyre et al., 2004; Courtine et al., 2008; van den Brand et al., 2012). After an incomplete spinal cord injury, axonal detour circuits have been shown to contribute to this functional recovery. This axonal remodeling is divided into three different phases, (i) the initiation of growth, (ii) the formation of collaterals which are guided into a certain target area and (iii) the formation of contacts and the followed refinement of those onto the target cells.

In my thesis, I was trying to find molecules which regulate the different phases of the formation of this detour circuit in order to better understand the underlying mechanisms of axonal remodeling. This could help guiding future studies and help finding therapeutic targets to support recovery and thereby prevent the devastating consequences after injury.

Looking at the research that has been done in the last years, it has become clearer that manipulation of a single molecule will not be sufficient to achieve successful recovery, but rather a combination of the manipulation of several cues. This also underlies the need of a combination of therapeutic interventions to overcome the lack of recovery such as gene therapy, physiotherapy or electrical stimulation. The field of spinal cord injury research has evolved very quickly in the last years, and thanks to progresses in many different experimental techniques such as *in vivo* imaging, electrophysiology, transgenic technologies or optogenetics, the chances of establishing experimentally combined therapies that could then be translated to help patients with SCI are coming closer and more realistic.

6. Bibliography

Aaronson DS, Horvath CM. A road map for those who don't know JAK-STAT. Science. (2002) May 31;296(5573):1653-5.

Akira S. Roles of STAT3 defined by tissue-specific gene targeting. Oncogene. (2000) 19:2607-11

Alstermark B, Lundberg A, Pinter M, Sasaki S. Subpopulations and functions of long C3-C5 propriospinal neurons. Brain Res. (1987) Feb 24;404(1-2):395-400.

Bagri A, Marin O, Plump AS, Mak J, Pleasure SJ, et al. Slit proteins prevent midline crossing and determine the dorsoventral position of major axonal pathways in the mammalian forebrain. Neuron (2002) 33(2):233–248.

Bamber NI, Li H, Lu X, Oudega M, Aebischer P, Xu XM. Neurotrophins BDNF and NT-3 promote axonal re-entry into the distal host spinal cord through Schwann cell-seeded mini-channels. European Journal of Neuroscience (2001) 13:257-68

Bareyre FM, Haudenschild B, Schwab ME. Long-lasting sprouting and gene expression changes induced by the monoclonal antibody IN-1 in the adult spinal cord. J Neurosci. 2002 Aug 15;22(16):7097-110.

Bareyre FM, Schwab ME. Inflammation, degeneration and regeneration in the injured spinal cord: insights from DNA microarrays. Trends in Neurosciences (2003).26:555-63

Bareyre FM, Kerschensteiner M, Raineteau O, Mettenleiter TC, Weinmann O, Schwab ME. The injured spinal cord spontaneously forms a new intraspinal circuit in adult rats. Nat Neurosci. (2004) Mar;7(3):269-77.

Bareyre FM, Garzorz N, Lang C, Misgeld T, Büning H, Kerschensteiner M. In vivo imaging reveals a phase-specific role of STAT3 during central and peripheral nervous system axon regeneration. Proc Natl Acad Sci USA (2011) Apr 12;108(15):6282-7.

Bartel M, Schaffer D and Buning H. "Enhancing the Clinical Potential of AAV Vectors by Capsid Engineering to Evade Pre-Existing Immunity." Front Microbiol (2011)2: 204.

Behar O, Golden JA, Mashimo H, Schoen FJ, Fishman MC. Semaphorin III is needed for normal patterning and growth of nerves, bones and heart. Nature (1996) Oct 10;383(6600):525-8.

Bellusci S, Grindley J, Emoto H, Itoh N, Hogan BL. Fibroblast growth factor 10 (FGF10) and branching morphogenesis in the embryonic mouse lung. Development (1997) Dec;124(23):4867-78.

Bethea JR and Dietrich DW. Targeting the host inflammatory response in traumatic spinal cord injury. Current Opinion in Neurology (2002) 15:355-360

Bibliography

Biederer T, Sara Y, Mozhayeva M, Atasoy D, Liu X, Kavalali ET, Südhof TC. SynCAM, a synaptic adhesion molecule that drives synapse assembly. Science (2002) Aug 30;297(5586):1525-31.

Biederer T. Hooking up new synapses. Nat Neurosci (2006) 9(10): 1203–1204.

Biederer T and Stagi M. Signaling by synaptogenic molecules. Current Opinion in Neurobiology (2008), 18:261–269.

Böttcher RT, Niehrs C. Fibroblast growth factor signaling during early vertebrate development. Endocr Rev. (2005) Feb;26(1):63-77.

Bracken MB, Collins WF, Freeman DF, Shepard MJ, Wagner FW, Silten RM, Hellenbrand KG, Ransohoff J, Hunt WE, Perot PL Jr. Efficacy of methylprednisolone in acute spinal cord injury. JAMA (1984) Jan 6;251(1):45-52.

Bracken MB. Methylprednisolone in the management of acute spinal cord injuries. Med J Aust. (1990) Sep 17;153(6):368.

Bracken MB, Shepard MJ, Holford TR, Leo-Summers L, Aldrich EF. Administration of Methylprednisolone for 24 or 48 Hours or Tirilazad Mesylate for 48 Hours in the Treatment of Acute Spinal Cord Injury. JAMA: The Journal of the American Medical Association (1997) 277:1597-604.

Brösamle C, Huber AB, Fiedler M, Skerra A, Schwab ME. Regeneration of Lesioned Corticospinal Tract Fibers in the Adult Rat Induced by a Recombinant, Humanized IN-1 Antibody Fragment. The Journal of Neuroscience (2000) 20:8061-8.

Brooks AN, Kilgour E, Smith PD. Molecular pathways: fibroblast growth factor signaling: a new therapeutic opportunity in cancer. Clinical Cancer Research (2012) 18:1855–62.

Brus-Ramer M, Carmel JB, Chakrabarty S, Martin JH. Electrical Stimulation of Spared Corticospinal Axons Augments Connections with Ipsilateral Spinal Motor Circuits after Injury. The Journal of Neuroscience (2007) 27:13793-801.

Bundesen LQ, Scheel TA, Bregman BS, Kromer LF. Ephrin-B2 and EphB2 regulation of astrocyte-meningeal fibroblast interactions in response to spinal cord lesions in adult rats. J Neurosci (2003) 23(21): 7789–800.

Burns SP, Golding DG, Rolle Jr WA, Graziani V, Ditunno Jr JF. Recovery of ambulation in motorincomplete tetraplegia. Archives of physical medicine and rehabilitation (1997) 78:1169-72.

Cafferty WB, Gardiner NJ, Gavazzi J, Powell J, McMahon SB, Heath JK, MunsonJ ,Cohen J and Thompson SW. Leukemia inhibitory factor determines the growth status of injured adult sensory neurons. J Neurosci (2001) 21(18): 7161-7170.

Bibliography

Cafferty WB, Gardiner NJ, Das P, Qiu J, McMahon SB and Thompson SW. Conditioning injury-induced spinal axon regeneration fails in interleukin-6 knock-out mice. J Neuroscience (2004) 24(18): 4432-4443.

Chen M, Huber A, van der Haar M, Frank M, Schnell L. Nogo-A is a myelin-associated neurite outgrowth inhibitor and an antigen for monoclonal antibody IN-1. Nature (2000) 403:434-9.

Courtine G, Song B, Roy RR, Zhong H, Herrmann JE. Recovery of supraspinal control of stepping via indirect propriospinal relay connections after spinal cord injury. Nat Med (2008) 14:69-74.

Croker BA, Kiu H and Nicholson SE. SOCS regulation of the JAK/STAT signaling pathway. Semin Cell Dev Biol (2008) 19(4): 414-422.

Curt A, Schwab ME, Dietz V. Providing the clinical basis for new interventional therapies: refined diagnosis and assessment of recovery after spinal cord injury. Spinal Cord (2004) Jan;42(1):1-6.

Dalva MB, McClelland AC, Kayser MS. Cell adhesion molecules: signalling functions at the synapse. Nat Rev Neurosci. (2007) Mar;8(3):206-20.

Dean C, Scholl FG, Choih J, DeMaria S, Berger J. Neurexin mediates the assembly of presynaptic terminals. Nat Neurosci (2003) 6: 708 –716.

Deng K, He H, Qiu J, Lorber B, Bryson JB and Filbin MT. Increased synthesis of spermidine as a result of upregulation of arginase I promotes axonal regeneration in culture and in vivo. J Neurosci (2009) 29(30): 9545-9552.

Dietz V, Wirz M, Colombo G, Curt A. Locomotor capacity and recovery of spinal cord function in paraplegic patients: a clinical and electrophysiological evaluation. Electroencephalogr Clin Neurophysiol. (1998) 109:140-53.

Dietz V. Recent advances in spinal cord neurology. J Neurol. (2010) Oct;257(10):1770-3.

Dietz V, Fouad K. Restoration of sensorimotor functions after spinal cord injury. Brain. (2014) Mar;137(Pt 3):654-67.

Dietz V, Harkema SJ. Locomotor activity in spinal cord-injured persons. J Appl Physiol (1985). 2004 May;96(5):1954-60.

Ditunno JF, Little JW, Tessler A, Burns AS. Spinal shock revisited: a four-phase model. Spinal Cord (2004) 42:383-95

Doherty P, Walsh FS. CAM-FGF Receptor Interactions: A Model for Axonal Growth. Mol Cell Neurosci (1996) Aug;8(2/3):99-111.

Dusart I, Schwab ME. Secondary Cell Death and the Inflammatory Reaction after Dorsal Hemisection of the Rat Spinal Cord. European Journal of Neuroscience (1994) 6:712-24.

Bibliography

Dziennis S, Alkayed NJ. Role of signal transducer and activator of transcription 3 in neuronal survival and regeneration. Rev Neurosci. (2008) ;19(4-5):341-61.

Edgerton V, Tillakaratne N, Bigbee A, de Leon R, Roy R. Plasticity of the spinal neural circuitry after injury. Annu Rev Neurosci.(2004) 27:145-67

Eberhart J, Swartz M, Koblar SA, Pasquale EB, Tanaka H. Expression of EphA4, ephrin-A2 and ephrin-A5 during axon outgrowth to the hindlimb indicates potential roles in pathfinding. Dev Neurosci (2000) 22(3): 237–250.

Fawcett JW, Curt A, Steeves JD, Coleman WP, Tuszynski MH, Lammertse D, Bartlett PF, Blight AR, Dietz V, Ditunno J, Dobkin BH, Havton LA, Ellaway PH, Fehlings MG, Privat A, Grossman R, Guest JD, Kleitman N, Nakamura M, Gaviria M, Short D. Guidelines for the conduct of clinical trials for spinal cord injury as developed by the ICCP panel: spontaneous recovery after spinal cord injury and statistical power needed for therapeutic clinical trials. Spinal Cord. (2007) Mar;45(3):190-205.

Filbin MT. Myelin-associated inhibitors of axonal regeneration in the adult mammalian CNS. Nat Rev Neurosci (2003) 4:703-13

Filli L, Schwab ME. The rocky road to translation in spinal cord repair. Ann Neurol. (2012) Oct;72(4):491-501.

Fitch MT, Doller C, Combs CK, Landreth GE, Silver J. Cellular and Molecular Mechanisms of Glial Scarring and Progressive Cavitation: In Vivo and In Vitro Analysis of Inflammation-Induced Secondary Injury after CNS Trauma. The Journal of Neuroscience (1999) 19:8182-98

Fouad K, Pedersen V, Schwab ME, Brösamle C. Cervical sprouting of corticospinal fibers after thoracic spinal cord injury accompanies shifts in evoked motor responses. Curr Biol. (2001) Nov 13;11(22):1766-70.

Fox MA, Umemori H. Seeking long-term relationship: axon and target communicate to organize synaptic differentiation. J Neurochem (2006) 97(5): 1215– 1231.

Fox MA, Sanes JR, Borza DB, Eswarakumar VP, Fässler R, Hudson BG, John SW, Ninomiya Y, Pedchenko V, Pfaff SL, Rheault MN, Sado Y, Segal Y, Werle MJ, Umemori H. Distinct target-derived signals organize formation, maturation, and maintenance of motor nerve terminals. Cell. (2007) Apr 6;129(1):179-93.

Gautron L, De Smedt-Peyrusse V, Layé S. Characterization of STAT3-expressing cells in the postnatal rat brain. Brain Res. (2006) Jul 7;1098(1):26-32.

George ER, Scholten DJ, Büchler M, Jordan-Tibbs J,Mattice C, Albrecht RM: Failure of methylprednisolone to improve the outcome of spinal cord injuries. Am Surg 61(1995) 659-663.

Bibliography

Gerhart KA, Johnson RL, Menconi J, Hoffman RE,Lammertse DP: Utilization and effectiveness of methylprednisolone in a population-based sample of spinal cord injured persons. Paraplegia 33 (1995) 316-321.

Gerrow K, El-Husseini A. Cell adhesion molecules at the synapse. Front Biosci. (2006) Sep 1;11:2400-19.

Giovanelli Barilari M, Kuypers HG. Propriospinal fibers interconnecting the spinal enlargements in the cat. Brain Res. (1969) Jul;14(2):321-30.

Graf ER, Zhang X, Jin SX, Linhoff MW, Craig AM. Neurexins induce differentiation of GABA and glutamate postsynaptic specializations via neuroligins. Cell (2004) 119(7): 1013–1026.

Greulich H, Pollock PM. Targeting mutant fibroblast growth factor receptors in cancer. Trends in Molecular Medicine (2011) 17:283–92.

Grillner S, Wallen P. Central pattern generators for locomotion, with special reference to vertebrates. Annu Rev Neurosci (1985) 8:233-61.

Guan KL, Rao Y. Signalling mechanisms mediating neuronal responses to guidance cues. Nat Rev Neurosci (2003) Dec; 4(12):941-56.

Guillemot F, Zimmer C. From cradle to grave: the multiple roles of fibroblast growth factors in neural development. Neuron (2011) Aug 25;71(4):574-88.

Hall H, Walsh FS, Doherty P. Review: a role for the FGF receptor in the axonal growth response stimulated by cell adhesion molecules? Cell Adhes Commun. (1996) Apr;3(6):441-50.

Hammond R, Vivancos V, NaeemA, Chilton J, Mambetisaeva E, et al. (2005) Slit-mediated repulsion is a key regulator of motor axon pathfinding in the hindbrain. Dev 132(20): 4483–4495.

Harel NY, Strittmatter SM. Can regenerating axons recapitulate developmental guidance during recovery from spinal cord injury? Nat Rev Neurosci. (2006) Aug;7(8):603-16.

Harel NY, Yigitkanli K, Fu Y, Cafferty WB, Strittmatter SM. Multimodal exercises simultaneously stimulating cortical and brainstem pathways after unilateral corticospinal lesion. Brain Res. (2013) Nov 13;1538:17-25.

Hassan B, Akcakanat A, Holder AM, Meric-Bernstam F. Targeting the PI3-kinase/Akt/mTOR signaling pathway. Surg Oncol Clin N Am. (2013) Oct;22(4):641-64.

Henkemeyer M, Itkis OS, Ngo M, Hickmott PW, Ethell IM. Multiple EphB receptor tyrosine kinases shape dendritic spines in the hippocampus. J Cell Biol (2003) 163(6): 1313–1326.

Herrmann JE, Imura T, Song B, Qi J, Ao Y, Nguyen TK, Korsak RA, Takeda K, Akira S and Sofroniew MV. STAT3 is a critical regulator of astrogliosis and scar formation after spinal cord injury. J Neurosci (2008) 28(28): 7231-7243.

Houweling DA, Bär PR, Gispen WH, Joosten EA. Spinal cord injury: bridging the lesion and the role of neurotrophic factors in repair. Prog Brain Res. (1998) 117:455-71.

Huang S. Regulation of metastases by signal transducer and activator of transcription 3 signaling pathway: clinical implications. Clin Cancer Res. (2007) Mar 1;13(5):1362-6.

Hulsebosch CE. Recent advances in pathophysiology and treatment of spinal cord injury. Adv Physiol Educ. (2002) Dec;26(1-4):238-55.

Hurlbert RJ and Hamilton MG. Methylprednisolone for acute spinal cord injury: 5-year practice reversal. Can J Neurol Sci. (2008) Mar;35(1):41-5.

Ishii H, Jin X, Ueno M, Tanabe S, Kubo T, Serada S, Naka T, Yamashita T. Adoptive transfer of Th1-conditioned lymphocytes promotes axonal remodeling and functional recovery after spinal cord injury. Cell Death Dis. (2012) Aug 9;3:e363.

Jakeman LB, Wei P, Guan Z, Stokes BT. Brain-derived neurotrophic factor stimulates hindlimb stepping and sprouting of cholinergic fibers after spinal cord injury. Exp Neurol. (1998) Nov;154(1):170-84.

Jain A, Kim YT, McKeon RJ, Bellamkonda RV. In situ gelling hydrogels for conformal repair of spinal cord defects, and local delivery of BDNF after spinal cord injury. Biomaterials. (2006) Jan;27(3):497-504.

Jankowska E. Interneuronal relay in spinal pathways from proprioceptors. Prog. Neurobiol. (1992) 38:335-78

Jevince AR, Kadison SR, Pittman AJ, Chien CB and Kaprilian Z. Distribution of EphB Receptors and Ephrin-B1 in the Developing Vertebrate Spinal Cord. The Journal of Comparative Neurology (2006) 497:734–750.

Katoh M. FGFR2 Abnormalities Underlie a Spectrum of Bone, Skin, and Cancer Pathologies. Journal of Investigative Dermatology (2009) 129, 1861–1867.

Kerschensteiner M, Bareyre FM, Buddeberg BS, Merkler D, Stadelmann C, Brück W, Misgeld T, Schwab ME. Remodeling of axonal connections contributes to recovery in an animal model of multiple sclerosis. J Exp Med. (2004) Oct 18;200(8):1027-38.

Kennedy TE, Wang H, Marshall W, Tessier-Lavigne M. Axon guidance by diffusible chemo attractants: a gradient of netrin protein in the developing spinal cord. J Neurosci. (2006) Aug 23;26(34):8866-74.

Kigerl KA, Gensel JC, Ankeny DP, Alexander JK, Donnelly DJ, Popovich PG. Identification of two distinct macrophage subsets with divergent effects causing either neurotoxicity or regeneration in the injured mouse spinal cord. J Neurosci. (2009) Oct 28;29(43):13435-44.

Klein R. Eph/ephrin signalling during development.t Development. (2012) Nov;139(22):4105-9.

Kolodkin AL, Tessier-Lavigne M. Mechanisms and molecules of neuronal wiring: a primer. Cold Spring Harb Perspect Biol (2011) 3(6).

Köning W, Frowein RA. Incidence of spinal cord injury in the Federal Republic of Germany. Neurosurg Rev. (1989) ;12 Suppl 1:562-6.

Kopp MA, Brommer B, Gatzemeier N, Schwab JM, Prüss H. Spinal cord injury induces differential expression of the profibrotic semaphorin 7A in the developing and mature glial scar. Glia (2010) 58(14): 1748–1756.

Kouhara H, Hadari YR, Spivak-Kroizman T, Schilling J, Bar-Sagi D, Lax I, Schlessinger J. A lipid-anchored Grb2-binding protein that links FGF-receptor activation to the Ras/MAPK signaling pathway. Cell. (1997) May 30;89(5):693-702.

Kunisada K, Hirota H, Fujio Y, Matsui H, Tani Y. Activation of JAK-STAT and MAP Kinases by Leukemia Inhibitory Factor Through gp130 in Cardiac Myocytes. Circulation (1996) 94:2626-32

Lang C, Guo X, Kerschensteiner M, Bareyre FM. Single collateral reconstructions reveal distinct phases of corticospinal remodeling after spinal cord injury. PLoS One (2012) ;7(1):e30461.

Lang C, Bradley PM, Jacobi A, Kerschensteiner M, Bareyre FM. STAT3 promotes corticospinal remodelling and functional recovery after spinal cord injury. EMBO Rep. (2013) Oct;14(10):931-7.

Lee CH, Umemori H. Suppression of epileptogenesis-associated changes in response to seizures in FGF22-deficient mice. Front Cell Neurosci. (2013) Apr 18;7:43.

Li Y, Field PM, Raisman G. Regeneration of Adult Rat Corticospinal Axons Induced by Transplanted Olfactory Ensheathing Cells. The Journal of Neuroscience (1998) 18:10514-24.

Li M, Jayandharan GH, Li B, Ling C, Ma W, Srivastava A and Zhong L. Highefficiency transduction of fibroblasts and mesenchymal stem cells by tyrosine-mutant AAV2 vectors for their potential use in cellular therapy. Hum Gene Ther (2010) 21(11): 1527- 1543.

Lim ST, Airavaara M, Harvey BK. Viral vectors for neurotrophic factor delivery: A gene therapy approach for neurodegenerative diseases of the CNS. Pharmacological Research (2010) 61:14-26.

Liu XZ, Xu XM, Hu R, Du C, Zhang SX, McDonald JW, Dong HX, Wu YJ, Fan GS, Jacquin MF, Hsu CY, Choi DW. Neuronal and glial apoptosis after traumatic spinal cord injury. J Neurosci. (1997) Jul 15;17(14):5395-406.

Liu K, Lu Y, Lee JK, Samara R, Willenberg R, Sears-Kraxberger I, Tedeschi A, Park KK, Jin D, Cai B, Xu B, Connolly L, Steward O, Zheng B and He Z. PTEN deletion enhances the regenerative ability of adult corticospinal neurons. Nat Neurosci (2010) 13(9): 1075-1081.

López-Bendito G, Flames N, Ma L, Fouquet C, Di Meglio T, Chedotal A, Tessier-Lavigne M, Marín O. Robo1 and Robo2 cooperate to control the guidance of major axonal tracts in the mammalian forebrain. J Neurosci. (2007) Mar 28;27(13):3395-407.

Lu YJ, Xu NW, Yang WQ. Immunofluorescence laser confocal expression and localization study of rat nerve growth guidance cues Netrin-1 and Slit2 after spinal cord injury. Chin J Traumatol (2008) 11(2): 98–103.

Maegele M, Müller S, Wernig A, Edgerton VR, Harkema SJ. Recruitment of spinal motor pools during voluntary movements versus stepping after human spinal cord injury. J Neurotrauma (2002) Oct;19(10):1217-29.

Mann F, Chauvet S, Rougon G. Semaphorins in development and adult brain: Implication for neurological diseases. Prog Neurobiol (2007) 82: 57–79.

Markus A, Zhong J, Snider WD. Raf and Akt Mediate Distinct Aspects of Sensory Axon Growth. Neuron (2002) 35:65-76.

Marillat V, Cases O, Nguyen-Ba-Charvet KT, Tessier-Lavigne M, Sotelo C. Spatiotemporal expression patterns of slit and robo genes in the rat brain. J Comp Neurol (2002) 442(2): 130–155.

Martin GR. The roles of FGFs in the early development of vertebrate limbs. Genes Dev (1998) 12:1571-1586.

Martirosyan NL, Feuerstein JS, Theodore N, Cavalcanti DD, Spetzler RF, Preul MC. Blood supply and vascular reactivity of the spinal cord under normal and pathological conditions. Journal of Neurosurgery: Spine (2011) 15:238-51.

Nakamura M and Okano H. Cell transplantation therapies for spinal cord injury focusing on induced pluripotent stem cells. Cell Research (2013) 23:70–80.

Matis GK, Birbilis TA. Erythropoietin in spinal cord injury. Eur Spine J. (2009) Mar;18(3):314-23.

Mingozzi F and High KA. Immune responses to AAV in clinical trials. Curr Gene Ther (2011) 11(4): 321-330.

Mofidi A, Bader A, Pavlica S. The use of erythropoietin and its derivatives to treat spinal cord injury. Mini Rev Med Chem. (2011) Aug;11(9):763-70.

Moreno-Flores MT, Wandosell F. Up-regulation of Eph tyrosine kinase receptors after excitotoxic injury in adult hippocampus. Neurosci (1999) 91(1): 193– 201.

Morrison RS, Yamaguchi F, Saya H, Bruner JM, Yahanda AM, Donehower LA, Berger M. Basic fibroblast growth factor and fibroblast growth factor receptor I are implicated in the growth of human astrocytomas. J Neurooncol. (1994);18(3):207-16.

Moss RB, Milla C, Colombo J, Accurso F, Zeitlin PL, Clancy JP, Spencer LT, Pilewski J, Waltz DA, Dorkin HL, Ferkol T, Pian M, Ramsey B, Carter BJ, Martin DB, Heald AE. Repeated

aerosolized AAV-CFTR for treatment of cystic fibrosis: a randomized placebo-controlled phase 2B trial. Hum Gene Ther. (2007) Aug;18(8):726-32.

Moss RB, Rodman D, Spencer LT, Aitken ML, Zeitlin PL, Waltz D, Milla C, Brody AS, Clancy JP, Ramsey B, Hamblett N, Heald AE. Repeated adeno-associated virus serotype 2 aerosol-mediated cystic fibrosis transmembrane regulator gene transfer to the lungs of patients with cystic fibrosis: a multicenter, double-blind, placebo-controlled trial. Chest. (2004) Feb;125(2):509-21.

Mueller BK. Growth cone guidance: first steps towards a deeper understanding. Annu Rev Neurosci (1999) 22: 351–358.

Muramatsu R, Takahashi C, Miyake S, Fujimura H, Mochizuki H, Yamashita T. Angiogenesis induced by CNS inflammation promotes neuronal remodeling through vessel-derived prostacyclin. Nat Med. (2012) Nov;18(11):1658-64.

Nesathurai S. Steroids and spinal cord injury: revisiting the NASCIS 2 and NASCIS 3 trials. J Trauma. (1998) Dec;45(6):1088-93.

Neumann S, Bradke F, Tessier-Lavigne M, Basbaum AI. Regeneration of Sensory Axons within the Injured Spinal Cord Induced by Intraganglionic cAMP Elevation. Neuron (2002) 34:885-93.

Nicholson DW. From bench to clinic with apoptosis-based therapeutic agents. Nature (2000) 407:810-6

Niclou SP, Ehlert EM, Verhaagen J. Chemorepellent axon guidance molecules in spinal cord injury. J Neurotrauma. (2006) Mar-Apr;23(3-4):409-21.

Novikova LN, Novikov LN, Kellerth JO. Survival effects of BDNF and NT-3 on axotomized rubrospinal neurons depend on the temporal pattern of neurotrophin administration. Eur J Neurosci. (2000) Feb;12(2):776-80.

Okada S, Nakamura M, Katoh H, Miyao T, Shimazaki T, Ishii K, Yamane J, Yoshimura A, Iwamoto Y, Toyama Y and Okano H. Conditional ablation of Stat3 or Socs3 discloses a dual role for reactive astrocytes after spinal cord injury. Nat Med (2006) 12(7): 829-834.

Ornitz DM and Itoh N. Fibroblast growth factors. Genome Biology (2001) Vol 2 No 3.

Ornitz DM, Xu J, Colvin JS, McEwen DG, MacArthur CA, Coulier F, Gao G, and Goldfarb M. Receptor specificity of the fibroblast growth factor family. J. Biol. Chem.(1996) 271, 15292–15297.

Ozdinler PH, Macklis JD. IGF-I specifically enhances axon outgrowth of corticospinal motor neurons. Nat Neurosci (2006) 9:1371-81.

Paradiso B, Zucchini S and Simonato M. Implication of fibroblast growth factors in epileptogenesis-associated circuit rearrangements. Frontiers in Cellular Neuroscience (2013) Volume 7, 152.

Park KK, Liu K, Hu Y, Smith PD, Wang C, Cai B, Xu B, Connolly L, Kramvis I, Sahin M and He Z. Promoting axon regeneration in the adult CNS by modulation of the PTEN/mTOR pathway. Science (2008) 322(5903): 963-966.

Park KK, Liu K, Hu Y, Kanter JL and He Z. PTEN/mTOR and axon regeneration. Exp Neurol (2010) 223(1): 45-50.

Pasterkamp RJ, Peschon JJ, Spriggs MK, Kolodkin AL Semaphorin 7A promotes axon outgrowth through integrins and MAPKs. Nature (2003) 424(6947): 398–405.

Pernet V, Schwab ME. The role of Nogo-A in axonal plasticity, regrowth and repair. Cell Tissue Res. (2012) Jul;349(1):97-104.

Pernet V, Joly S, Jordi N, Dalkara D, Guzik-Kornacka A, Flannery JG, Schwab ME .Misguidance and modulation of axonal regeneration by Stat3 and Rho/ROCK signaling in the transparent optic nerve. Cell Death Dis. (2013) Jul 18;4:e734.

Popovich PG, Guan Z, Wei P, Huitinga I, van Rooijen N, Stokes BT. Depletion of Hematogenous Macrophages Promotes Partial Hindlimb Recovery and Neuroanatomical Repair after Experimental Spinal Cord Injury. Experimental Neurology (1999) 158:351-65.

Qiu J, Cai D, Dai H, McAtee M, Hoffman PN. Spinal Axon Regeneration Induced by Elevation of Cyclic AMP. Neuron (2002) 34:895-903.

Qiu J, Cafferty WB, McMahon SB and Thompson SW. Conditioning injuryinduced spinal axon regeneration requires signal transducer and activator of transcription 3 activation. J Neurosci (2005) 25(7): 1645-1653.

Raineteau O, Schwab ME. Plasticity of motor systems after incomplete spinal cord injury. Nat Rev Neurosci. (2001) Apr;2(4):263-73.

Raivich G, Makwana M. The making of successful axonal regeneration: genes, molecules and signal transduction pathways. Brain Res Rev. (2007) Feb;53(2):287-311.

Rajan P, Stewart CL and Fink JS. LIF-mediated activation of STAT proteins after neuronal injury in vivo. Neuroreport (1995) 6(16): 2240-2244.

Rogers GL, Martino AT, Aslanidi GV, Jayandharan GR, Srivastava A and Herzog RW. Innate Immune Responses to AAV Vectors. Front Microbiol (2011) 2: 194.

Rünker AE, Little GE, Suto F, Fujisawa H, Mitchell KJ. Semaphorin-6A controls guidance of corticospinal tract axons at multiple choice points. Neural Dev (2008) 3: 34.

Sadowsky C, Volshteyn O, Schultz L, McDonald JW. Spinal cord injury. Disabil Rehabil. (2002) Sep 10;24(13):680-7.

Sang Q, Wu JY, Rao Y, Hsueh Y-P, Tan S-S. Slit promotes branching and elongation of neurites of interneurons but not projection neurons from the developing telencephalon. Mol Cell Neurosci (2002) 21: 250–265.

Sasaki M, Radtke C, Tan AM, Zhao P, Hamada H, Houkin K, Honmou O, Kocsis JD. BDNF-hypersecreting human mesenchymal stem cells promote functional recovery, axonal sprouting, and protection of corticospinal neurons after spinal cord injury. J Neurosci. (2009) Nov 25;29(47):14932-41.

Scheiffele P, Fan J, Choih J, Fetter R, Serafini T. Neuroligin expressed in nonneuronal cells triggers presynaptic development in contacting axons. Cell (2000) Jun 9;101(6):657-69.

Schnell L, Schwab ME. Axonal regeneration in the rat spinal cord produced by an antibody against myelin-associated neurite growth inhibitors. Nature (1990) 343:269-72.

Schoch S and Gundelfinger ED. Molecular organization of the presynaptic active zone. Cell Tissue Res. (2006) Nov;326(2):379-91.

Seijffers R, Mills CD and Woolf JC. ATF3 increases the intrinsic growth state of DRG neurons to enhance peripheral nerve regeneration. J Neurosci (2007) 27(30): 7911- 7920.

Serafini T, Colamarino SA, Leonardo ED, Wang H, Beddington R, Skarnes WC, Tessier-Lavigne M. Netrin-1 is required for commissural axon guidance in the developing vertebrate nervous system. Cell. (1996) Dec 13;87(6):1001-14.

Shapiro L, Love J, Colman DR. Adhesion molecules in the nervous system: structural insights into function and diversity. Annu Rev Neurosci. (2007);30:451-74.

Sharma HS, Olsson Y, Dey PK. Early accumulation of serotonin in rat spinal cord subjected to traumatic injury. Relation to edema and blood flow changes. Neuroscience. (1990) 36(3):725-30.

Shepard MJ, Bracken MB The effect of methylprednisolone, naloxone, and spinal cord trauma on four liver enzymes: observations from NASCIS 2. National Acute Spinal Cord Injury Study. Paraplegia. (1994) Apr;32(4):236-45.

Shim SO, Cafferty WB, Schmidt EC, Kim BG, Fujisawa H. PlexinA2 limits recovery from corticospinal axotomy by mediating oligodendrocyte- derived Sema6A growth inhibition. Mol Cell Neurosci (2012) 50(2): 193–200.

Shen K and Cowan CW. Guidance Molecules in Synapse Formation and Plasticity. Cold Spring Harb Perspect Biol (2010).

Smith PD, Sun F, Park KK, Cai B, Wang C, Kuwako K, Martinez-Carrasco I, Connolly L and He Z. SOCS3 deletion promotes optic nerve regeneration in vivo. Neuron (2009) 64(5): 617-623.

Smith RP, Lerch-Haner JK, Pardinas JR, Buchser WJ, Bixby JL, Lemmon VP. Transcriptional

profiling of intrinsic PNS factors in the postnatal mouse. Molecular and Cellular Neuroscience (2011) 46:32-44.

Song JY, Ichtchenko K, Suedhof TC, Brose N. Neuroligin 1 is a postsynaptic call-adhesion molecule of excitatory synapses. Proc Natl Acad Sci USA (1999) 96: 1100–1105.

Starkey ML, Bartus K, Barritt AW and Bradbury EJ. Chondroitinase ABC promotes compensatory sprouting of the intact corticospinal tract and recovery of forelimb function following unilateral pyramidotomy in adult mice. European Journal of Neuroscience, (2012) 36, 3665–3678.

Stokes BT, Jakeman LB. Experimental modelling of human spinal cord injury: a model that crosses the species barrier and mimics the spectrum of human cytopathology. Spinal Cord. (2002) Mar;40(3):101-9.

Sun F and He Z. Neuronal intrinsic barriers for axon regeneration in the adult CNS. Curr Opin Neurobiol (2010) 20(4): 510-518.

Sun F, Park KK, Belin S, Wang D, Lu T, Chen G, Zhang K, Yeung C, Feng G, Yankner BA, He Z. Sustained axon regeneration induced by co-deletion of PTEN and SOCS3. Nature. (2011) Nov 6;480(7377):372-5.

Suto F, Tsubio M, Kamiya H, Mizuno H, Kiyama Y. Interactions between Plexin-A2, Plexin-A4, and Semaphorin6A controls lamina-restricted projection of hippocampal mossy fibers. Neuron (2007) 53: 535–547.

Tagashira S, Harada H, Katsumata T, Itoh N, Nakatsuka M. Cloning of mouse FGF10 and up-regulation of its gene expression during wound healing. Gene (1997) Sep 15;197(1-2):399-404.

Takahashi JA, Mori H, Fukumoto M, Igarashi K, Jaye M, Oda Y, Kikuchi H, Hatanaka M. Gene expression of fibroblast growth factors in human gliomas and meningiomas: demonstration of cellular source of basic fibroblast growth factor mRNA and peptide in tumor tissues. Proc Natl Acad Sci USA (1990) Aug;87(15):5710-4.

Tallafuss A, Constable JR, Washbourne P. Organization of central synapses by adhesion molecules Eur J Neurosci (2010) Jul;32(2):198-206.

Taylor L, Jones L, Tuszynski MH, Blesch A. Neurotrophin-3 gradients established by lentiviral gene delivery promote short-distance axonal bridging beyond cellular grafts in the injured spinal cord. J Neurosci (2006) Sep 20;26(38):9713-21.

Terashima T. Anatomy, development and lesion-induced plasticity of rodent corticospinal tract. Neuroscience Research (1995) 22:139-61.

Terauchi A, Johnson-Venkatesh EM, Toth AB, Javed D, Sutton MA, Umemori H. Distinct FGFs promote differentiation of excitatory and inhibitory synapses. Nature (2010) Jun 10;465(7299):783-7.

Tessier-Lavigne MT, Goodman CS. The molecular biology of axon guidance. Science, (1996) 274

Thomas LA, Akins MR, Biederer T. Expression and adhesion profiles of SynCAM molecules indicate distinct neuronal functions. J Comp Neurol (2008) 510(1): 47–67.

Thuret S, Moon LDF, Gage FH. Therapeutic interventions after spinal cord injury. Nat Rev Neurosci (2006) 7:628-43.

Turner N and Grose R. Fibroblast growth factor signalling: from development to cancer. Nature Reviews Cancer (2010), Vol 10.

Umemori H, Linhoff MW, Ornitz DM, Sanes JR. FGF22 and its close relatives are presynaptic organizing molecules in the mammalian brain. Cell (2004) Jul 23;118(2):257-70.

Ushkaryov YA, Petrenko AG, Geppert M, Südhof TC. Neurexins: synaptic cell surface proteins related to the alpha- latrotoxin receptor and laminin. Science(1992) 257: 50 –56.

Ushkaryov YA, Südhof TC. Neurexin III alpha: extensive alternative splicing generates membrane-bound and soluble forms. Proc Natl Acad Sci USA (1993) 90: 6410–6414.

van den Brand R, Heutschi J, Barraud Q, DiGiovanna J, Bartholdi K, Huerlimann M, Friedli L, Vollenweider I, Moraud EM, Duis S, Dominici N, Micera S, Musienko P, Courtine G Restoring voluntary control of locomotion after paralyzing spinal cord injury. Science (2012) Jun 1;336(6085):1182-5.

Wang JK, Xu H, Li HC, Goldfarb M. Broadly expressed SNT-like proteins link FGF receptor stimulation to activators of Ras. Oncogene (1996) Aug 15;13(4):721-9.

Wehrle R, Camand E, Chedotal A, Sotelo C, Dusart I. Expression of netrin-1, slit-1 and slit-3 but not of slit-2 after cerebellar and spinal cord lesions. Eur J Neurosci (2005) 22(9): 2134–2144.

Weidner N, Ner A, Salimi N, Tuszynski MH. Spontaneous corticospinal axonal plasticity and functional recovery after adult central nervous system injury. Proceedings of the National Academy of Sciences (2001) 98:3513-8.

Wernig A, Nanassy A, Müller S. Maintenance of locomotor abilities following Laufband (treadmill) therapy in para- and tetraplegic persons: follow-up studies. Spinal Cord (1998) Nov;36(11):744-9.

Wernig A, Müller S. Laufband locomotion with body weight support improved walking in persons with severe spinal cord injuries. Paraplegia (1992) Apr;30(4):229-38.

Westgren N, Levi R. Quality of life and traumatic spinal cord injury. Arch Phys Med Rehabil. (1998) Nov;79(11):1433-9.

Wiessner C, Bareyre F, Allegrini P, Mir A, Frentzel S. Anti-Nogo-A antibody infusion 24 hours after experimental stroke improved behavioral outcome and corticospinal plasticity in normotensive and spontaneously hypertensive rats. J Cereb Blood Flow Metab. (2003) 23:154-65.

Wirz M, Colombo G, Dietz V. Long term effects of locomotor training in spinal humans. J Neurol Neurosurg Psychiatry (2001) Jul;71(1):93-6.

Varoqueaux F, Aramuni G, Rawson RL, Mohrmann R, Missler M, Gottmann G , Zhang W, Südhof TC, Brose N. Neuroligins Determine Synapse Maturation and Function. Neuron (2006) 51, 741–754.

Xiao X, Li J, McCown TJ and Samulski RJ. Gene transfer by adeno-associated virus vectors into the central nervous system. Exp Neurol (1997) 144(1): 113-124.

Yip PK, Wong L-F, Sears TA, Yáñez-Muñoz RJ, McMahon SB. Cortical Overexpression of Neuronal Calcium Sensor-1 Induces Functional Plasticity in Spinal Cord Following Unilateral Pyramidal Tract Injury in Rat. PLoS Biol (2010) 8:e1000399.

Yokoyama N, Romero MI, Cowan CA, Galvan P, Helmbacher F. Forward signaling mediated by ephrin-B3 prevents contralateral corticospinal axons from recrossing the spinal cord midline. Neuron(2001) 29: 85–97.

You SW, Chen BY, Liu HL, Lang B, Xia JL, Jiao XY, Ju G. Spontaneous recovery of locomotion induced by remaining fibers after spinal cord transection in adult rats. Restor Neurol Neurosci (2003) 21:39-45

H. Yu, D. Pardoll and R. Jove. STATs in cancer inflammation and immunity: a leading role for STAT3. Nat Rev Cancer (2009) 9(11): 798-809.

Zelano J, Berg A, Thams S, Hailer NP, Cullheim S. SynCAM1 expression correlates with restoration of central synapses on spinal motoneurons after two different models of peripheral nerve injury. J Comp Neurol (2009) 517(5): 670–682.

Zhai R. Temporal appearance of the presynaptic cytomatrix protein bassoon during synaptogenesis. Mol Cell Neurosci (2000) 15, 417–428

Zhang X, Ibrahimi OA, Olsen SK, Umemori H, Mohammadi M, Ornitz DM. Receptor specificity of the fibroblast growth factor family. The complete mammalian FGF family. J Biol Chem (2006) Jun 9;281(23):15694-700.

Zhang Z, Krebs CJ, Guth L. Experimental Analysis of Progressive Necrosis after Spinal Cord Trauma in the Rat: Etiological Role of the Inflammatory Response. Experimental Neurology (1997) 143:141-52

Zhong Z, Wen Z and Darnell JE, Jr. Stat3: a STAT family member activated by tyrosine phosphorylation in response to epidermal growth factor and interleukin-6. Science (1994) 264(5155): 95-98.

Zhou L, Shine HD. Neurotrophic factors expressed in both cortex and spinal cord induce axonal plasticity after spinal cord injury. Journal of Neuroscience Research (2003) 74:221-6

Zou H, Ho C, Wong K and Tessier-Lavigne M. Axotomy-induced Smad1 activation promotes axonal growth in adult sensory neurons. J Neurosci (2009) 29(22): 7116-7123.

Dear Anne

Thank you for your permission request.

We hereby grant you permission to reprint the material below at no charge **in your thesis** subject to the following conditions:

1. If any part of the material to be used (for example, figures) has appeared in our publication with credit or acknowledgement to another source, permission must also be sought from that source. If such permission is not obtained then that material may not be included in your publication/copies.

2. Suitable acknowledgment to the source must be made, either as a footnote or in a reference list at the end of your publication, as follows:

   "This article was published in Publication title, Vol number, Author(s), Title of article, Page Nos, Copyright Elsevier (or appropriate Society name) (Year)."

3. Your thesis may be submitted to your institution in either print or electronic form.

4. Reproduction of this material is confined to the purpose for which permission is hereby given.

5. This permission is granted for non-exclusive world **English** rights only. For other languages please reapply separately for each one required. Permission excludes use in an electronic form other than submission. Should you have a specific electronic project in mind please reapply for permission.

6. Should your thesis be published commercially, please reapply for permission.

Regards

Banita Samantray
Global Rights Department

Elsevier
(A division of Reed Elsevier India Pvt. Ltd.)

From: Rebecca Laming
To: Jacobi, Anne
Subject: Re: Permission to reprint a figure from your homepage
Date: Dienstag, 24. Juni 2014 14:09:05

Hello Anne,

Thank you for reaching out. You are welcome to cite the Reeve Foundation study in your thesis as long as you include a proper citation for the stat.

I certainly appreciate you checking and good luck with your thesis. Please reach out if you need anything else and have a wonderful day.

Rebecca Laming
Senior Director, Marketing & Communications
Christopher & Dana Reeve Foundation
Today's Care. Tomorrow's Cure.®

636 Morris Turnpike, Suite 3A
Short Hills, NJ 07078
O: (973) 379-2690 ext. 7115
M: (917) 558-1828
rlaming@christopherreeve.org
www.ChristopherReeve.org

NATURE PUBLISHING GROUP LICENSE
TERMS AND CONDITIONS

Oct 08, 2014

This is a License Agreement between Institut for clinical Neuroimmunology ("You") and Nature Publishing Group ("Nature Publishing Group") provided by Copyright Clearance Center ("CCC"). The license consists of your order details, the terms and conditions provided by Nature Publishing Group, and the payment terms and conditions.

All payments must be made in full to CCC. For payment instructions, please see information listed at the bottom of this form.

License Number	3418740070710
License date	Jun 30, 2014
Licensed content publisher	Nature Publishing Group
Licensed content publication	Nature Reviews Neuroscience
Licensed content title	Can regenerating axons recapitulate developmental guidance during recovery from spinal cord injury?
Licensed content author	Noam Y. HarelandStephen M. Strittmatter
Licensed content date	Aug 1, 2006
Volume number	7
Issue number	8
Type of Use	reuse in a dissertation / thesis
Requestor type	academic/educational
Format	print and electronic
Portion	figures/tables/illustrations
Number of figures/tables /illustrations	1
High-res required	no
Figures	Figure 2a Corticospinal tract response to injury
Author of this NPG article	no
Your reference number	None
Title of your thesis / dissertation	Identification and Manipulation of Molecules Regulating Axonal Outgrowth and Synapse Formation during Post-Injury Axonal Remodeling
Expected completion date	Jun 2014
Estimated size (number of pages)	160
Total	0.00 EUR
Terms and Conditions	

NATURE PUBLISHING GROUP LICENSE TERMS AND CONDITIONS

Oct 08, 2014

This is a License Agreement between Institut for clinical Neuroimmunology ("You") and Nature Publishing Group ("Nature Publishing Group") provided by Copyright Clearance Center ("CCC"). The license consists of your order details, the terms and conditions provided by Nature Publishing Group, and the payment terms and conditions.

All payments must be made in full to CCC. For payment instructions, please see information listed at the bottom of this form.

License Number	3415360795862
License date	Jun 24, 2014
Licensed content publisher	Nature Publishing Group
Licensed content publication	Journal of Investigative Dermatology
Licensed content title	FGFR2 Abnormalities Underlie a Spectrum of Bone, Skin, and Cancer Pathologies
Licensed content author	Masaru Katoh
Licensed content date	Apr 23, 2009
Volume number	129
Issue number	8
Type of Use	reuse in a dissertation / thesis
Requestor type	academic/educational
Format	print and electronic
Portion	figures/tables/illustrations
Number of figures/tables /illustrations	1
High-res required	no
Figures	Figure 1: FGFR2 signaling cascades
Author of this NPG article	no
Your reference number	None
Title of your thesis / dissertation	Identification and Manipulation of Molecules Regulating Axonal Outgrowth and Synapse Formation during Post-Injury Axonal Remodeling
Expected completion date	Jun 2014
Estimated size (number of pages)	160
Total	0.00 EUR
Terms and Conditions	

NATURE PUBLISHING GROUP LICENSE TERMS AND CONDITIONS

Oct 08, 2014

This is a License Agreement between Institut for clinical Neuroimmunology ("You") and Nature Publishing Group ("Nature Publishing Group") provided by Copyright Clearance Center ("CCC"). The license consists of your order details, the terms and conditions provided by Nature Publishing Group, and the payment terms and conditions.

All payments must be made in full to CCC. For payment instructions, please see information listed at the bottom of this form.

License Number	3415360154497
License date	Jun 24, 2014
Licensed content publisher	Nature Publishing Group
Licensed content publication	Nature Reviews Neuroscience
Licensed content title	Therapeutic interventions after spinal cord injury
Licensed content author	Sandrine Thuret,Lawrence D. F. MoonandFred H. Gage
Licensed content date	Aug 1, 2006
Volume number	7
Issue number	8
Type of Use	reuse in a dissertation / thesis
Requestor type	academic/educational
Format	print and electronic
Portion	figures/tables/illustrations
Number of figures/tables /illustrations	1
High-res required	no
Figures	Box 1 | The ASIA Impairment Scale
Author of this NPG article	no
Your reference number	None
Title of your thesis / dissertation	Identification and Manipulation of Molecules Regulating Axonal Outgrowth and Synapse Formation during Post-Injury Axonal Remodeling
Expected completion date	Jun 2014
Estimated size (number of pages)	160
Total	0.00 EUR
Terms and Conditions	

NATURE PUBLISHING GROUP LICENSE TERMS AND CONDITIONS

Oct 08, 2014

This is a License Agreement between Institut for clinical Neuroimmunology ("You") and Nature Publishing Group ("Nature Publishing Group") provided by Copyright Clearance Center ("CCC"). The license consists of your order details, the terms and conditions provided by Nature Publishing Group, and the payment terms and conditions.

All payments must be made in full to CCC. For payment instructions, please see information listed at the bottom of this form.

License Number	3415350994100
License date	Jun 24, 2014
Licensed content publisher	Nature Publishing Group
Licensed content publication	Cell Research
Licensed content title	Cell transplantation therapies for spinal cord injury focusing on induced pluripotent stem cells
Licensed content author	Masaya Nakamura and Hideyuki Okano
Licensed content date	Dec 11, 2012
Volume number	23
Issue number	1
Type of Use	reuse in a dissertation / thesis
Requestor type	academic/educational
Format	print and electronic
Portion	figures/tables/illustrations
Number of figures/tables /illustrations	1
High-res required	no
Figures	Figure 1 Microenvironment of the injured spinal cord
Author of this NPG article	no
Your reference number	None
Title of your thesis / dissertation	Identification and Manipulation of Molecules Regulating Axonal Outgrowth and Synapse Formation during Post-Injury Axonal Remodeling
Expected completion date	Jun 2014
Estimated size (number of pages)	160
Total	0.00 USD
Terms and Conditions	

NATURE PUBLISHING GROUP LICENSE TERMS AND CONDITIONS

Oct 08, 2014

This is a License Agreement between Institut for clinical Neuroimmunology ("You") and Nature Publishing Group ("Nature Publishing Group") provided by Copyright Clearance Center ("CCC"). The license consists of your order details, the terms and conditions provided by Nature Publishing Group, and the payment terms and conditions.

All payments must be made in full to CCC. For payment instructions, please see information listed at the bottom of this form.

License Number	3415350449674
License date	Jun 24, 2014
Licensed content publisher	Nature Publishing Group
Licensed content publication	Nature
Licensed content title	Distinct FGFs promote differentiation of excitatory and inhibitory synapses
Licensed content author	Akiko Terauchi, Erin M. Johnson-Venkatesh, Anna B. Toth, Danish Javed, Michael A. Sutton, Hisashi Umemori
Licensed content date	May 26, 2010
Volume number	465
Issue number	7299
Type of Use	reuse in a dissertation / thesis
Requestor type	academic/educational
Format	print and electronic
Portion	figures/tables/illustrations
Number of figures/tables /illustrations	1
High-res required	no
Figures	Figure 4g : Altered synaptic transmission and seizure susceptibility in FGFKO mice, and a model for the role of FGF22 and FGF7 in specific presynaptic differentiation. Page 786.
Author of this NPG article	no
Your reference number	None
Title of your thesis / dissertation	Identification and Manipulation of Molecules Regulating Axonal Outgrowth and Synapse Formation during Post-Injury Axonal Remodeling
Expected completion date	Jun 2014
Estimated size (number of pages)	160
Total	0.00 USD
Terms and Conditions	

THE AMERICAN ASSOCIATION FOR THE ADVANCEMENT OF SCIENCE LICENSE TERMS AND CONDITIONS

Oct 08, 2014

This is a License Agreement between Institut for clinical Neuroimmunology ("You") and The American Association for the Advancement of Science ("The American Association for the Advancement of Science") provided by Copyright Clearance Center ("CCC"). The license consists of your order details, the terms and conditions provided by The American Association for the Advancement of Science, and the payment terms and conditions.

All payments must be made in full to CCC. For payment instructions, please see information listed at the bottom of this form.

License Number	3415341199599
License date	Jun 24, 2014
Licensed content publisher	The American Association for the Advancement of Science
Licensed content publication	Science
Licensed content title	The Molecular Biology of Axon Guidance
Licensed content author	Marc Tessier-Lavigne, Corey S. Goodman
Licensed content date	Nov 15, 1996
Volume number	274
Issue number	5290
Type of Use	Thesis / Dissertation
Requestor type	Scientist/individual at a research institution
Format	Print and electronic
Portion	Figure
Number of figures/tables	1
Order reference number	None
Title of your thesis / dissertation	Identification and Manipulation of Molecules Regulating Axonal Outgrowth and Synapse Formation during Post-Injury Axonal Remodeling
Expected completion date	Jun 2014
Estimated size(pages)	160
Total	0.00 EUR
Terms and Conditions	

AMERICAN ASSOCIATION FOR CANCER RESEARCH LICENSE TERMS AND CONDITIONS

Oct 08, 2014

This is a License Agreement between Institut for clinical Neuroimmunology ("You") and American Association for Cancer Research ("American Association for Cancer Research") provided by Copyright Clearance Center ("CCC"). The license consists of your order details, the terms and conditions provided by American Association for Cancer Research, and the payment terms and conditions.

All payments must be made in full to CCC. For payment instructions, please see information listed at the bottom of this form.

License Number	3415350665636
License date	Jun 24, 2014
Licensed content publisher	American Association for Cancer Research
Licensed content publication	Clinical Cancer Research
Licensed content title	Regulation of Metastases by Signal Transducer and Activator of Transcription 3 Signaling Pathway: Clinical Implications
Licensed content author	Suyun Huang
Licensed content date	March 1, 2007
Volume number	13
Issue number	5
Type of Use	Thesis/Dissertation
Requestor type	academic/educational
Format	print and electronic
Portion	figures/tables/illustrations
Number of figures/tables /illustrations	1
Will you be translating?	no
Circulation	2
Territory of distribution	Worldwide
Title of your thesis / dissertation	Identification and Manipulation of Molecules Regulating Axonal Outgrowth and Synapse Formation during Post-Injury Axonal Remodeling
Expected completion date	Jun 2014
Estimated size (number of pages)	160
Total	0.00 USD
Terms and Conditions	

7. Acknowledgements

There are many people I would like to thank for their support throughout the time of this thesis.
First and outer most, I would like to thank Dr. Florence Bareyre and Prof. Martin Kerschensteiner. Thank you, for giving me the opportunity to work on such an interesting and also challenging project. You both were always there with positive energy, fruitful discussions, continuous support and encouragement in tough times! Thank you for the opportunity to learn from you as great scientists and giving me the chance to discover this great and highly interesting field of neuroscience research!

Next, I would like to thank my supervisor from the biology faculty, Prof. Hans Straka, who showed a lot of interest in my work and help me through the time of my thesis studies.

Also I would like to thank all members of the lab who created a great and joyful work environment! Next to great work atmosphere, I enjoyed our lab excursions, our BBQ parties and the nights out a lot! It is truly a wonderful place to work at! Most important to mention, Anja! Thank you for being there from the first day of work, for helping doing countless in situs, for always supporting me (in anger ☺ and laugh) and for being a great friend who made long hours of work to a lot of fun! I will miss you!
Room 007, with all its current and former members, was great and a lot of fun!! Special thanks goes to Elisa, for sharing the desk with me and the van during hot days of summer, for the hours you spent laughing with me and this way becoming a very good friend.

Cathy, who started the doctoral studies at the same time as me and was a great company during joyful times! Also a big thank you to Kristina, for your unique help and the many hours you spent in the animal room to help finishing up the FGF paper! You joined our lab at the right time ☺.Finally, a special thanks to Peter, for your help, our critical discussions about techniqual challenges and even though you don't remember, for all your help to finish up my thesis as quick as possible ☺.

Next to the great support at work, I would like to thank all my friends! Especially worth mentioning, Anschi, Meike and Sandra! I am very grateful to have you in my life and thankful for your support! A special Thank You to my dear friend Susi! Thank you for all your support, for encouraging and motivating me after long days or weekends of work! You were always there for me!

Finally, my family, my brother with his family, my two grandmas'! I thank you for your constant support and care during the last years! A special Thanks goes to my dear parents, you have always been there for me, supported me and encouraged me in tougher times. I am extremely grateful for your support during my whole life!

Multitasking PhD (Winner of the 2.price award of the Graduate Center, LMU Fotocompetition 2011)